

DESIGN AND DEVELOPMENT OF ELECTROMAGNETIC WAVE
ABSORBING COMPOSITES EFFECTIVE AT MICROWAVE FREQUENCIES

A THESIS SUBMITTED TO
THE GRADUATE SCHOOL OF NATURAL AND APPLIED SCIENCES
OF
MIDDLE EAST TECHNICAL UNIVERSITY

BY

ÖZGÜR HAMAT

IN PARTIAL FULFILLMENT OF THE REQUIREMENTS
FOR
THE DEGREE OF MASTER OF SCIENCE
IN
METALLURGICAL AND MATERIALS ENGINEERING

NOVEMBER 2014

Approval of the thesis:

**DESIGN AND DEVELOPMENT OF ELECTROMAGNETIC WAVE
ABSORBING COMPOSITES EFFECTIVE AT MICROWAVE
FREQUENCIES**

submitted by **ÖZGÜR HAMAT** in partial fulfillment of the requirements for the degree of **Master of Science in Metallurgical and Materials Engineering Department, Middle East Technical University** by,

Prof. Dr. Gülbin Dural Ünver

Dean, **Graduate School of Natural and Applied Sciences**

Prof. Dr. C. Hakan Gür

Head of Department, **Metallurgical and Materials Engineering**

Assoc. Prof. Dr. Arcan F. Dericioğlu

Supervisor, **Metallurgical and Materials Eng. Dept., METU**

Examining Committee Members:

Prof. Dr. C. Hakan Gür

Metallurgical and Materials Engineering Dept., METU

Assoc. Prof. Dr. Arcan F. Dericioğlu

Metallurgical and Materials Engineering Dept., METU

Prof. Dr. Cevdet Kaynak

Metallurgical and Materials Engineering Dept., METU

Assoc. Prof. Dr. Demirkan Çöker

Aerospace Engineering Dept., METU

Assist. Prof. Dr. Mert Efe

Metallurgical and Materials Engineering Dept., METU

Date: 21.11.2014

I hereby declare that all information in this document has been obtained and presented in accordance with academic rules and ethical conduct. I also declare that, as required by these rules and conduct, I have fully cited and referenced all material and results that are not original to this work.

Name, Last name: Özgür Hamat

Signature :

ABSTRACT

DESIGN AND DEVELOPMENT OF ELECTROMAGNETIC WAVE ABSORBING COMPOSITES EFFECTIVE AT MICROWAVE FREQUENCIES

Hamat, Özgür

M.S., Department of Metallurgical and Materials Engineering

Supervisor: Assoc. Prof. Dr. Arcan F. Dericioğlu

November 2014, 143 pages

In the scope of this study, EM wave absorbing composites effective at microwave frequencies having crucial properties for their structural applicability will be designed and developed making use of a novel approach originating from our research group. For this purpose, surfaces of glass and polymeric fiber woven fabrics were modified via metal coatings with nm order thickness, where EM wave absorbing structural composites were formed by incorporating multilayered combinations of these surface-modified woven fabrics within polymer matrices. EM wave reflection and transmission properties, and hence absorption characteristics of surface-modified single layer and multilayer fiber woven fabrics were investigated using Free-Space test method. Based on the experimental data achieved on single layer woven fabrics, simulation studies were conducted in order to predict the EM wave absorption

characteristics of multilayered reinforcement structures. In the last phase of the study, structural prototype EM wave absorbing polymer matrix composite is produced by placing surface modified multilayer fiber woven reinforcement materials with the highest EM wave absorption. More than 90% EM wave absorption was achieved with the fabricated composites in 18-40 GHz frequency range. Critical design principles required to reach to this challenging target were presented using simulations and experimental studies.

Keywords: Electromagnetic wave absorption, electromagnetic interference, glass fiber woven fabrics, aramid fiber woven fabrics, surface modification, free-space method, microwave frequency.

ÖZ

MİKRODALGA FREKANSLARINDA ETKİN ELEKTROMANYETİK DALGA SOĞURUCU KOMPOZİTLERİN TASARIMI VE GELİŞTİRİLMESİ

Hamat, Özgür

Yüksek Lisans, Metalurji ve Malzeme Mühendisliği Bölümü

Tez Yöneticisi: Doç. Dr. Arcan F. Dericioğlu

Kasım 2014, 143 sayfa

Bu çalışma kapsamında, mikrodalga frekanslarında etkin elektromanyetik dalga soğurma özelliğine sahip ve aynı zamanda kullanım alanları bakımından gerekli olabilecek yapısal özellikleri de barındıran kompozit malzemelerin tasarlanması ve geliştirilmesi hedeflenmiştir. Bu amaç doğrultusunda, cam ve aramid elyaf dokumaların yüzeyleri nanometre mertebesinde kalınlıklara sahip metalik kaplamalarla modifiye edilmiş ve bu modifiye edilmiş dokumalardan oluşan çok katmanlı yapılar, polimer matrisler içerisine takviye malzemesi olarak yerleştirilerek EM dalga soğurucu yapısal kompozit malzemeler geliştirilmiştir. Yüzeyleri modifiye edilen tek katmanlı ve çok katmanlı fiber dokumaların EM dalga geçirim ve yansıtma ve dolayısıyla soğurma özellikleri Serbest Uzay (Free-Space) yöntemi kullanılarak incelenmiştir. Çalışmanın son aşamasında ise, en yüksek EM dalga soğurma özelliğine

sahip, yüzey modifikasyonlu elyaf dokumalardan oluşan çok katmanlı takviye malzemesi epoksi matris içerisine yerleştirilerek, prototip EM dalga soğurucu polimer matrisli yapısal kompozit üretilmiştir. Sonuç olarak, elde edilen kompozit malzemede 18-40 GHz frekans aralığında %90'ın üzerinde EM dalga soğurma sağlanmıştır. Yapılan simülasyonlar ve deneysel çalışmalarla bu hedefe ulaşmak için gerekli tasarım prensipleri ortaya konmuştur.

Anahtar Kelimeler: Elektromanyetik dalga soğurumu, elektromanyetik girişim, cam elyaf dokuma, aramid elyaf dokuma, yüzek modifikasyonu, serbest-uzay yöntemi, mikrodalga frekansları.

To My Family

ACKNOWLEDGEMENTS

This work has been funded by TUBİTAK.

I would like to thank my advisor Assoc. Prof. Dr. Arcan F. Dericiođlu for his guidance and supervision and providing me the possibility to work in such a sophisticated facility.

I would like to thank to Prof. Dr. C. Hakan Gr, Prof. Dr. Cevdet Kaynak, Assoc. Prof. Dr. Demirkan oker and Assist Prof. Dr. Mert Efe for being on my thesis committee.

I am grateful to all the staff of the Department of Metallurgical and Materials Engineering and my lab mates Aylin Gneş, Eda Aydođan, Gney Dalođlu, Selen Nimet Grbz Gner, Seray Kaya and Simge Tlbez.

I would like to thank Ali Naci Erdem, Arda Gleş, Ođuzhan Temel and Ođuzhan Orkut Okudur, for their support through thesis writing period.

Finally, I owe a debt to my family and Burcu Arslan for their endless support, patience, encouragements and especially for their love.

TABLE OF CONTENTS

ABSTRACT	v
ÖZ	vii
ACKNOWLEDGEMENTS	x
TABLE OF CONTENTS	xi
LIST OF TABLES	xv
LIST OF FIGURES	xvi
INTRODUCTION	1
LITERATURE REVIEW.....	3
2.1 Electromagnetic Spectrum and Electromagnetic Waves	3
2.2 Microwave Frequency and Applications.....	5
2.3 Electromagnetic Wave – Material Interactions	7
2.3.1 Mechanisms of Electromagnetic Loss	7
2.3.1.1 Dielectric Loss	8
2.3.1.2 Magnetic Loss.....	9
2.4 Electromagnetic Wave Absorbing Materials.....	9
EXPERIMENTAL PROCEDURE.....	15
3.1 Materials and Surface Modification Treatment	15
3.2 Surface Modification & Thin Film Characterization.....	16
3.2.1 Characterization with FESEM	16
3.2.2 Characterization with AFM	16

3.3 Composite Production	17
3.3.1 Silanization	17
3.3.2 Prototype Composite Fabrication.....	19
3.4 Characterization of EM Wave Absorbers by Free-Space Method	22
3.5 Mathematical Simulation for Multilayer EM Wave Absorbers	29
3.6 Mechanical Testing of EM Wave Absorber Composites	29
RESULTS AND DISCUSSION	33
4.1 Surface Modification and Electrical Conductivity of Thin Films	33
4.2 Surface Modification Characterization	35
4.2.1 Surface Morphology Examination using FESEM	35
4.2.2 Surface Topography Examination using AFM.....	40
4.3 Electromagnetic Measurements and Results.....	47
4.3.1 Electromagnetic Measurements and Results of Surface Modified Glass Fiber Woven Fabrics.....	48
4.3.1.1 EM Measurement Results of Glass Fiber Woven Fabrics Surface Modified with Silver.....	49
4.3.1.2 EM Measurement Results of Glass Fiber Woven Fabrics Surface Modified with Gold	58
4.3.1.3 EM Measurement Results of Glass Fiber Woven Fabrics Surface Modified with Nickel	65
4.3.2 Electromagnetic Measurement Results of Surface Modified Aramid Fiber Woven Fabrics.....	71
4.3.2.1 EM Measurement Results of Aramid Fiber Woven Fabrics Surface Modified with Gold	71
4.3.2.2 EM Measurement Results of Aramid Fiber Woven Fabrics Surface Modified with Nickel	78

4.3.3 Electromagnetic Measurements Results of Surface Modified PET Sheets	82
4.3.4 Electromagnetic Measurements and Results of Prototype Composite Structures	87
4.3.4.1 Electromagnetic Measurement Results of Gold Surface Modified Multilayered Glass Fiber Woven Fabric Containing Prototype Composites	87
4.3.4.2 Electromagnetic Measurement Results of Nickel Surface Modified Multilayered Glass Fiber Woven Fabric Containing Prototype Composites	91
4.3.4.3 Electromagnetic Measurement Results of Gold Surface Modified Multilayered Aramid Fiber Woven Fabric Containing Prototype Composites	94
4.3.4.4 Electromagnetic Measurement Results of Nickel Surface Modified Multilayered Aramid Fiber Woven Fabric Containing Prototype Composites	98
4.3.5 Electromagnetic Measurement Simulation Studies	101
4.4 Mechanical Test Results	104
4.5 Summary of Achievements	111
CONCLUSION	115
REFERENCES	117
APPENDIX A	123
A.1 EM Wave Measurements and Results of Silanized and Surface Modified Woven Fabrics	123
A.1.1 EM Wave Measurements and Results of Silanized and Gold Surface Modified Glass Fiber Woven Fabrics	123

A.1.2 EM Wave Measurements and Results of Silanized and Nickel Surface Modified Glass Fiber Woven Fabrics	127
A.1.3 EM Wave Measurements and Results of Silanized and Gold Surface Modified Aramid Fiber Woven Fabrics	131
A.1.4 EM Wave Measurements and Results of Silanized and Nickel Surface Modified Aramid Fiber Woven Fabrics	135
A.2 Electromagnetic Measurement Simulation Studies	139

LIST OF TABLES

TABLES

Table 3.1 Technical specification of horn antennas used in Free-space method.	25
Table 3.2 Composite samples used in three-point bending tests.....	30
Table 3.3 Dimensions of 36 three point bending test specimens.	31
Table 4.1 Electrical conductivity of Ag, Au, Ni thin films with changing thickness.	34
Table 4.2 Measured average nuclei sizes for 15 nm, 20 nm, 25 nm thick Au thin films.	40
Table 4.3 Surface parameters obtained by AFM examination.	47

LIST OF FIGURES

FIGURES

Figure 2.1 Electromagnetic spectrum [6].	4
Figure 2.2 Atmospheric opacity [7].	5
Figure 2.3 Microwave frequency applications and frequency bands [8].	6
Figure 2.4 Schematic of interaction between EM wave and material.	10
Figure 2.5 Schematic model of “Salisbury Screen”.	12
Figure 2.6 Schematic model of Jaumann Absorber.	13
Figure 3.1 Structural formula of aminopropyl trimethoxy silane.	17
Figure 3.2 Schematics of chemical reactions taking place during silane treatment.	18
Figure 3.3 Constructed vacuum bagging system.	20
Figure 3.4 Photographs of fabricated composites without surface modifications.	21
Figure 3.5 Cross-sections of composite structures without surface modifications.	21
Figure 3.6 Horn antenna used in free-space measurement system.	24
Figure 3.7 Schematic view of horn antennas used in free-space measurement system with their dimensions (dimensions are in unit of mm).	25
Figure 3.8 Schematic view of layout for free-space method and polymeric lenses with specific dimensions [43].	26
Figure 3.9 Polymeric lenses used in free-space measurement system.	27
Figure 3.10 Isometric view of designed layout of Free-space method.	28
Figure 3.11 Custom-designed and built free-space measurement system and the utilized network analyzer.	28
Figure 4.1 Electrical conductivity of Ag, Au, Ni thin films with changing film thickness.	34

Figure 4.2 Surface morphology of 15 nm Au thin film on silicon wafer, photo taken by FESEM under x120000 magnification.....	36
Figure 4.3 Surface morphology of 20 nm Au thin film on silicon wafer, photo taken by FESEM under x120000 magnification.....	37
Figure 4.4 Surface morphology of 25 nm Au thin film on silicon wafer, photo taken by FESEM under x120000 magnification.....	37
Figure 4.5 Edge morphology of 15 nm Au thin film on silicon wafer, photo taken by FESEM under x240000 magnification.	38
Figure 4.6 Edge morphology of 20 nm Au thin film on silicon wafer, photo taken by FESEM under x240000 magnification.	39
Figure 4.7 Edge morphology of 25 nm Au thin film on silicon wafer, photo taken by FESEM under x240000 magnification.	39
Figure 4.8 3D microstructure photo taken using AFM of 15 nm thick Au film on silicon wafer (500 nm x 500 nm area).	42
Figure 4.9 2D microstructure photo taken using AFM of 15 nm thick Au film on silicon wafer (500 nm x 500 nm area) and nuclei size determination.	42
Figure 4.10 3D microstructure photo taken using AFM of 25 nm thick Au film on silicon wafer (500 nm x 500 nm area).	43
Figure 4.11 2D microstructure photo taken using AFM of 25 nm thick Au film on silicon wafer (500 nm x 500 nm area) and nuclei size determination.	43
Figure 4.12 3D microstructure of the scratch, photo taken using AFM on the 15 nm thick Au film on silicon wafer (60 μm x 60 μm area).	45
Figure 4.13 2D microstructure of the scratch, photo taken using AFM on the 15 nm thick Au film on silicon wafer (60 μm x 60 μm area) and thickness measurement. ...	45
Figure 4.14 3D microstructure of the scratch, photo taken using AFM on the 25 nm thick Au film on silicon wafer (20 μm x 20 μm area).	46
Figure 4.15 2D microstructure of the scratch, photo taken using AFM on the 25 nm thick Au film on silicon wafer (20 μm x 20 μm area) and thickness measurement. ...	46
Figure 4.16 EM wave reflection loss varying with frequency in silver surface modified single layered glass fiber woven fabrics.	50

Figure 4.17 EM wave transmission loss varying with frequency in silver surface modified single layered glass fiber woven fabrics.	50
Figure 4.18 EM wave reflection loss varying with frequency in silver surface modified multilayered glass fiber woven fabrics.	52
Figure 4.19 EM wave transmission loss varying with frequency in silver surface modified multilayered glass fiber woven fabrics.	52
Figure 4.20 EM wave absorption varying with frequency in silver surface modified multilayered glass fiber woven fabrics.	53
Figure 4.21 EM wave reflection loss varying with frequency in silver surface modified multilayered (5-layered) glass fiber woven fabric with metallic backing plate.....	54
Figure 4.22 EM wave reflection loss varying with frequency in oxidized silver surface modified single layered glass fiber woven fabrics.	55
Figure 4.23 EM wave transmission loss varying with frequency in oxidized silver surface modified single layered glass fiber woven fabrics.	56
Figure 4.24 EM wave reflection loss varying with frequency in oxidized silver surface modified multilayered glass fiber woven fabrics.	56
Figure 4.25 EM wave transmission loss varying with frequency in oxidized silver surface modified multilayered glass fiber woven fabrics.	57
Figure 4.26 EM wave absorption percentage varying with frequency in oxidized silver surface modified multilayered glass fiber woven fabrics.	57
Figure 4.27 EM wave reflection loss varying with frequency in oxidized silver surface modified 5-layered glass fiber woven fabric with metallic backing plate.....	58
Figure 4.28 EM wave reflection loss varying with frequency in gold surface modified single layer glass fiber woven fabrics.....	60
Figure 4.29 EM wave transmission loss varying with frequency in gold surface modified single layer glass fiber woven fabrics.....	60
Figure 4.30 EM wave reflection loss varying with frequency in gold surface modified multilayered glass fiber woven fabrics.	62
Figure 4.31 EM wave transmission loss varying with frequency in gold surface modified multilayered glass fiber woven fabrics.	62

Figure 4.32 EM wave absorption percentage varying with frequency in gold surface modified multilayered glass fiber woven fabrics.	63
Figure 4.33 EM wave reflection loss varying with frequency in gold surface modified 5-layered glass fiber woven fabrics with metallic backing plate.....	64
Figure 4.34 EM wave reflection loss varying with frequency in nickel surface modified single layer glass fiber woven fabrics.	66
Figure 4.35 EM wave transmission loss varying with frequency in nickel surface modified single layer glass fiber woven fabrics.	66
Figure 4.36 EM wave reflection loss varying with frequency in nickel surface modified multilayered glass fiber woven fabrics.	68
Figure 4.37 EM wave transmission loss varying with frequency in nickel surface modified multilayered glass fiber woven fabrics.	68
Figure 4.38 EM wave absorption percentages varying with frequency in nickel surface modified multilayered glass fiber woven fabrics.	69
Figure 4.39 EM wave reflection loss varying with frequency in nickel surface modified 5-layered glass fiber woven fabrics with metallic backing plate.....	70
Figure 4.40 EM wave reflection loss varying with frequency in gold surface modified single layer aramid fiber woven fabrics.	72
Figure 4.41 EM wave transmission loss varying with frequency in gold surface modified single layer aramid fiber woven fabrics.	73
Figure 4.42 EM wave reflection loss varying with frequency in gold surface modified multilayered aramid fiber woven fabrics.	74
Figure 4.43 EM wave transmission loss varying with frequency in gold surface modified multilayered aramid fiber woven fabrics.	75
Figure 4.44 EM wave absorption percentage varying with frequency in gold surface modified multilayered aramid fiber woven fabrics.	75
Figure 4.45 EM wave reflection loss varying with frequency in gold surface modified 5-layered aramid fiber woven fabrics with metallic backing plate.....	76
Figure 4.46. Aramid fiber woven fabrics with gold surface modification as (a) non-silanized and (b) silanized.	77

Figure 4.47 EM wave reflection loss varying with frequency in nickel surface modified single layer aramid fiber woven fabrics.....	78
Figure 4.48 EM wave transmission loss varying with frequency in nickel surface modified single layer aramid fiber woven fabrics.....	79
Figure 4.49 EM wave reflection loss varying with frequency in nickel surface modified multilayered aramid fiber woven fabrics.	80
Figure 4.50 EM wave transmission loss varying with frequency in nickel surface modified multilayered aramid fiber woven fabrics.	80
Figure 4.51 EM wave absorption percentage varying with frequency in nickel surface modified multilayered aramid fiber woven fabrics.	81
Figure 4.52 EM wave reflection loss varying with frequency in nickel surface modified 5-layered aramid fiber woven fabrics with metallic backing plate.	82
Figure 4.53 EM wave reflection loss varying with frequency in gold surface modified single layer PET sheets.	83
Figure 4.54 EM wave transmission loss varying with frequency in gold surface modified single layer PET sheets.	84
Figure 4.55 EM wave reflection loss varying with frequency in gold surface modified multilayered PET sheets.	85
Figure 4.56 EM wave transmission loss varying with frequency in gold surface modified multilayered PET sheets.	86
Figure 4.57 EM wave absorption percentage varying with frequency in gold surface modified multilayered PET sheets.	86
Figure 4.58 EM wave reflection loss varying with frequency in silanized and non-silanized composites containing gold surface modified multilayered glass fiber woven fabrics.	88
Figure 4.59 EM wave transmission loss varying with frequency in silanized and non-silanized composites containing gold surface modified multilayered glass fiber woven fabrics.	89
Figure 4.60 EM wave absorption percentage varying with frequency in silanized and non-silanized composites containing gold surface modified multilayered glass fiber woven fabrics.	90

Figure 4.61 EM wave reflection loss varying with frequency in silanized and non-silanized composites containing gold surface modified multilayered glass fiber woven fabrics under the presence of a metallic backing plate.	91
Figure 4.62 EM wave reflection loss varying with frequency in silanized and non-silanized composites containing nickel surface modified multilayered glass fiber woven fabrics.....	92
Figure 4.63 EM wave transmission loss varying with frequency in silanized and non-silanized composites containing nickel surface modified multilayered glass fiber woven fabrics.....	92
Figure 4.64 EM wave absorption percentage varying with frequency in silanized and non-silanized composites containing nickel surface modified multilayered glass fiber woven fabrics.....	93
Figure 4.65 EM wave reflection loss varying with frequency in silanized and non-silanized composites containing nickel surface modified multilayered glass fiber woven fabrics under the presence of a metallic backing plate.	94
Figure 4.66 EM wave reflection loss varying with frequency in silanized and non-silanized composites containing gold surface modified multilayered aramid fiber woven fabrics.....	95
Figure 4.67 EM wave transmission loss varying with frequency in silanized and non-silanized composites containing gold surface modified multilayered aramid fiber woven fabrics.....	96
Figure 4.68 EM wave absorption percentage varying with frequency in silanized and non-silanized composites containing gold surface modified multilayered aramid fiber woven fabrics.....	97
Figure 4.69 EM wave reflection loss varying with frequency in silanized and non-silanized composites containing gold surface modified multilayered aramid fiber woven fabrics under the presence of a metallic backing plate.	98
Figure 4.70 EM wave reflection loss varying with frequency in silanized and non-silanized composites containing nickel surface modified multilayered aramid fiber woven fabrics.....	99

Figure 4.71 EM wave transmission loss varying with frequency in silanized and non-silanized composites containing nickel surface modified multilayered aramid fiber woven fabrics.	99
Figure 4.72 EM wave absorption percentage varying with frequency in silanized and non-silanized composites containing nickel surface modified multilayered aramid fiber woven fabrics.	100
Figure 4.73 EM wave reflection loss varying with frequency in silanized and non-silanized composites containing nickel surface modified multilayered aramid fiber woven fabrics under the presence of a metallic backing plate.....	101
Figure 4.74 Comparison of measured and simulated EM wave reflection loss of gold surface modified 5-layered glass fiber woven fabric structure.	103
Figure 4.75 Comparison of measured and simulated EM wave transmission loss of gold surface modified 5-layered glass fiber woven fabric structure.	103
Figure 4.76 Comparison of measured and simulated EM wave absorption percentage of gold surface modified 5-layered glass fiber woven fabric structure.	104
Figure 4.77 Three-point bending test results of prototype composites containing silanized and non-silanized as-received glass fiber woven fabrics.	105
Figure 4.78 Three-point bending test results of prototype composites containing silanized and non-silanized gold surface modified glass fiber woven fabrics.	107
Figure 4.79 Three-point bending test results of prototype composites containing silanized and non-silanized nickel surface modified glass fiber woven fabrics.	107
Figure 4.80 Three-point bending test results of prototype composites containing silanized and non-silanized as-received aramid fiber woven fabrics.	108
Figure 4.81 Three-point bending test results of prototype composites containing silanized and non-silanized gold surface modified aramid fiber woven fabrics.	109
Figure 4.82 Three-point bending test results of prototype composites containing silanized and non-silanized aramid surface modified aramid fiber woven fabrics. .	110
Figure 4.83 EM wave absorption percentage of the selected composites varying with frequency.....	112
Figure 4.84 EM wave reflection loss of selected composites varying with frequency.	112

Figure 4.85 Maximum flexural stress values achieved in 12 different composite types.	113
Figure A.1 EM wave reflection loss varying with frequency in silanized gold surface modified single layer glass fiber woven fabrics.	123
Figure A.2 EM wave transmission loss varying with frequency in silanized gold surface modified single layer glass fiber woven fabrics.	124
Figure A.3 EM wave reflection loss varying with frequency in silanized gold surface modified multilayered glass fiber woven fabrics.	124
Figure A.4 EM wave transmission loss varying with frequency in silanized gold surface modified multilayered glass fiber woven fabrics.	125
Figure A.5 EM wave absorption percentage varying with frequency in silanized gold surface modified multilayered glass fiber woven fabrics.	125
Figure A.6 EM wave reflection loss varying with frequency in silanized gold surface modified multilayered glass fiber woven fabrics with backing metallic plate.....	126
Figure A.7 EM wave reflection loss varying with frequency in silanized nickel surface modified single layer glass fiber woven fabrics.	127
Figure A.8 EM wave transmission loss varying with frequency in silanized nickel surface modified single layer glass fiber woven fabrics.	128
Figure A.9 EM wave reflection loss varying with frequency in silanized nickel surface modified multilayered glass fiber woven fabrics.	128
Figure A.10 EM wave transmission loss varying with frequency in silanized nickel surface modified multilayered glass fiber woven fabrics.	129
Figure A.11 EM wave absorption percentage varying with frequency in silanized nickel surface modified multilayered glass fiber woven fabrics.	129
Figure A.12 EM wave reflection loss varying with frequency in silanized nickel surface modified multilayered glass fiber woven fabrics with backing metallic plate.	130
Figure A.13 EM wave reflection loss varying with frequency in silanized gold surface modified single layer aramid fiber woven fabrics.	131
Figure A.14 EM wave transmission loss varying with frequency in silanized gold surface modified single layer aramid fiber woven fabrics.	132

Figure A.15 EM wave reflection loss varying with frequency in silanized gold surface modified multilayered aramid fiber woven fabrics.	132
Figure A.16 EM wave transmission loss varying with frequency in silanized gold surface modified multilayered aramid fiber woven fabrics.	133
Figure A.17 EM wave absorption percentage varying with frequency in silanized gold surface modified single layer aramid fiber woven fabrics.	133
Figure A.18 EM wave reflection loss varying with frequency in silanized gold surface modified multilayered aramid fiber woven fabrics with backing metallic plate.	134
Figure A.19 EM wave reflection loss varying with frequency in silanized nickel surface modified single layer aramid fiber woven fabrics.	135
Figure A.20 EM wave transmission loss varying with frequency in silanized nickel surface modified single layer aramid fiber woven fabrics.	136
Figure A.21 EM wave reflection loss varying with frequency in silanized nickel surface modified multilayered aramid fiber woven fabrics.	136
Figure A.22 EM wave transmission loss varying with frequency in silanized nickel surface modified multilayered aramid fiber woven fabrics.	137
Figure A.23 EM wave absorption percentage varying with frequency in silanized nickel surface modified multilayered aramid fiber woven fabrics.	137
Figure A.24 EM wave reflection loss varying with frequency in silanized nickel surface modified multilayered aramid fiber woven fabrics with backing metallic plate.	138
Figure A.25 EM wave reflection loss comparison of five layer nickel surface modified glass fiber structure and its simulation.	139
Figure A.26 EM wave transmission loss comparison of five layer nickel surface modified glass fiber structure and its simulation.	140
Figure A.27 EM wave absorption percentage comparison of five layer nickel surface modified glass fiber structure and its simulation.	140
Figure A.28 EM wave reflection loss comparison of five layer gold surface modified aramid fiber structure and its simulation.	141
Figure A.29 EM wave transmission loss comparison of five layer gold surface modified aramid fiber structure and its simulation.	141

Figure A.30 EM wave absorption percentage comparison of five layer gold surface modified aramid fiber structure and its simulation.	142
Figure A.31 EM wave reflection loss comparison of five layer nickel surface modified aramid fiber structure and its simulation.	142
Figure A.32 EM wave transmission loss comparison of five layer nickel surface modified aramid fiber structure and its simulation.	143
Figure A.33 EM wave absorption percentage comparison of five layer nickel surface modified aramid fiber structure and its simulation.	143

CHAPTER 1

INTRODUCTION

As electromagnetic technology advances, various systems transferring data between terminals have become common in engineering applications. Various systems utilizing electromagnetic (EM) waves with different service frequencies are being used widespread in wireless communication, satellite broadcasting, medical treatment and military applications etc. Interference of EM waves emitted from different sources constitutes problems related to information loss and misinterpretation of the data transferred. In order to eliminate electromagnetic interference (EMI), to reduce radar cross-section and provide operational security to EM wave based systems, electromagnetic shielding and/or absorber materials have been developed. For this purpose, conventionally EM wave absorbing structures or lossy coatings are integrated to the structural elements as additional components. Problems related to weight and thickness increase are considered as the major disadvantage of classical EMI shielding approaches [1]. In order to minimize performance loss due to conventional EMI shielding methods, development of novel EM wave absorbing structural materials is essential. In EM wave absorption applications, simultaneous absorption of electric and magnetic fields is expected to provide higher attenuation, and thus higher power loss due to electromagnetic absorption.

Alternatively, electromagnetic energy can be dissipated by destructive interference of reflected EM waves with certain frequency from reflective surfaces. Such arrangements like Salisbury screens have been used in the past [2]. However, obligation to cover a wide frequency range for EM wave absorbing materials arose following the development of multi-frequency devices. In order to provide broadband effectiveness multilayered methods such as Jaumann absorbers and Dallenbach layers

have been developed. Main disadvantage of such EM wave absorption structures were reported as the problems due to extra weight and oversized thickness [1].

In this study, based on the novel approach emerged from our research group development of multilayered reinforcement structures for EM wave absorption capable glass fiber reinforced polymer (GFRP) and aramid fiber reinforced polymer (AFRP) matrix composites have been discussed. GFRP and AFRP composites are widely utilized in structural applications due to the advantages they possess such as high specific material properties, toughness and damping capacity [3]. They are typically used in mobile structures and energy harvesting devices such as wind turbines. Ultimate aim of the study is to achieve EM wave absorbing structural composites of reasonable thickness and weight. In the scope of our novel approach, electromagnetic energy dissipation is provided by controlling electrical properties of fiber glass and aramid woven fabric layers via modifying their surfaces with metallic thin films. Thermal evaporation technique was used for the application of metallic thin films with a thickness from 15 to 35 nm. Gold, nickel and silver were used as target materials for being conductive, diamagnetic and/or ferromagnetic, which can easily be charged by the electric and magnetic field applied simultaneously.

Electromagnetic properties of surface-modified woven glass and aramid fabric layers and PET sheets were characterized in 18 – 40 GHz (IEEE K and K_a band) range by “free – space” method [4]. Considering fundamental principles of EM wave absorbing structures, surface-modified single layer samples were cascaded according to increasing intrinsic impedance to form multilayered reinforcement structures. Enhancement in EM wave absorption characteristic via utilization of intrinsic loss mechanisms and multilayer effect has been achieved resulting in the absorption of more than 90% of the incident EM wave energy. Mechanical tests have been conducted on composite samples revealing 90% EM wave energy absorption; in order to examine the mechanical strength, and hence the structural capability of the developed EM wave absorber GFRP and AFRP composites. Consequently, multilayered reinforcement structure with high electromagnetic energy absorption potential has been obtained for GFRP and AFRP applications.

CHAPTER 2

LITERATURE REVIEW

In this chapter, information about electromagnetic (EM) spectrum and electromagnetic waves, their applications in broadband, their interactions with materials will be met, basically. Material interactions of EM waves will be discussed over electromagnetic loss mechanisms. Additionally, characterization method for determining EM characteristics, free-space method and its mathematical background will be introduced. Finally, basic EM wave absorber materials given in literature and their applications will be explained.

2.1 Electromagnetic Spectrum and Electromagnetic Waves

The term electromagnetic spectrum corresponds to electromagnetic radiation for all frequencies; and, electromagnetic radiation is caused by moving photons which carry energy and act as both waves and particles. The first discovery of electromagnetic radiation was done by William Herschel and electromagnetic radiation was correlated to electromagnetism by Michael Faraday. After these developments, fundamental laws of electromagnetism was first propounded by James Clerk Maxwell with mathematical expressions. These expressions are Gauss' law, Faraday's law and Ampere's law. According to Maxwell's equations, it can be said that varying electrical fields generates changes in magnetic fields in free-space or change in magnetic field constitutes variations in electric fields and these variations in electric and magnetic fields are perpendicular to each other [5]. Besides all these, analysis of Maxwell on speed of variations in electric and magnetic fields caused Maxwell to think electromagnetic waves should travel at known speed of light. This thought was experimented and supported by studies of Heinrich Hertz. These findings lead to much known equation:

$$c = \lambda f \quad (2-1)$$

where (c) is the known speed of light, $3,00 \times 10^8$ m/s, (f) is frequency and (λ) is wavelength. Application of this formula to all frequencies gives the electromagnetic spectrum which can be seen in Figure 2.1.

In free-space, EM waves carry energy associated with magnetic field and electric field. This energy is carried by photons and energy (E) of photons can be stated with equation (2-2), where (h) is the Planck's constant, $6,63 \times 10^{-34}$ J.s.

$$E = \frac{hc}{\lambda} \quad (2-2)$$

This equation demonstrate that EM waves with shorter wavelength carry higher energy or, similarly, EM waves with lower frequency have lower energy.

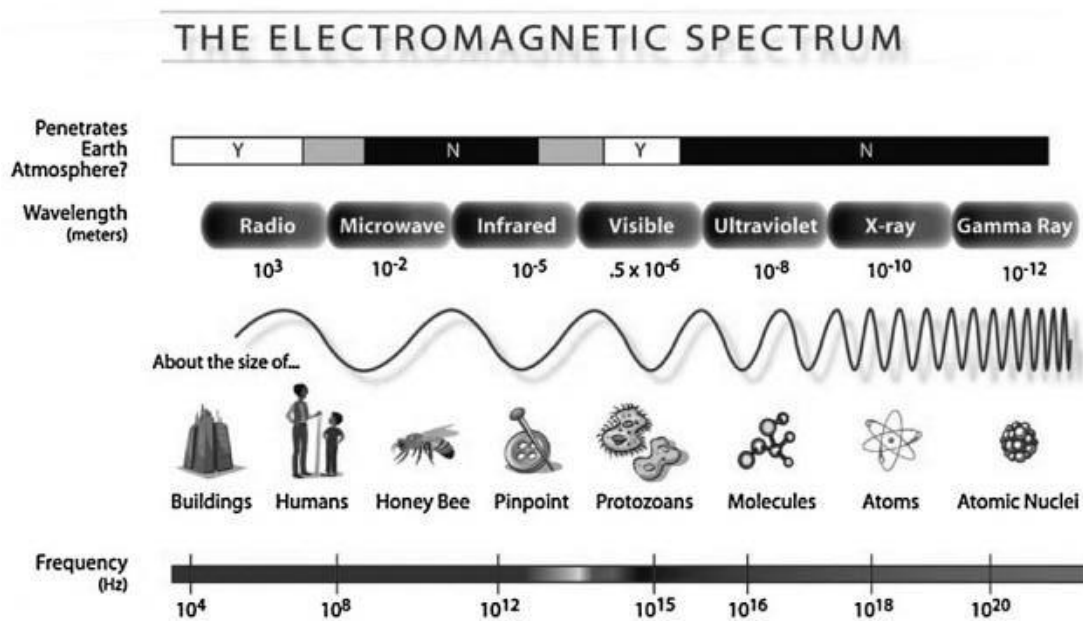


Figure 2.1 Electromagnetic spectrum [6].

EM waves can be produced by natural events or electronic devices and can be transmitted from one point to another in space. Possibility of EM waves to complete the transmission is about the energy and wavelength of EM waves. In free-space, it is possible to transmit the EM waves to any point; however, conditions in atmosphere prevent this behavior of EM waves. There is an atmospheric opacity which has different permittivity levels for different wavelengths. Beside that atmospheric opacity prevents harmful electromagnetic radiations to reach earth, it specifies the frequency of electronic devices working on. Atmospheric opacity for whole EM spectrum can be seen in Figure 2.2. This figure explains that the reason of using microwave frequency on electronic devices, satellites, cell phones, radars etc.

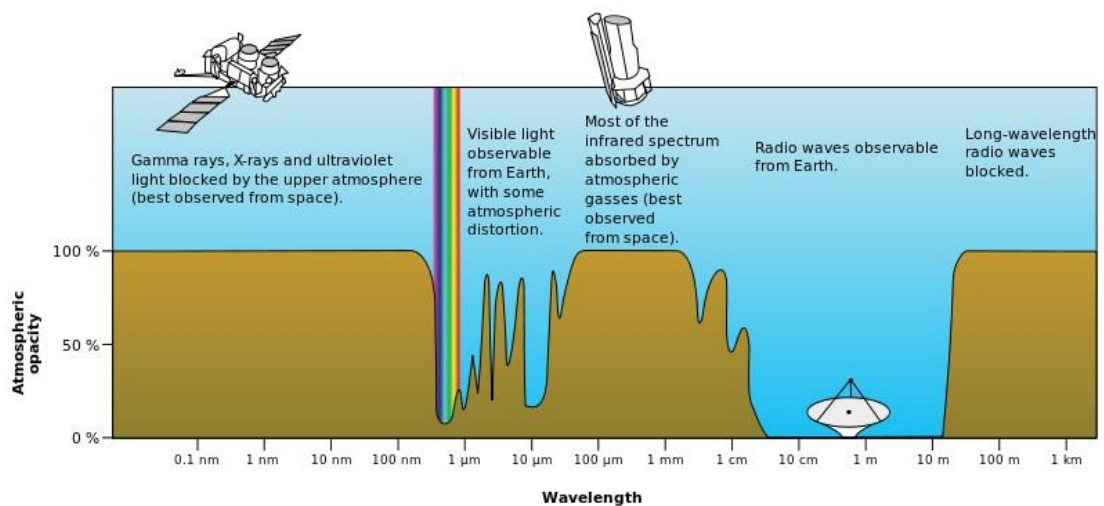


Figure 2.2 Atmospheric opacity [7].

2.2 Microwave Frequency and Applications

Microwave frequency corresponds to frequency range between 300 MHz and 300 GHz [8]. This frequencies are equal to wavelengths between 1 mm and 1 m.

Nowadays, electronic devices operates with using microwave frequency, generally. Because of atmospheric opacity which is mentioned previously and required precision,

microwave frequency is the best option for electronic devices to operate. In today’s world, communication devices, satellites, aerospace applications, radars, wireless devices, mobile phones, military applications, medical applications etc. are being operated in microwave frequency. All of these devices works in different frequency bands of microwave frequency. This classification can be seen in Figure 2.3. As number of electronic devices increase, interference of EM waves is inevitable. Interference of EM waves cause misinterpretations, miscommunications, wrong weather forecasts, wrong monitoring etc. In order to solve this problem, electromagnetic shielding is necessary. This study introduces electromagnetic interference (EMI) shielding or EM wave absorber for K and K_a (18-40 GHz) band.

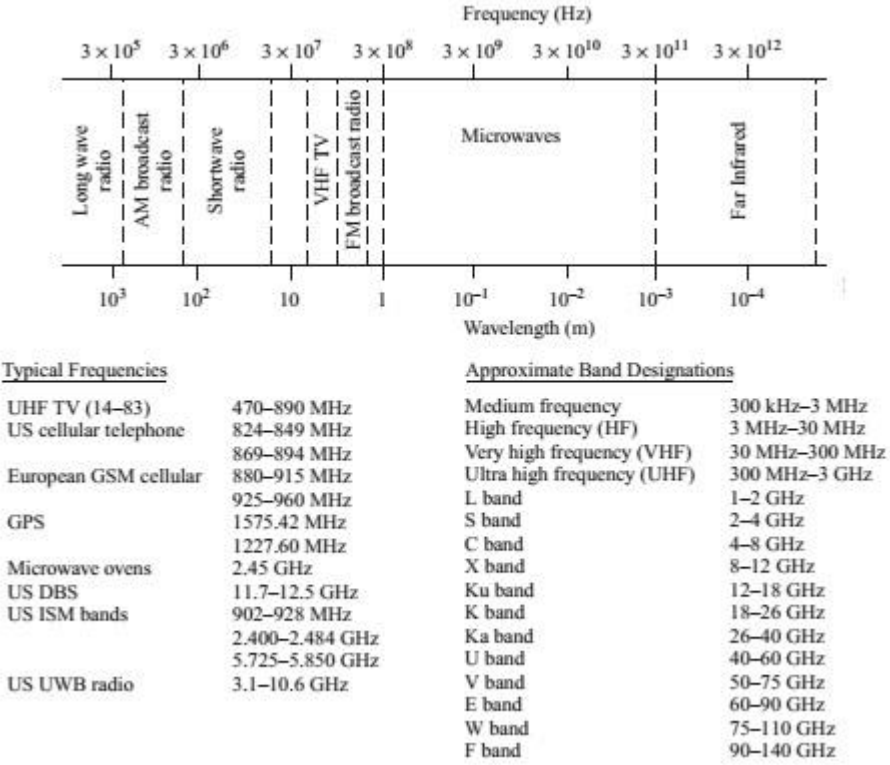


Figure 2.3 Microwave frequency applications and frequency bands [8].

2.3 Electromagnetic Wave – Material Interactions

EM waves spreading throughout the space can be encountered by any matter. Energy or power of EM waves decrease when they interact with any other EM wave or matter. Interactions of different electric fields and magnetic fields is the reason of energy decrease for EM waves. When EM waves are confronted by matter or other EM waves, they can act in three behavior; reflection, transmission and absorption. Due to the conservation of energy, initial energy must be equal to the final energy of system. Therefore, power of reflection, transmission and absorption of EM waves after confrontation must be equal to initial power of EM waves. This leads to equation (2-3). In equation P_0 , P_R , P_T , P_A represent initial power, power of reflected part, power of transmitted part and power of absorbed part, respectively. EMI shielding materials and EM wave absorber materials are being designed according to this rule. In this study, power of reflection and transmission parts was tried to be attenuated; in order to increase the absorption of EM waves. This is only possible with utilization of electromagnetic loss mechanisms.

$$1 = \frac{P_R}{P_0} + \frac{P_T}{P_0} + \frac{P_A}{P_0} \quad (2-3)$$

2.3.1 Mechanisms of Electromagnetic Loss

Basic principle for electromagnetic wave absorbing is to restrain the EM wave in absorber materials. EM wave energy can be absorbed by absorber materials with conversion of energy. According to conservation of energy principles, non-reflected and non-transmitted EM energy must be converted to other energy forms. Because of the fact that EM energy is the combination of electrical and magnetic energy, EM energy can be transformed to electrical and magnetic energy forms in EM wave absorber materials, easily. This is possible with adjusting absorber materials' electrical and magnetic properties for appropriate frequency range. Therefore; absorber characteristics can be achieved by the utilization of dielectric loss and magnetic loss.

2.3.1.1 Dielectric Loss

Dielectric material, as a definition, is electrical insulator can be polarized in the presence of electric field. Polarization can be described as alignment of electric dipoles with the applied field. This process needs force to rotate the dipoles [9]. Dielectric loss in materials is composed of three types of loss mechanism; conductance loss, dielectric relaxation loss and resonance loss [5].

- Conductance Loss

Electrical conductance is the results of moving free electrons in materials. For conductive materials, applied electric field is sufficient to change positions of electrons; however, dielectric materials are not capable of that due there is not sufficient free electrons. Because of this, dielectric materials have limited conductivity.

In this study, surface modification generates conductive layer on the surface of woven fabrics. This means that EM waves met with surface modified woven fabrics will be confronted by resistance of conductive layer.

- Dielectric Relaxation Loss

Dielectric relaxation means the delay in response of dipole polarization due to changing electric field. Dipole rotation is a more time dependent and slower movement compared to variations in electric field with higher frequency [10]. Therefore, when material interacts with higher frequency EM waves, dipoles cannot respond as fast as frequency change. This results in change in dielectric constant of materials and leads to change in polarization types which are frequency dependent [9].

- Resonance Loss

When natural oscillation frequency of atoms, ions and electrons in materials meet with the electric or magnetic field has same frequency, absorption occurs [10].

2.3.1.2 Magnetic Loss

Magnetism is a phenomenon of materials' behaviors when there is applied magnetic field. Number of unpaired electrons determine the magnetism type in materials. Materials have balanced magnetic spins are diamagnetic materials and materials have unpaired electrons; that results in unbalanced magnetic spin, are paramagnetic materials. There is third kind of magnetism; ferromagnetism. Ferromagnetic materials, like paramagnetic materials, have unpaired electrons but their magnetic moments stands parallel to applied magnetic field [9].

- Eddy Current Loss

Eddy current, as a definition, electric currents that is formed by variation of applied magnetic field on conducting materials. [11]. The principle of eddy current loss mechanism is to produce a current in material that opposes the applied magnetic field. Eddy current loss can be increased by increasing the thickness of sheet materials [10]. Moreover, eddy current loss can be affected by grain size, surface roughness and morphology [12, 13].

- Magnetic Hysteresis Loss

Irreversible magnetic domain movements and magnetic moment rotations cause magnetic hysteresis loss [11].

- Residual Loss

Residual loss is a frequency dependent loss mechanism. While thermal fluctuations and hysteresis of electrons in materials cause the residual loss at low frequencies, ferromagnetic resonance, domain wall resonance and size resonance result in residual loss at high frequencies. Residual loss can be adjusted by changing particle size and anisotropy of magnetic materials [11, 14].

2.4 Electromagnetic Wave Absorbing Materials

Main purpose of EM wave absorber materials is to limit EM energy in a specific area and specific value and to prevent its spreading [2]. Schematic of reflection,

transmission and absorption phenomena which created by the interaction of EM waves and materials can be seen in Figure 2.4. A material to be used as EM wave absorber should suppress or scatter the incident EM waves. This is possible with electromagnetic loss mechanisms explained before. Basic properties that defines the interaction between EM wave absorber and EM waves are related with absorbers' magnetic and electric permittivities and impedances (Z_m) [15]. EM wave absorbers can be classified as radar absorber materials (RAM), electromagnetic interference shielding (EMI), noise suppression materials and materials used in high frequency communication.

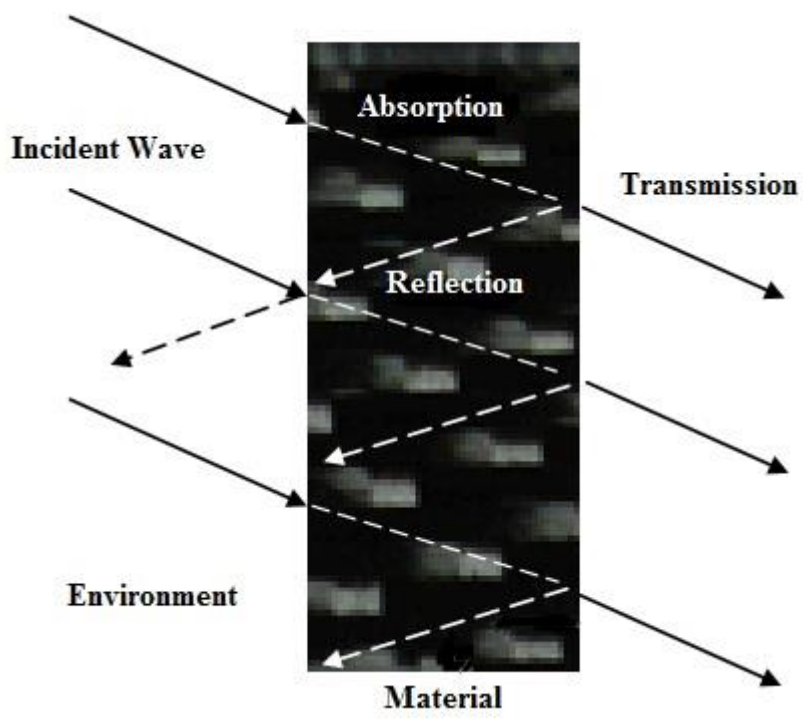


Figure 2.4 Schematic of interaction between EM wave and material.

In today's technology, working principle of radar is based on pulse that is first broadcasted by a transmitter, then, reflected by a target and finally, caught by a receiver. Receiver can detect the direction, velocity, position of target by analyzing

reflected EM wave. There are two possible way to suppress the reflection from target; changing the geometry of target in order to scatter the EM waves to other directions or decreasing reflected energy by absorbing EM waves [16]. Studies show that changing the geometry of target influences aerodynamics of target and decrease its efficiency, negatively. Therefore, studies about EM wave absorber composites are being increased due to weight, low environmental resistance and low mechanical properties of monolithic materials [17, 18, 19]

RAMs are designed to become a stealthy for radars by reducing radar cross-sectional area (RCS) of an assault or defending systems [1]. Insulator composites, conductive particle infused polymers and ceramics and ferrites are being used as RAMs [20, 21, 22, 23] Dielectric, metallic, carbon, ferrite powder or fiber dispersed composite materials can be applied to surfaces in form of paint or tiles. Moreover, ferrite type materials can be used in form of furnaced tiles as RAMs [24, 25, 26, 27, 28].

Absorption capability of all mentioned materials is related with thickness, geometry, surface topography, amount of additive part in RAMs, size and interaction between each of them. Superior radar absorbing materials requires to be light, practical, cost effective and resistant to heat, moisture and impurity erosion.

Composites of metallic and non-metallic particle (silver, carbon etc.) dispersed in polymeric resin matrix [29, 21, 30, 31] or composites reinforced with stainless steel and carbon fiber [32, 33, 34, 35, 36] are used as EM wave absorbers in different frequency ranges. Moreover, particles like ferrite and nickel providing magnetic losses are being used as EM wave absorber reinforcement materials [29, 18, 37].

First developed RAM is known as “Salisbury Screen”. In this type of RAMs, porous graphite added thin material is placed over metallic backing plate with distance of quarter of wavelength ($\lambda/4$). According to transmission line theory, metallic plate which placed quarter of any wavelength away from lossy material creates efficient open circuit on lossy material. In this situation, incident wavelength behaves like in free-space and reflection cannot take place. This results in absorption of incident EM energy.

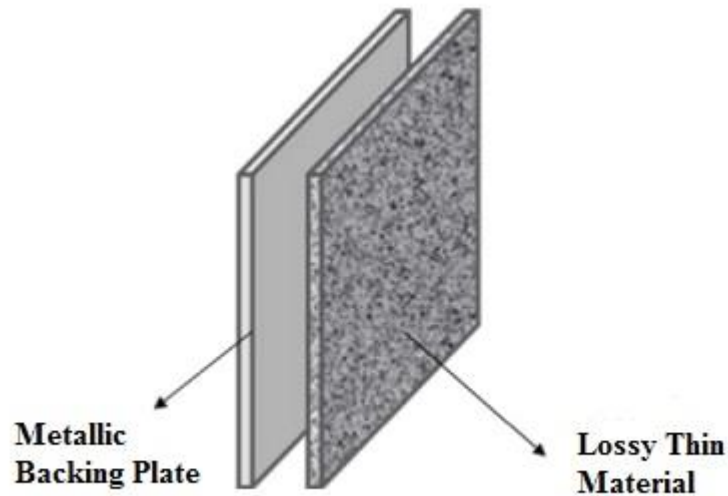


Figure 2.5 Schematic model of “Salisbury Screen”.

When distance between plate and lossy material is not quarter of wavelength, incident wave is encountered by an impedance parallel to resistance of plate. This impedance is different than impedance of free space; therefore, part of incident wave reflects. In situations like this, as deviation increases, undesired reflection increases. For this reason, “Salisbury Screen” works in narrow frequency range, this makes it not useful for RAM.

Increase of efficient frequency range can be possible with graded arrangements of more than one lossy thin materials. Resistance of each lossy material gradually decreases as getting closer to metallic backing plate in this system. This system is known as “Jaumann Absorber” in literature. Addition of each layer increases the efficient frequency range; however, thickness of system also increases [1]. This affects practicality and cost negatively; therefore, this type of absorbers generally does not preferred.

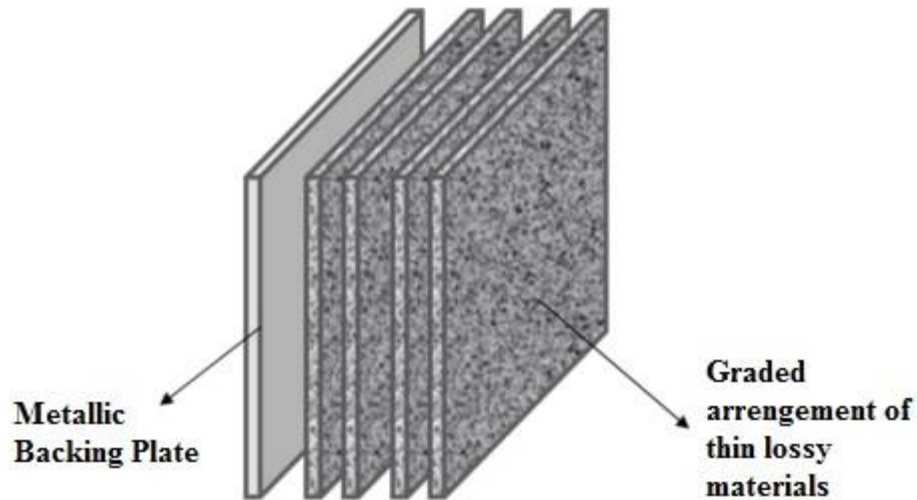


Figure 2.6 Schematic model of Jaumann Absorber.

In order to obtain tapered transmission loss, graded absorbers are being used. In this type of absorbers, energy of incident wave is decreased systematically within the structure. Strong reflections from materials' surfaces are prevented by the gradual difference of interface between air and metal. Graded absorbers can be produced by filling geometries like pyramids are filled with lossy dielectric materials and tapered line absorbers [5].

In the light of literature, development and design of EM wave absorbers should consist of lightweight, cost effectiveness, operating in broadband frequency range, acceptable mechanical strength. In this context, it is determined in studies [5, 38] that surface modified fiber woven fabrics can be used as polymer matrix composite structures. In this study, application and efficiency of surface modified fiber woven fabrics in polymeric composite structures was improved with the help of literature.

CHAPTER 3

EXPERIMENTAL PROCEDURE

3.1 Materials and Surface Modification Treatment

Reinforcement materials used in this study were Quadriaxial ($0^\circ / \pm 45^\circ / 90^\circ$ reinforcement angles) woven glass fabrics (METYX[®], Telateks Textile Products, Co., Ltd., Istanbul, Turkey), aramid fiber woven fabrics and PET sheets [39]. Secondly, in order to measure the electrical conductivities of applied thin films, coverglass substrates were used, and in order to characterize thin film structures single crystal silicon wafers were used. Metals to be used for surface modifications were gold, nickel and silver and their purity levels were %99.99, %99.99 and %99.9, respectively.

Surface modifications of two different types of woven fabrics, PET sheets, coverglass substrates and silicon wafers were done using thermal evaporation technique with different coating parameters applied for each metal. Gold was coated with 74.0 A evaporation current and 0.15 Å/s evaporation rate in the 1.5×10^{-6} torr chamber vacuum. Nickel was coated with 80.4 A evaporation current and 1.10 Å/s in the 2.5×10^{-6} torr chamber vacuum. Finally, silver was coated with 44.2 A evaporation current and 1.36 Å/s in the 4×10^{-6} torr chamber vacuum. Using same parameters for all thermal evaporations, glass and aramid fiber woven fabrics were modified with 15, 20, 25, 30 and 35 nm thick gold, nickel and silver thin films. Because of the restrictions in thermal evaporation system, size of surface modified reinforcement materials was limited to 70×70 mm.

In order to examine the surface topography dependence of EM absorption characteristics, PET sheets were modified with gold layers having four different thickness: 15, 20, 25 and 30 nm. Additionally, in order to examine the morphology

and microstructure of gold thin films, silicon wafers were modified with gold layers having three different thickness: 15, 20 and 25 nm.

3.2 Surface Modification & Thin Film Characterization

Structural characterization of surface modified glass fiber (GF) and aramid fiber (AF) woven fabrics under scanning electron microscope (SEM) and atomic force microscope (AFM) were almost impossible because thin layer of gold on GF and AF was charging under SEM and rough surface of fiber woven fabrics prevented the AFM imaging and thin film XRD scanning. Therefore, sample characterizations were done on silicon wafers that are modified with 15, 20, 25 nm thick gold thin films.

3.2.1 Characterization with FESEM

Surface modifications on silicon wafers, 15 nm, 20 nm and 25 nm thick gold thin films were monitored with field emission scanning electron microscope (FESEM). Electromagnetic properties of thin films can be developed and controlled by film continuity, grain size and distribution. Therefore, film continuity and grain size and morphology were examined under FESEM. FESEM photos taken were classified in two groups based on the position on the thin film applied substrate surface, namely as “from edge of thin film” and “from center of thin film”. While film continuity and morphology were observed on FESEM photos taken from the center of thin films, grain size was determined on FESEM photos taken from the edge of thin films.

3.2.2 Characterization with AFM

In order to support obtained data from FESEM and get more information about thin film morphology (AFM) was used. 15 nm and 25 nm thick gold thin films on silicon wafers were examined for grain size determination and film continuity.

There is a possibility of making wrong thickness measurement in thermal evaporation. In order to control the film thickness which was read from thermal evaporation device, real film thickness was measured with AFM. Using Stanley knife, a scratch was

opened on thin film surface with a little pressure without damaging the surface of the silicon wafer.

3.3 Composite Production

3.3.1 Silanization

Silane treatment is a chemical process used for improving the interaction between organic and inorganic phases. Mechanical properties of materials, especially composites, can be enhanced with the application of chemical bridges. In this study, aminopropyl trimethoxy silane (APS) was used in order to increase the mechanical strength of composites. APS was selected as silanization agent, because it provides efficient interaction with epoxy used as the matrix material in the composite structures of the current study. Structural formula of aminopropyl trimethoxy silane can be seen in Figure 3.1.

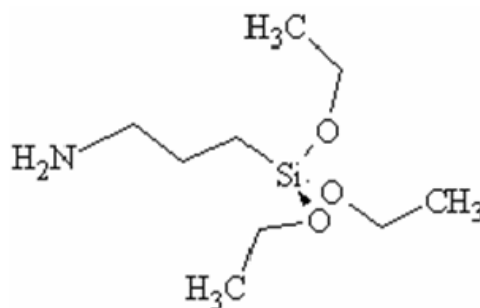


Figure 3.1 Structural formula of aminopropyl trimethoxy silane.

Silanization process takes place as a result of three chemical reactions; hydrolysis, condensation and hydrogen bonding. Hydrolysis reaction takes place in a specific pH environment via forming $-OH$ bonds by removing alcohol in order to provide bonding between silane molecule and inorganic surface. In condensation reaction, molecules

are united with each other to create larger molecules. Finally, hydrogen bonding takes place to join the organic side and the inorganic substrate surface. Schematics of these reactions can be seen in Figure 3.2.

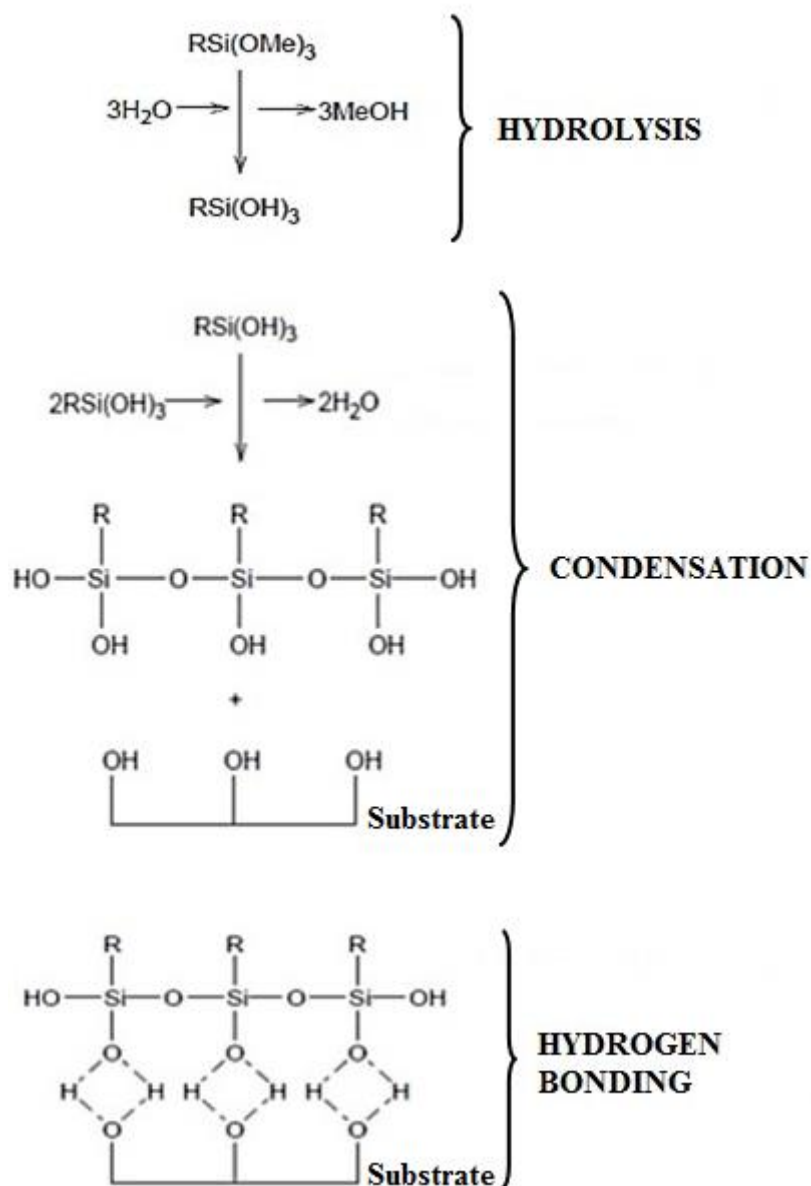


Figure 3.2 Schematics of chemical reactions taking place during silane treatment.

In this study, silanization was applied on surface modified glass and aramid fiber woven fabrics by spraying. Sprayed solution was prepared using the procedure explained below. pH of the solution of 95% alcohol – 5% distilled water was adjusted to value between 4.5 – 5.5 by adding acetic acid. 17 μ l APS was poured into liquid solution and obtained new solution was stirred for 90 minutes using magnetic stirrer. Hydrolysis reaction took place in the liquid solution. Then, the final solution was sprayed to surface modified woven fabrics with air brush. After this, in order condensation reaction to take place silane solution applied surface modified woven fabrics were held at 120 °C for 1 hour.

3.3.2 Prototype Composite Fabrication

Vacuum bagging method was selected as the polymer composite fabrication method. Vacuum bagging is a practical composite fabrication method which can provide the required pressure to hold reinforcement and matrix material together until the completion of curing.

In this study, firstly epoxy resin matrix was prepared by mixing epoxy and its special hardener in 74:26 weight ratio. Then, surface modified woven fabrics were wetted by epoxy resin one by one on a wax applied glass surface. Woven fabrics which were wetted by epoxy resin were stiffed together in order to obtain sandwich structures. Sandwich structures were closed with peel ply, air breather and vacuum bag. Obtained closed bag over the glass surface was sealed and inside of the bag was isolated from the environment. Bag was vacuumed for 3 hours by a rotary vacuum pump in order to apply the required pressure to the sandwich structure. After 3 hours the bag was opened and composite fabrication was ended by peeling the ply from the surface of the composites. Constructed system before the process of vacuum bagging can be seen in Figure 3.3.

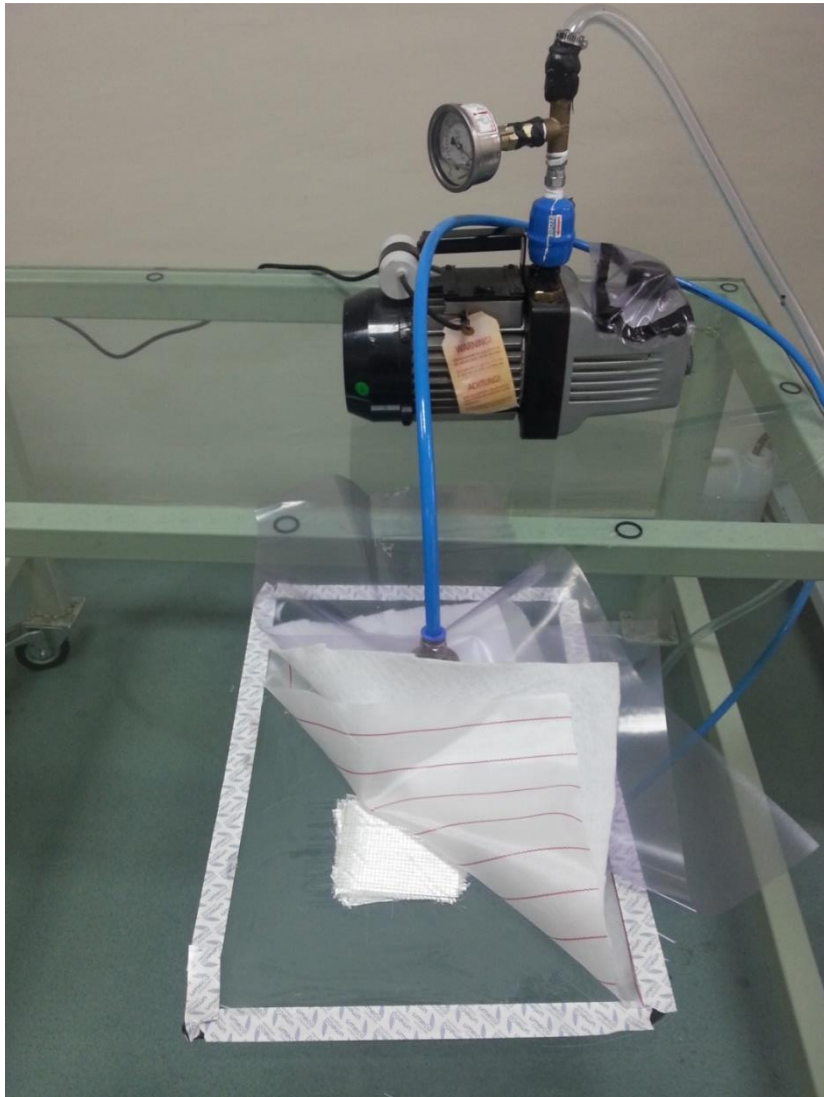


Figure 3.3 Constructed vacuum bagging system.

Composite fabricated by vacuum bagging which consist of aramid or glass fiber woven fabrics as the reinforcement material and epoxy as the matrix material can be seen in Figure 3.4. Moreover, cross-sectional views of these composite structures are also provided in Figure 3.5.

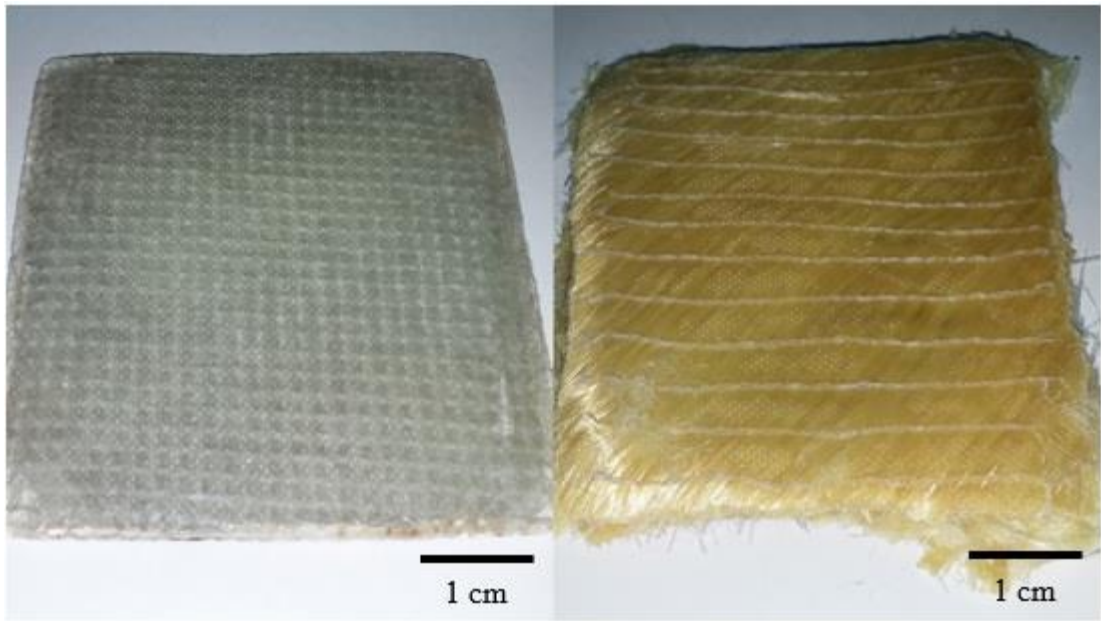


Figure 3.4 Photographs of fabricated composites without surface modifications.

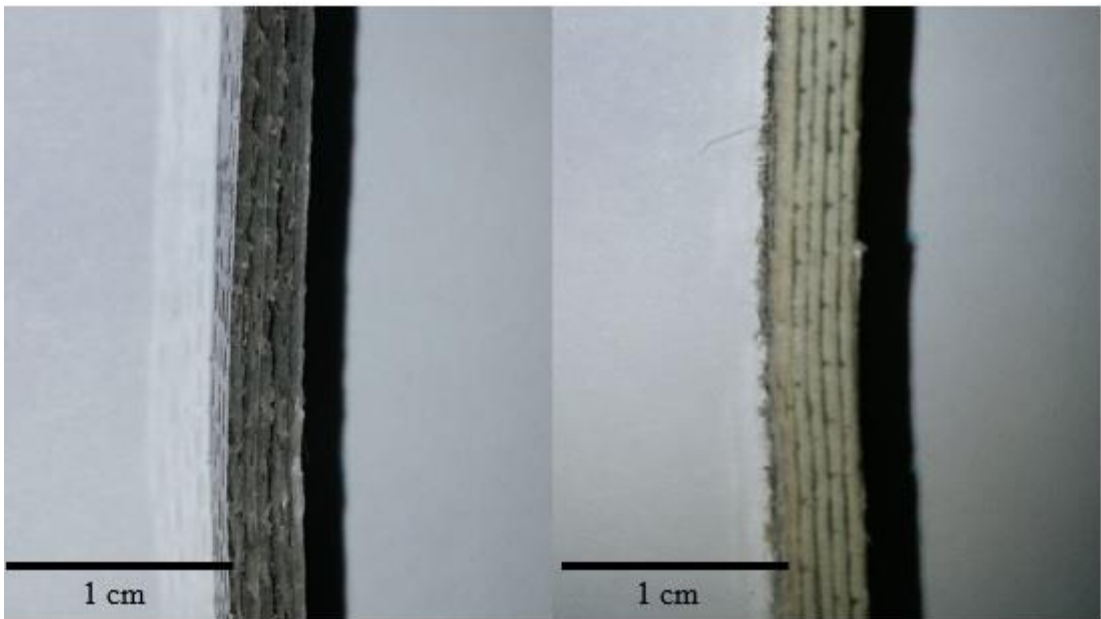


Figure 3.5 Cross-sections of composite structures without surface modifications.

3.4 Characterization of EM Wave Absorbers by Free-Space Method

EM waves travelling in free space is reflected when they encounter a medium with electrical parameters different than those of vacuum. Degree of electromagnetic reflection depends on the difference between intrinsic impedance of the medium (Z_m) and free-space impedance (Z_0) which is expressed by reflection coefficient, Γ [40]. Reflection coefficient can be obtained by Eqn. 3.1 and Eqn. 3.2

$$\Gamma = \frac{Z_m - Z_0}{Z_m + Z_0} \quad (3-1)$$

$$Z_m = Z_0 \sqrt{\frac{\mu_R}{\epsilon_R}} \quad (3-2)$$

where μ_R and ϵ_R are complex material properties known as complex permeability and complex permittivity, respectively. By combining Eqn.1 and Eqn.2, a hypothetical medium with equal complex permittivity and complex permeability results in an intrinsic impedance equal to free space impedance. In such a case, reflection coefficient becomes zero. Fabrication of materials or composite structures with comparable complex material properties provide low EM wave reflection required for certain applications.

Free-space method is a technique to characterize complex electromagnetic properties and EM wave reflection – transmission behavior of a medium with certain thickness. Main advantage of the free- space method is its applicability to inhomogeneous and/or anisotropic media [41]. Free-space measurement system consists of two different horn antennas and a lens system facing each other. Power generated by network analyzer transferred via coaxial cables and power waves are emitted and received by horn antennas. Condensing lenses focus emitted waves to an area on the sample surface. Network analyzer measures S-parameters i.e. both magnitude and phase of reflection and transmission coefficients from the ports as a function of frequency. Reflection coefficient related to the EM waves emitted from horn1 and reflected back to horn1 is

expressed as S11. Transmission coefficient related to the EM waves emitted from horn1 and transmitted to horn2 is expressed as S21. Reflection and transmission coefficients are called as S22 and S12 in the case of the second port, respectively.

Reflection loss (3-3) and transmission loss (3-4) are logarithmic descriptions of the ratio of the power reflected (P_R) or power transmitted (P_T) to total power supplied by the system (P_0), respectively. Ratio of the power neither reflected nor transmitted is absorbed by the sample which can be given by Eqn. (3-5) according to the principle of energy conservation.

$$R_{dB} = 10 \log \frac{P_R}{P_0} \quad (3-3)$$

$$T_{dB} = 10 \log \frac{P_T}{P_0} \quad (3-4)$$

$$\text{Absorption Percentage (\%)} = 100 \times \left(1 - \frac{P_R}{P_0} - \frac{P_T}{P_0} \right) \quad (3-5)$$

As received and surface-modified glass and aramid fiber woven fabrics were characterized by free-space method in 18 – 40 GHz frequency range. With this method reflectance and transmittance measurements of EM waves through a medium placed into certain opening was done. In order to eliminate environmental effects related to hardware line(1) – reflect – line(2) (LRL) calibration was applied and time domain gating was used. In line(1) calibration system is calibrated for direct EM wave passage. In reflection calibration two reflective faces of a metallic calibration block with a certain thickness is introduced. Line(2) calibration requires setting aperture value to the quarter wavelength (2.5 mm) of the central frequency of the frequency band to be tested, which is accepted as 30 GHz in this study, and application of a through calibration [42]. After calibration, measurements were done with respect to reference

planes of front face of the sample (port1) and back face of the sample (port 2). Reflection/Transmission losses (S_{11} , S_{22} , S_{21} , and S_{12}) and phase angles of reflecting/transmitting EM waves were evaluated by E26379 PNA Network Analyzer (Anritsu, Kanagawa, Japan) within IEEE K and Ka band.

Installation of Free-Space Method Setup:

There are several critical issues for the utilization of the free space measurement method in terms of the measurement system requirements. These can be given as keeping the specimens perpendicular to the propagation axis of electromagnetic waves which must be passing through the center of the specimen surface and aligning all components precisely in the measurement system parallel to each other. These conditions made it compulsory to custom-design and build a free-space measurement system which holds two antennas and two EM lenses along with the specimen on the same horizontal axis very precisely.

The antennas used in the free-space measurement system can be seen in Figure 3.6 where the dimensions of the antennas are given in Figure 3.7. Technical specification of the horn antennas are provided in Table 3.1.

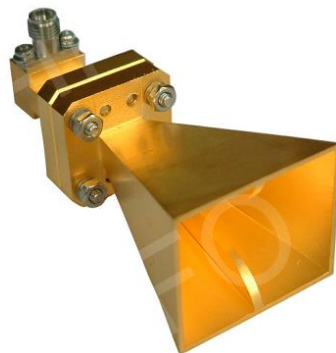


Figure 3.6 Horn antenna used in free-space measurement system.

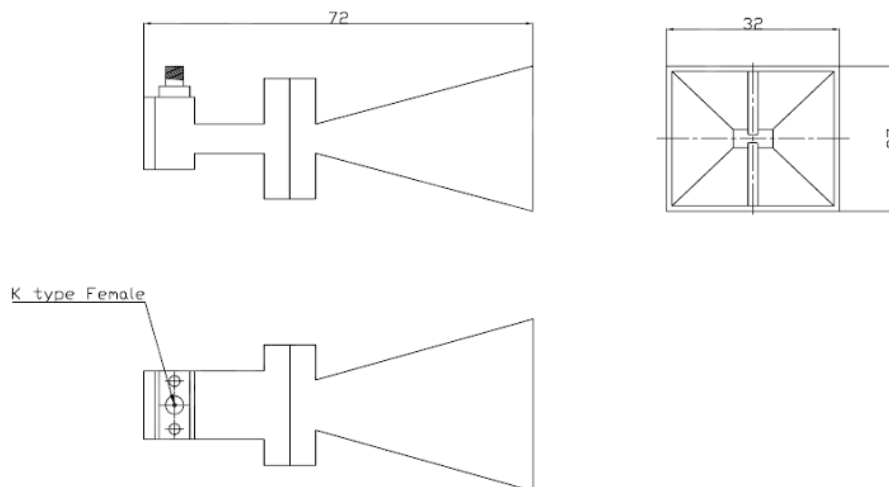


Figure 3.7 Schematic view of horn antennas used in free-space measurement system with their dimensions (dimensions are in unit of mm).

Table 3.1 Technical specification of horn antennas used in free-space measurement system.

Polarization	Linear
Frequency Range (GHz)	18-40
Gain (dBi)	14-18
Power Handling Capability (W)	10
VSWR	2:1 Typ.
Connector	K-Female
Size (mm)	32x27x72
Net Weight (Kg)	0.075 Around

In free-space measurement technique, polymeric lenses suitable for horn antennas must be designed and produced in order to create planar wave front for EM waves emitted from the horn antennas. Dimensions of polymeric lenses used in the free-space measurement system were calculated for 18-40 GHz frequency range which are given in Figure 3.8. For the custom-designed free-space measurement system w_{out} was determined as 17.9 mm, and f was determined as 62.05 mm (Figure 3.8). Using equation (3-6), and taking the dielectric constant (ϵ_r) of the polymeric material as 2.6 (supplied by the manufacturer), D and T were determined as 62.05 mm and 10.39 mm, respectively. According to these calculations, polymeric lenses were machined with CNC. Machined polymeric lenses used in the free-space measurement system can be seen in Figure 3.9.

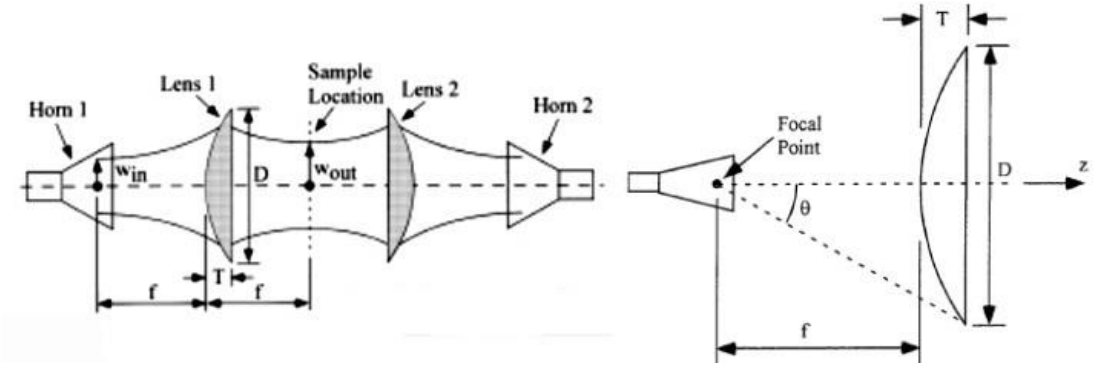


Figure 3.8 Schematic view of layout for free-space method and polymeric lenses with specific dimensions [43].

$$x^2+y^2 = (\epsilon_r-1)z^2+2f((\epsilon_r)^{1/2}-1) \tag{3-6}$$



Figure 3.9 Polymeric lenses used in free-space measurement system.

The free-space measurement system custom-designed to attach to the network analyzer through coaxial cables consisted of two antenna holders and two polymeric lens holders to surround and lock the antennas and lenses was machined from polyamide. Design layout of the free-space measurement system is provided in Figure 3.10. Custom-designed and built free-space measurement system and the utilized network analyzer can be seen in Figure 3.11.

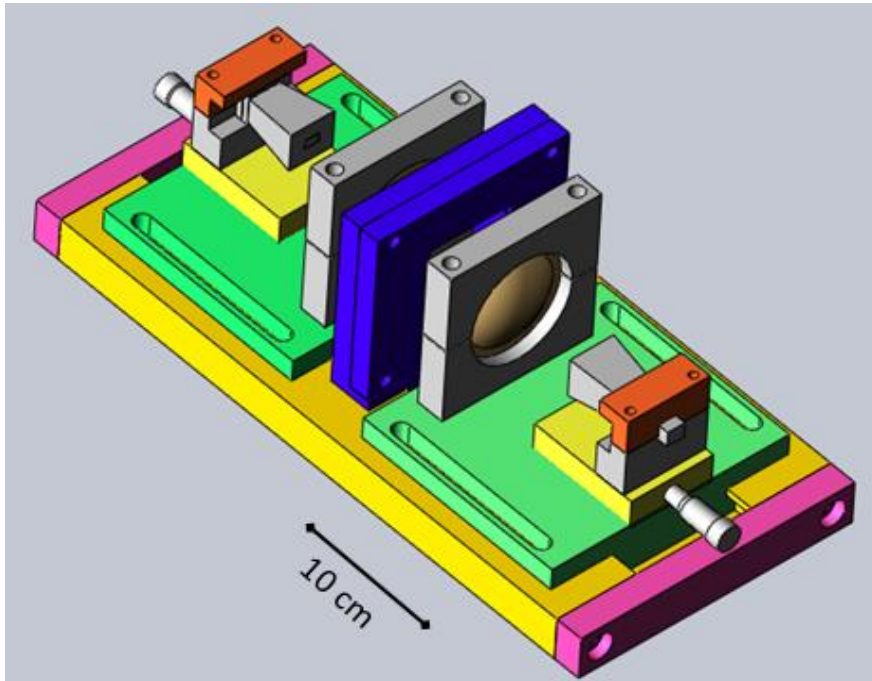


Figure 3.10 Isometric view of designed layout of Free-space method.



Figure 3.11 Custom-designed and built free-space measurement system and the utilized network analyzer.

3.5 Mathematical Simulation for Multilayer EM Wave Absorbers

EM wave absorption behavior of single layered and multilayered surface modified fiber woven fabrics were characterized with free-space method. In the light of the obtained results, know-how for suitable materials to be used in EM wave absorber composites has been gained. In addition to this, to be able to predict the EM behavior of multilayered structures, simulation studies were conducted. The purpose of simulation studies was to decrease the time and supplies to minimum level in designing the EM wave absorber structure.

Basics of this study rely on the prediction of EM behavior of multilayered structures and composites using known EM wave characteristics of the single layered structures. In this study, mathematical simulation was done by the commercial AWR Microwave Office software. Obtained EM wave characteristics of the single layered structures were inputted to the software database and desired multilayered structure was created by the software. Software calculated the EM wave characteristics of cascaded structures using the mathematical derivations of the S-parameters that have been measured using free-space method. Mathematical background of the simulation was explained in detail in reference [5].

During the study, simulation experiments were conducted frequently and the results, especially transmission characteristics, were found to be close to measured EM wave characteristics. However, it was seen that EM wave reflection characteristics obtained from simulation show significant differences compared to results obtained by the free-space method. On the other hand, EM wave absorption characteristics obtained from the simulation are satisfactory, and results close to measured ones were achieved.

3.6 Mechanical Testing of EM Wave Absorber Composites

Multilayered surface modified glass and aramid fiber woven fabrics with silane treatment revealing the highest EM wave absorption were used in composite fabrication. In order to determine the mechanical strength of the composite structures,

three point bending test was conducted. Epoxy was used as the matrix and surface modified glass and aramid fiber woven fabrics were used as reinforcement material in composites.

Mechanical testing was done on 36 composite samples of 12 different composite types. These 12 types of composites consisted of one single type of matrix material, two different types of reinforcement materials, two different types of surface modification metal with or without silanization. Classification of the fabricated composite samples is presented in Table 3.2.

Table 3.2 Composite samples used in three-point bending tests.

Type	Matrix	Reinforcement Material	Surface Modification Type	Silanization
Composite 1	Epoxy	Glass Fiber	None	Yes
Composite 2	Epoxy	Glass Fiber	None	No
Composite 3	Epoxy	Aramid Fiber	None	Yes
Composite 4	Epoxy	Aramid Fiber	None	No
Composite 5	Epoxy	Glass Fiber	Gold	Yes
Composite 6	Epoxy	Glass Fiber	Gold	No
Composite 7	Epoxy	Aramid Fiber	Gold	Yes
Composite 8	Epoxy	Aramid Fiber	Gold	No
Composite 9	Epoxy	Glass Fiber	Nickel	Yes
Composite 10	Epoxy	Glass Fiber	Nickel	No
Composite 11	Epoxy	Aramid Fiber	Nickel	Yes
Composite 12	Epoxy	Aramid Fiber	Nickel	No

Size of the composite structures was limited to 70×70 mm due to the restrictions of the thermal evaporation chamber used for the surface modification of the reinforcement materials. According to ASTM D-790 standard, thickness-to-span length ratio of samples to be subjected to three point bending tests should be between 1:16 and 1:40 [44]. Therefore, 12 different composite structures were cut by water jet to obtain 3 mechanical test specimens from each type according to ASTM D-790 standard. Due to the limitations in composite fabrication, thickness-to-span length ratio of some composite samples could not be cut in required dimensions. However, this did not have a remarkable effect on the comparison of the mechanical strengths of the composites. Dimensions of 36 three point bending test specimens for 12 different composite types are given in Table 3.3.

Table 3.3 Dimensions of 36 three point bending test specimens.

Type	Width	Thickness	Span Length	Type	Width	Thickness	Span Length
1	13.50	3.50	56.00	7	12.75	3.70	59.20
	13.42	3.61	57.76		13.15	3.90	60.00
	13.70	3.77	60.00		12.20	3.80	60.00
2	13.30	4.78	60.00	8	12.70	3.00	48.00
	13.45	4.80	60.00		13.60	3.00	48.00
	12.82	4.79	60.00		13.50	3.00	48.00
3	13.56	4.20	60.00	9	13.05	3.40	54.40
	13.48	4.12	60.00		12.95	3.40	54.40
	13.34	4.19	60.00		12.50	3.40	54.40
4	13.40	4.25	60.00	10	12.70	3.10	49.60
	13.10	3.80	60.00		12.90	3.15	50.40
	13.60	4.35	60.00		12.90	3.15	50.40
5	13.25	4.15	60.00	11	11.70	3.10	49.60
	13.50	4.10	60.00		12.90	3.10	49.60
	13.10	4.10	60.00		12.40	3.10	49.60
6	13.30	4.40	60.00	12	14.30	2.90	46.40
	13.50	3.90	60.00		13.30	2.80	44.80
	13.25	4.10	60.00		13.00	2.80	44.80

CHAPTER 4

RESULTS AND DISCUSSION

4.1 Surface Modification and Electrical Conductivity of Thin Films

Gold, nickel and silver metals were coated on cover glass substrates as thin films in this study in order to measure the surface electrical conductivity of thin films in different thicknesses. Thickness of metallic films; hence, electrical conductivities are related with electromagnetic (EM) behaviors in the way that has been explained in Chapter 2 under electromagnetic loss mechanisms. Cover glass surfaces were modified with silver (Ag), gold (Au) and nickel (Ni) and metals with thickness 15 nm, 20 nm and 25 nm using thermal evaporation technique. These thin films' electrical conductivities were measured using two probe technique [45]. Results can be seen in both Table 4.1 and Figure 4.1 Electrical conductivity of Ag, Au, Ni thin films with changing film thickness.. As it can be seen, increasing film thickness results in increasing electrical conductivity. In addition, as the metallic film gets thicker, its surface electrical conductivity approaches to that of the bulk given in the literature. However, none of them shows as high electrical conductivity as that of their bulk version. System resistances in the two probe technique can be the reason of this difference; however, the main reason is that as the film thickness decreases its impedance increases [46].

Table 4.1 Electrical conductivity of Ag, Au, Ni thin films with changing thickness.

Film Thickness	Ag	Au	Ni
15 nm	6.1×10^6 S/m	4.0×10^6 S/m	8.3×10^5 S/m
20 nm	9.1×10^6 S/m	8.3×10^6 S/m	1.4×10^6 S/m
25 nm	1.0×10^7 S/m	8.9×10^6 S/m	1.6×10^6 S/m
Lit. Bulk [47]	6.3×10^7 S/m	4.1×10^7 S/m	1.4×10^7 S/m

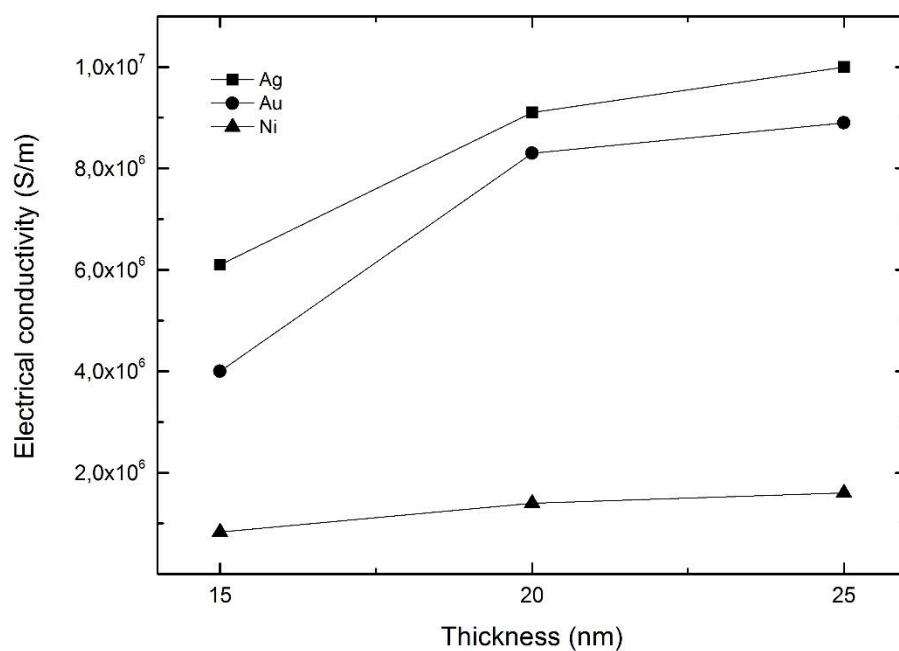


Figure 4.1 Electrical conductivity of Ag, Au, Ni thin films with changing film thickness.

4.2 Surface Modification Characterization

4.2.1 Surface Morphology Examination using FESEM

Gold metal was coated on silicon wafers with thickness 15 nm, 20 nm and 25 nm. Studies under FESEM have been done in order to examine film continuity and size of the nuclei forming the film structure separated by micro cracks. Under FESEM, photos have been taken from two different locations on the specimen surface; namely the center and the edge of the thin films. Film continuity has been examined from the central position and nuclei sizes have been examined on the edge of thin film.

FESEM micrographs in Figure 4.2 - Figure 4.4 show the microstructure, at 120000 magnification, of the central regions of 15 nm, 20 nm and 25 nm thick Au thin films where there is only growth not nucleation. As it can be seen in Figure 4.2-4.4, as thickness of the thin film increases, micro cracks which separate granular regions slowly disappear. In Figure 4.2, while relatively higher number of micro cracks are noteworthy on 15 nm thick thin film, in Figure 4.3, these micro cracks' clarity starts to disappear. In Figure 4.4, this effect is getting bigger, where number and clarity of micro cracks decreases. In these figures, there are boundaries visible between the granular regions and number of these boundaries gets smaller with increasing film thickness. This change does not show the presence of a continuous film structure; however, increasing electrical conductivity with increasing film thickness which is explained in Section 4.1 shows that there is a film continuity, and it has a tendency to get higher with increasing film thickness.

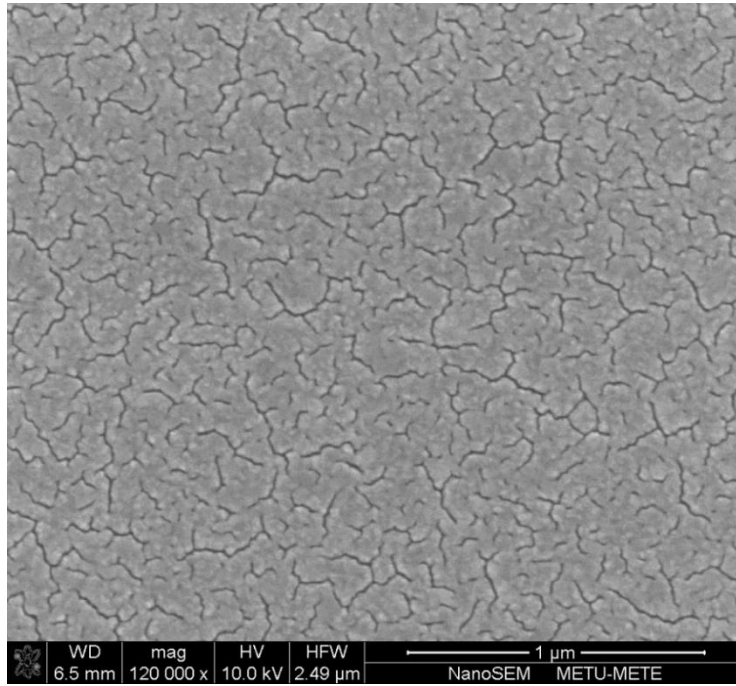


Figure 4.2 Surface morphology of 15 nm Au thin film on silicon wafer, photo taken by FESEM under x120000 magnification.

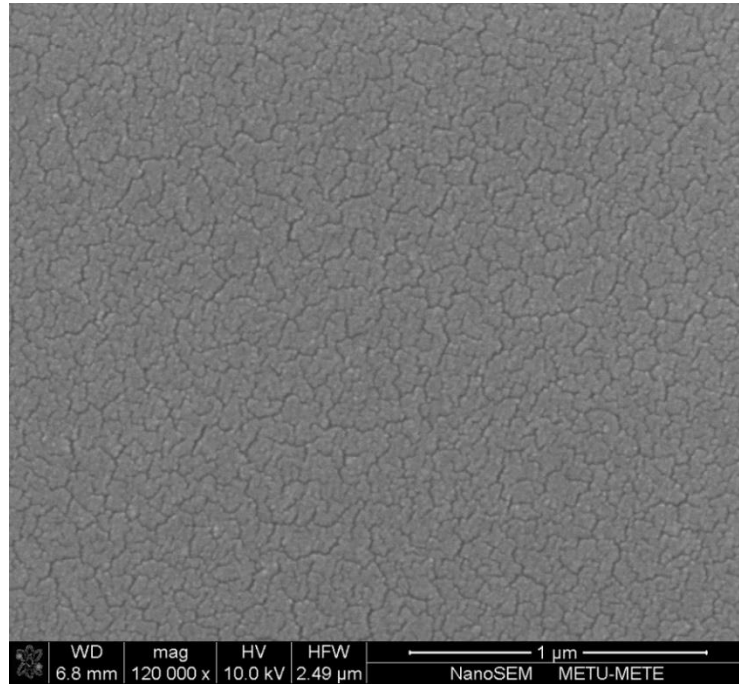


Figure 4.3 Surface morphology of 20 nm Au thin film on silicon wafer, photo taken by FESEM under x120000 magnification.

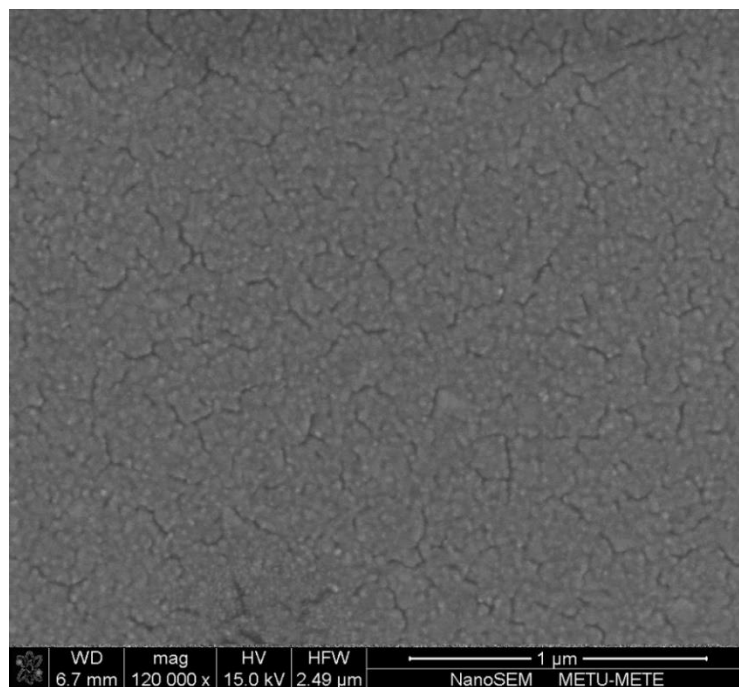


Figure 4.4 Surface morphology of 25 nm Au thin film on silicon wafer, photo taken by FESEM under x120000 magnification.

In Figure 4.5 - Figure 4.7, FESEM photos taken from the edges of 15 nm, 20 nm and 25 nm thick Au thin films on silicon wafers, respectively, are shown. In order to examine the morphology and size of the nuclei forming the film structure, FESEM photos were focused on the edges of the thin films, where the nuclei can be seen clearly being isolated from each of them. In Figure 4.5 - Figure 4.7, nuclei sizes were measured using the software ImageJ. In each FESEM photo, size of ten random nuclei was measured drawing lines through their diameter. In Table 4.2, measured nuclei sizes and average nuclei size for changing film thickness can be seen.

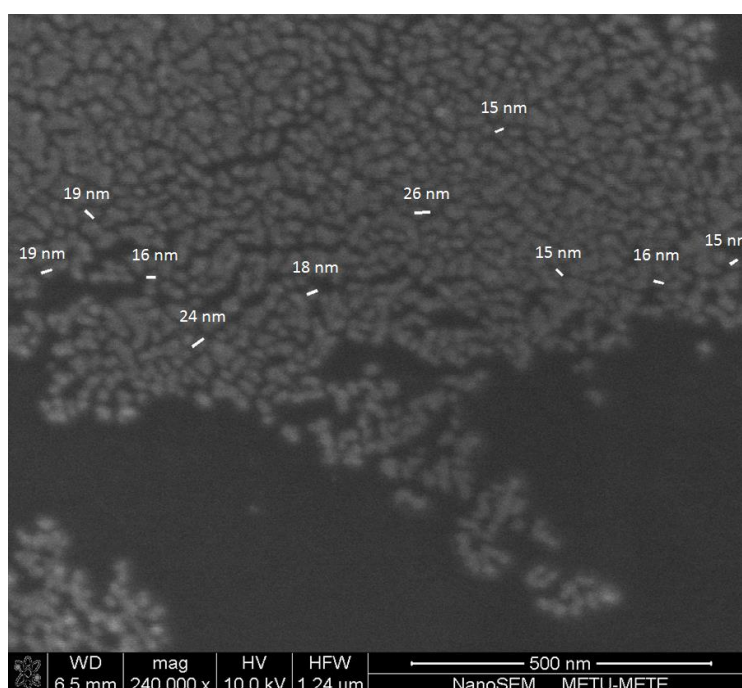


Figure 4.5 Edge morphology of 15 nm Au thin film on silicon wafer, photo taken by FESEM under x240000 magnification.

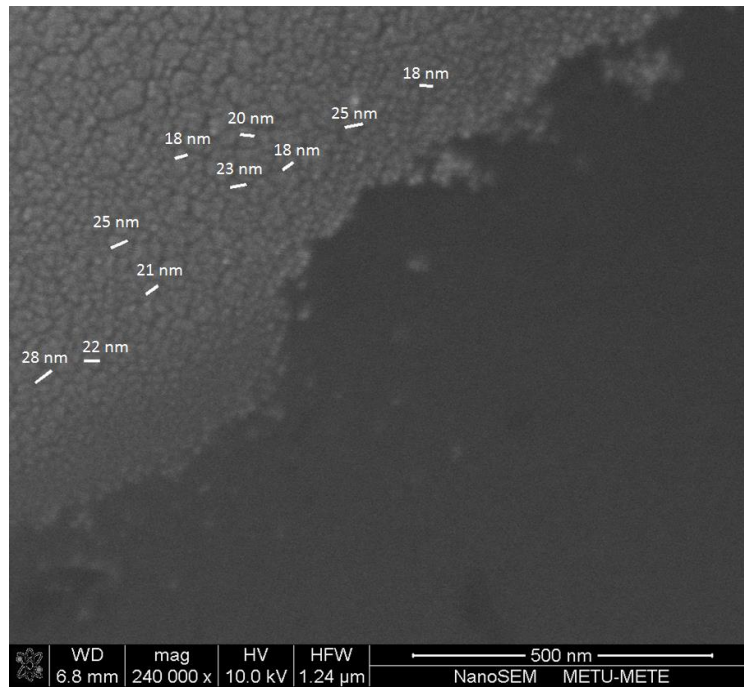


Figure 4.6 Edge morphology of 20 nm Au thin film on silicon wafer, photo taken by FESEM under x240000 magnification.

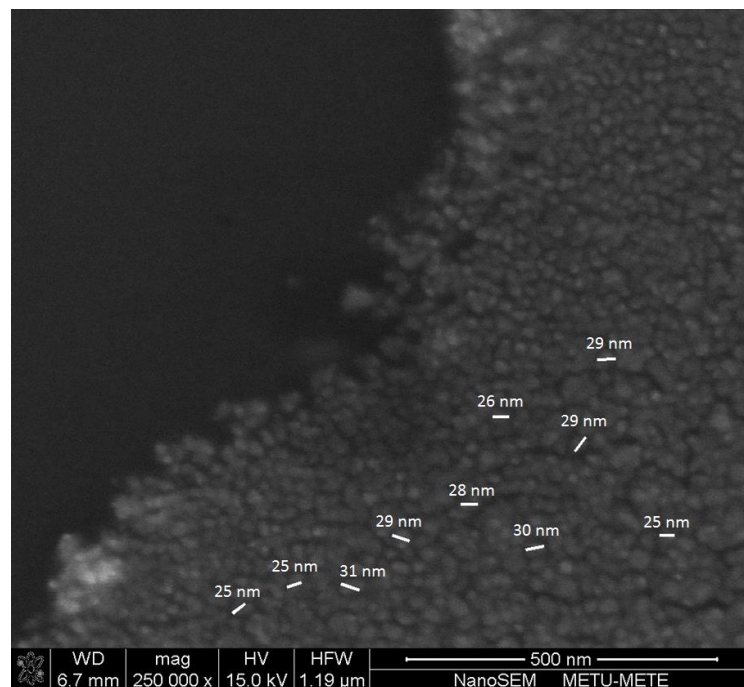


Figure 4.7 Edge morphology of 25 nm Au thin film on silicon wafer, photo taken by FESEM under x240000 magnification.

Table 4.2 Measured average nuclei sizes for 15 nm, 20 nm, 25 nm thick Au thin films.

	15 nm	20 nm	25 nm
1	15 nm	18 nm	25 nm
2	15 nm	18 nm	25 nm
3	15 nm	18 nm	25 nm
4	16 nm	20 nm	26 nm
5	16 nm	21 nm	28 nm
6	18 nm	22 nm	29 nm
7	19 nm	23 nm	29 nm
8	19 nm	25 nm	29 nm
9	24 nm	25 nm	30 nm
10	26 nm	28 nm	31 nm
Average	18.3 nm	21.8 nm	27.7 nm

As it can be seen in both Figure 4.5 - Figure 4.7 and Table 4.2, nuclei sizes are increasing with increasing film thickness. Additionally, the nuclei start to get in contact and form the continuous film structure at the central section of the thin films. This effect can be seen clearer when the edge and central sections of the thin films in Figure 4.5 - Figure 4.7 are compared.

Acquired FESEM photos show that 15 nm, 20 nm and 25 nm thick thin films tend to have continuous film structure. Therefore, it is considered that these thin films can provide the desired surface electrical conductivity, and hence electromagnetic properties.

4.2.2 Surface Topography Examination using AFM

Atomic force microscope (AFM) was used in order to examine the surface topography of the thin films in detail. 15 nm and 25 nm thick Au thin films on silicon wafer were observed using AFM in this study. Usage of AFM for surface topography examination

has provided 3D vision of nuclei and their distribution on silicon wafer along with the realistic film thickness.

In Figure 4.8-Figure 4.9, 2D and 3D microstructural views of 15 nm and 25 nm thick Au thin films obtained using AFM can be seen. These four AFM views were taken from a 500 x 500 nm square area, and all of these AFM photos are representing other similar AFM photos taken as 2D and 3D. Therefore, it can be said that the Au thin films are continuous, and nuclei forming those films have nearly half-spherical shapes as can be seen in Figure 4.8 and Figure 4.10. In Figure 4.9 and Figure 4.11, in the 2D view analysis of the microstructure and nuclei size can be seen as an example. According to the AFM based nuclei size measurements, average nucleus size is nearly 40 nm for 15 nm thick Au thin film and nearly 38 nm for 25 nm thick one. In Figure 4.9 and Figure 4.11, the technique used in the measurement of the average nucleus size is shown basically. Line intercepts with the nuclei were taken as the diameter of those nuclei. Average nucleus size of 15 nm thick Au film is larger than that of the 25 nm thick Au film. This is thought to be caused by the secondary nucleation over the first layer of the nuclei during prolonged thermal evaporation. When Figure 4.8 and Figure 4.10 are compared, this finding can be seen clearly in the 3D views. With the help of these results, uncertainties in the FESEM studies have been revealed.

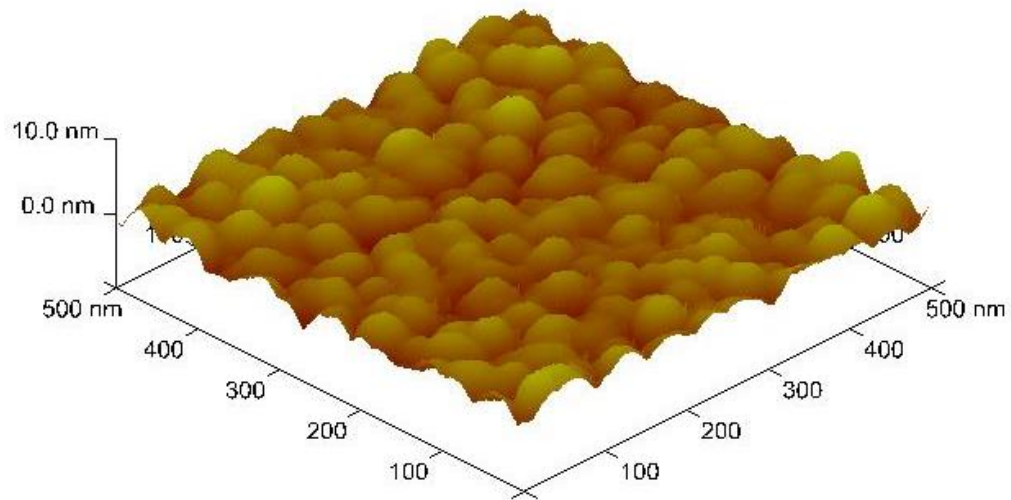


Figure 4.8 3D microstructure photo taken using AFM of 15 nm thick Au film on silicon wafer (500 nm x 500 nm area).

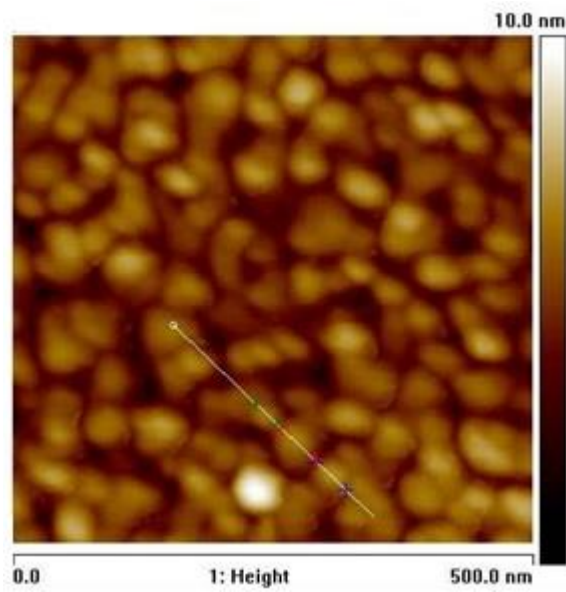


Figure 4.9 2D microstructure photo taken using AFM of 15 nm thick Au film on silicon wafer (500 nm x 500 nm area) and nuclei size determination.

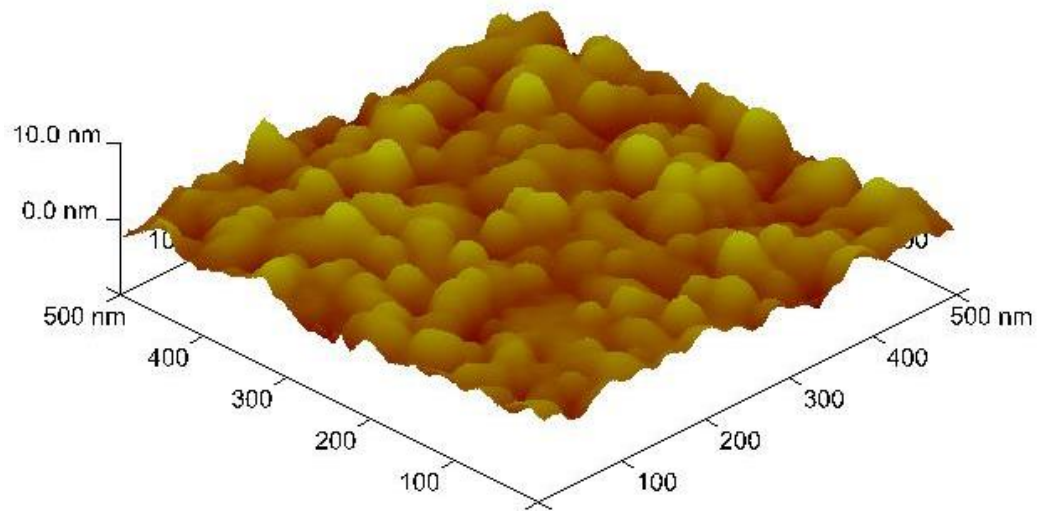


Figure 4.10 3D microstructure photo taken using AFM of 25 nm thick Au film on silicon wafer (500 nm x 500 nm area).

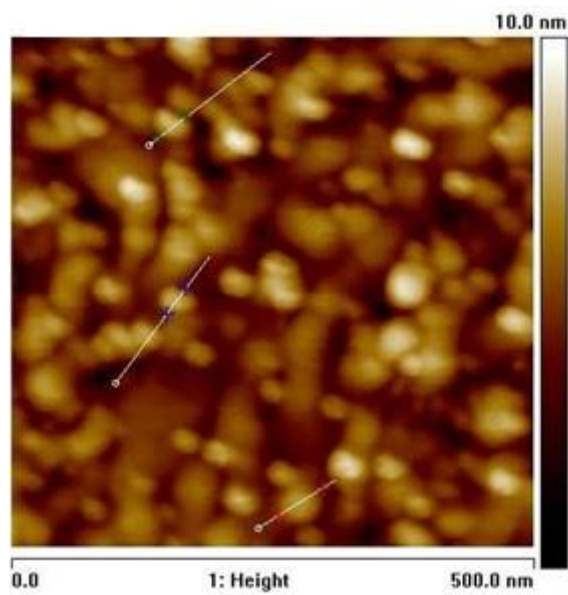


Figure 4.11 2D microstructure photo taken using AFM of 25 nm thick Au film on silicon wafer (500 nm x 500 nm area) and nuclei size determination.

Other than nuclei size measurement and film continuity observation, AFM was also used for measuring realistic film thickness which could not have been achieved from the thickness monitor of the thermal evaporator. 15 nm and 25 nm thick Au films on silicon wafers have been scratched with the help of stanley knife. In this process, only Au thin films were removed from the silicon wafers' surface, and silicon wafers were not deformed by the dint. As it can be seen from Figure 4.12-Figure 4.15, scratch did not deform the silicon wafer surface. AFM photos in Figure 4.12-Figure 4.15 helps in measuring the realistic thin film thickness. While Figure 4.12 and Figure 4.14 show that the AFM probe touched all of the points on given areas, Figure 4.13 and Figure 4.15 show the thickness measurement analysis. According to results obtained, 15 nm Au thick film has 18.3 nm average thickness and 25 nm thick Au film has 29.6 nm average thickness. There is a deviation between the real final thickness obtained by the surface modification and the desired surface modification thickness. This deviation can be measured as percentage using equation:

$$\% \text{ Error} = \frac{\text{Theoretical value} - \text{Experimental value}}{\text{Theoretical value}} \times 100 \quad (4-1)$$

Using Eqn. (4-1), % error of 15 nm thick Au film was determined to be 18.4% and that of the 25 nm thick Au film is 20%. With these results, it can be said that there is roughly 20% error in the thickness of the film obtained by the applied surface modification. Surface modification on glass and aramid fiber woven fabrics has been done considering this % error included in the thickness monitor of the used thermal evaporator.

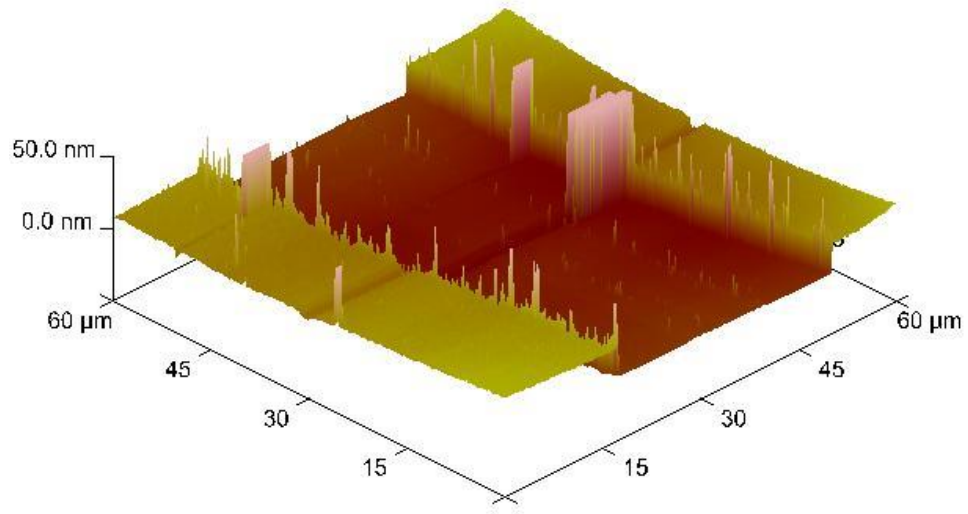


Figure 4.12 3D microstructure of the scratch, photo taken using AFM on the 15 nm thick Au film on silicon wafer (60 μm x 60 μm area).

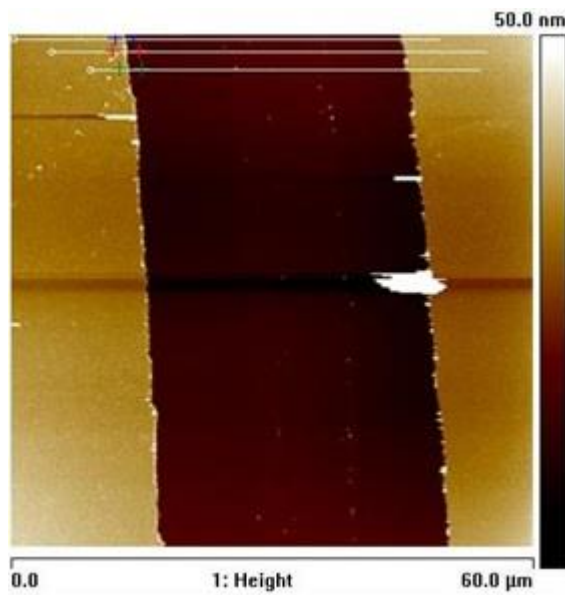


Figure 4.13 2D microstructure of the scratch, photo taken using AFM on the 15 nm thick Au film on silicon wafer (60 μm x 60 μm area) and thickness measurement.

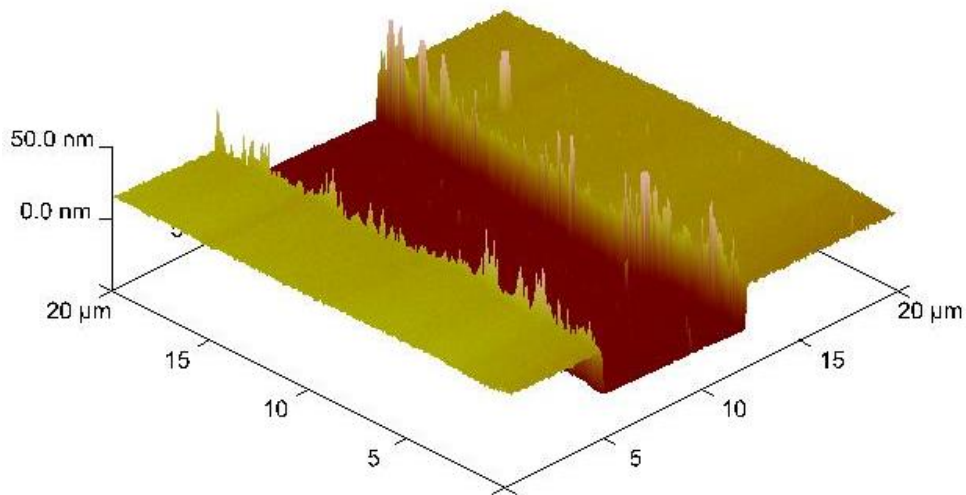


Figure 4.14 3D microstructure of the scratch, photo taken using AFM on the 25 nm thick Au film on silicon wafer (20 μm x 20 μm area).

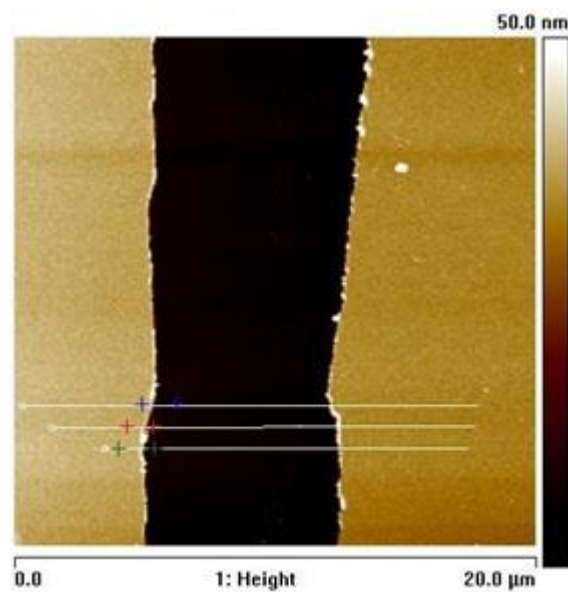


Figure 4.15 2D microstructure of the scratch, photo taken using AFM on the 25 nm thick Au film on silicon wafer (20 μm x 20 μm area) and thickness measurement.

In Figure 4.9 and Figure 4.11, surface data of 2D views were analyzed and surface geometrical parameters important for this study were summarized in Table 4.3. Surface roughness parameters are important for the current study in order to predict the relationship between the geometrical patterns which confront the EM waves and the resulting EM absorption. R_a , arithmetic average height, is the average deviation of roughness according to mean line of the system. R_z , ten-point height, difference between the average of five-highest and five lowest peaks [48].

Table 4.3 Surface parameters obtained by AFM examination.

	R_a	R_z	Real Film Thickness
15 nm Au thin film	0.83 nm	9.56 nm	18.30 nm
25 nm Au thin film	0.99 nm	11.90 nm	29.60 nm

As it can be seen in Table 4.3, increasing film thickness results in R_a and R_z to increase. Reason of the increase in R_a is thought to be the secondary nucleation of smaller nuclei over first layer. This shows that increase in thickness changes geometric pattern of thin films. Due to the low levels of R_a , it can be said that there is nearly homogenous distribution of surface modification on silicon wafer. Secondly, R_z value is considerably less than the real film thickness. This shows that there is a continuous film structure on the silicon wafer without any break offs.

All of the AFM results emphasize that surface modification can form continuous thin film structure. Moreover, this AFM study shows that data obtained from AFM and FESEM studies are in good agreement.

4.3 Electromagnetic Measurements and Results

In this part of the study, EM wave reflection, transmission, and hence absorption, characteristics of surface modified glass fiber and aramid fiber woven fabrics in single

and multilayer structure form were observed. Secondly, in order to show the effect of surface morphology of the woven fabrics on the resulting EM wave characteristics, EM wave absorption behavior of identically surface modified PET sheets were also examined. Additionally, EM wave absorption characteristics of fabricated prototype composites which are made of multilayered surface modified woven fabrics were investigated. Finally, computer aided simulation results on the EM wave absorption behavior of the multilayered reinforcement structures were analyzed. All of the EM measurements were done using free-space method.

EM measurements done using the free-space method should be separated in two groups; measurements on single layered and on multilayered structures. Reason of that is the difference in the EM characteristics of these structures. Basically, in single layer structures EM wave interacts with one conductive layer only. This single interaction results in the domination of either EM wave reflection or transmission. However; multilayered structures of surface modified woven fabrics behave in different way against EM waves. EM wave confronted by any of the layers in the structure reflects and transmits it at the same time. These reflections and transmissions create interference of EM waves in the multilayered structures. Interference can be both constructive and destructive. This results in unpredictable EM wave behavior, especially in case of reflection. Nevertheless, EM wave transmission characteristics are not affected in this way by the EM wave interactions mainly because of the direction of the incident EM wave used in the free-space method. Resulting EM measurements were analyzed based on the information explained above.

4.3.1 Electromagnetic Measurements and Results of Surface Modified Glass Fiber Woven Fabrics

In this study, electromagnetic wave reflection, transmission, and hence, absorption of surface modified glass fiber woven fabrics were observed. Surface modifications done with different metals; namely silver, gold and nickel on glass fiber woven fabrics. EM behaviors of these structures were examined in single layered and multilayered form both before and after silanization. In single layered structures, only EM wave reflection

and transmission results were compared. This is because either EM reflection or transmission behavior can be seen dominantly in results of single layered structures. Actually, EM wave absorption behavior is calculated using EM reflection and transmission together. In multilayered structures, which is formed by cascading single layered structures, EM wave reflection and transmission behaviors become developed and dominant simultaneously. Therefore, EM wave absorption characteristics can show significant results only in multilayered structure form.

Multilayered structures of surface modified glass fiber woven fabrics behave differently than their single layered versions. EM wave absorption mechanism can be used easier in multilayered structures as in the case of the Jaumann absorbers and graded absorbers for broad range of frequency [1].

4.3.1.1 EM Measurement Results of Glass Fiber Woven Fabrics Surface Modified with Silver

EM measurements began on silver surface modified fiber woven fabrics due to the reasons that silver is diamagnetic, has the highest electrical conductivity measured and has the easiest parameters to be obtained by thermal evaporation.

In 18-40 GHz frequency range, EM wave reflection and transmission characteristics of silver surface modified glass fiber woven fabrics were measured by free-space method. In Figure 4.16-Figure 4.17, EM wave reflection and transmission loss changes with frequency can be seen. As coating thickness increases, EM wave reflection loss is examined to increase. Similarly, EM wave transmission loss is decreasing with increasing thickness of coated silver. This outcome was expected due to the explained reason of impedance drop [46] with increasing film thickness. More conductive surfaces start to behave more reflective. While EM wave reflection loss of silver modified glass fiber woven fabrics is fluctuating between -5 dB and -15 dB, all EM wave transmission loss values are higher than -3 dB. These values correspond to ~10% EM wave reflection and ~80% EM wave transmission, respectively. This means that single layered silver surface modified glass fiber woven fabrics are almost transparent to EM waves in 18-40 GHz frequency range.

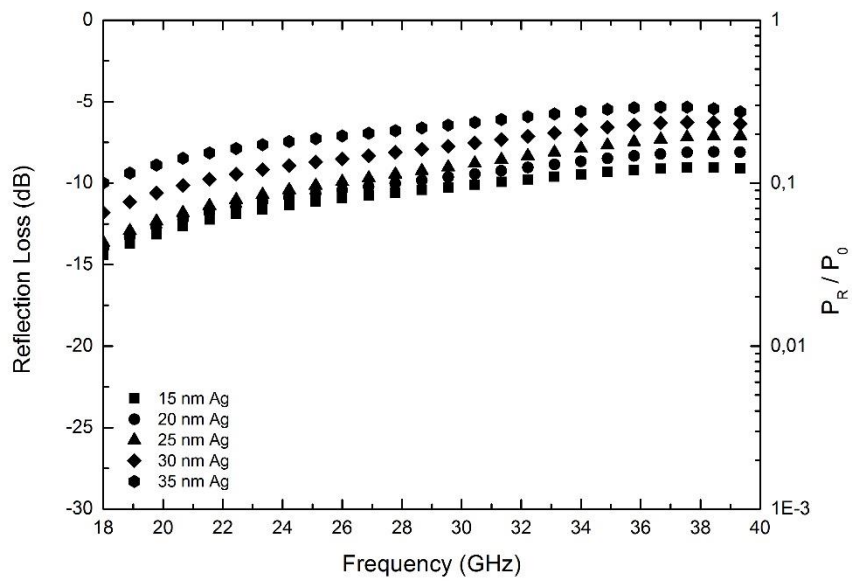


Figure 4.16 EM wave reflection loss varying with frequency in silver surface modified single layered glass fiber woven fabrics.

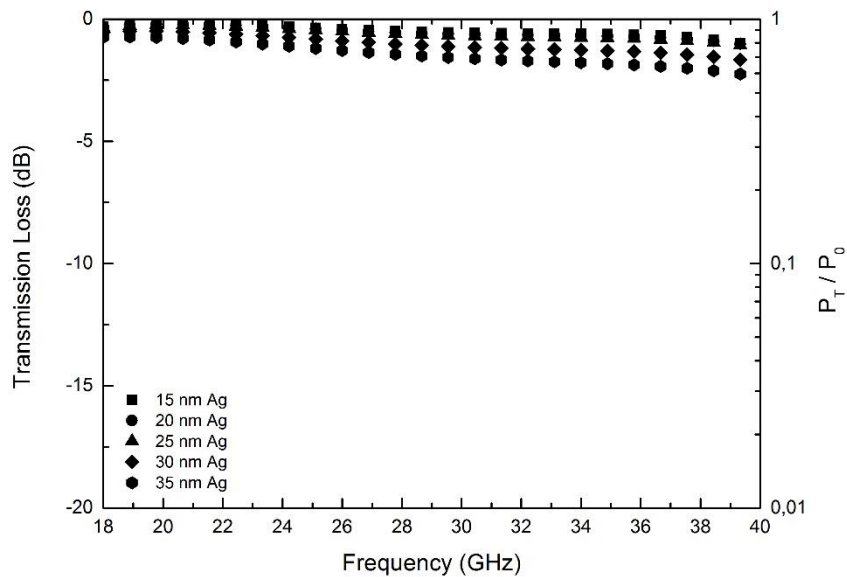


Figure 4.17 EM wave transmission loss varying with frequency in silver surface modified single layered glass fiber woven fabrics.

In the light of the information obtained from single layered structures, multilayered structures of silver surface modified glass fiber woven fabrics were examined. Surface modified single layers were cascaded according to their coating thickness, hence, electrical conductivity. Four different configurations of multilayered structures were formed in order to observe the effect of number of layers used in structure. In Figure 4.18-Figure 4.20, EM wave reflection, transmission and absorption measurement results of silver surface modified woven fabrics can be seen, respectively. As it was explained before, reflection loss results of the multilayered structures do not have a trend with increasing layer size or film thickness which was the case with the single layered structures. Interference of EM waves in multilayered structures causes fluctuations in EM wave reflection loss value with varying frequency. Although, there is no regular trend in the results, EM wave reflection loss values are less than -10 dB in high frequency range. This corresponds to 10% EM wave reflection. Analyzing more carefully, five layered structure shows less than 5% EM wave reflection without any fluctuations.

Unlike the EM wave reflection loss results, transmission loss results have a trend where EM wave transmission decreases with increasing number of layers. In Figure 4.19, it can be seen that EM wave transmission is decreasing with increase in frequency and the lowest EM transmission was 5% obtained for the five layered structure. Using both EM wave reflection and transmission loss results, EM wave absorption percentage can be calculated and results of this can be seen in Figure 4.20. Absorption percentages are increasing with the number of layers in the structure. Absorption results obtained for five layered structure are between 45% and 90%, and absorption is increasing directly with frequency. Therefore, it can be said that usage of silver surface modified glass fiber woven fabrics as EM wave absorbing materials can only be possible at higher frequencies.

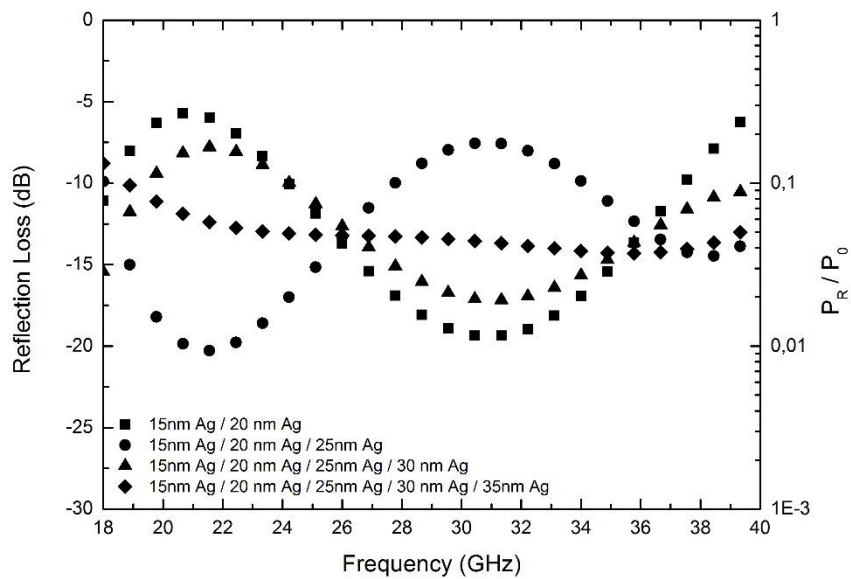


Figure 4.18 EM wave reflection loss varying with frequency in silver surface modified multilayered glass fiber woven fabrics.

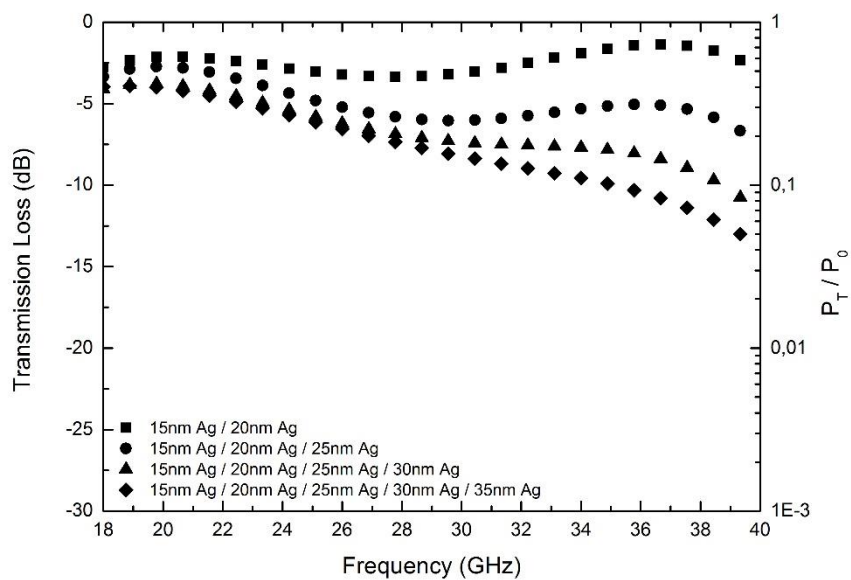


Figure 4.19 EM wave transmission loss varying with frequency in silver surface modified multilayered glass fiber woven fabrics.

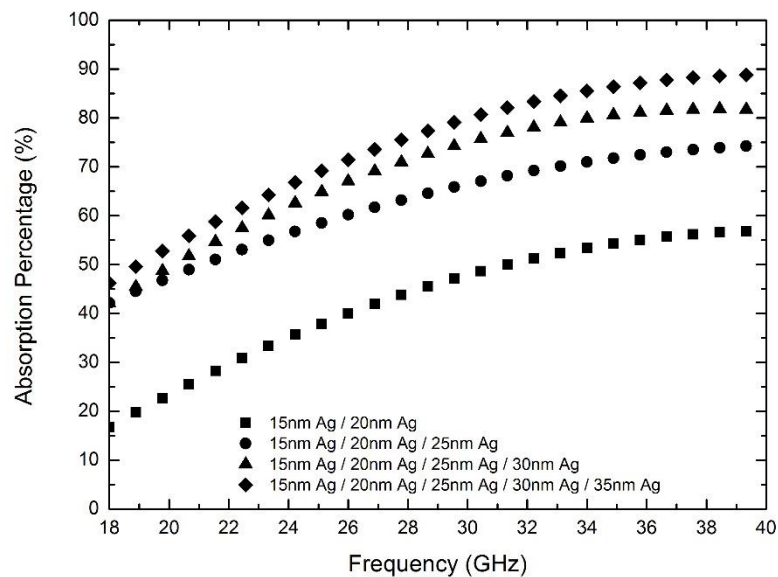


Figure 4.20 EM wave absorption varying with frequency in silver surface modified multilayered glass fiber woven fabrics.

A following study has been conducted on silver surface modified multilayered glass fiber woven fabrics. A fully reflective metallic plate was placed at back of the obtained five layered structure, and the EM measurement was repeated. It was intended to measure the change in EM wave reflection of a fully reflective metallic plate when an absorber multilayered structure is placed on its surface. This measurement revealed the possibility of using mentioned multilayered structure as an EM wave absorbing material on any device.

In Figure 4.21, it can be seen that EM wave reflection value changes between -8 dB and -15 dB. This means that EM wave reflection percentage changes between 3% and 15%. Because of the fact that there is a backing fully reflective metallic plate, there can be no EM behavior other than reflection and absorption. Therefore, the reflection percentage changing between 3% and 15% corresponds to EM wave absorption

percentage between 85% and 97%. In conclusion, developed silver surface modified 5-layered glass fiber woven fabric configuration has a potential to be used as a non-reflective material on metallic surfaces, especially on electronic devices and vehicles.

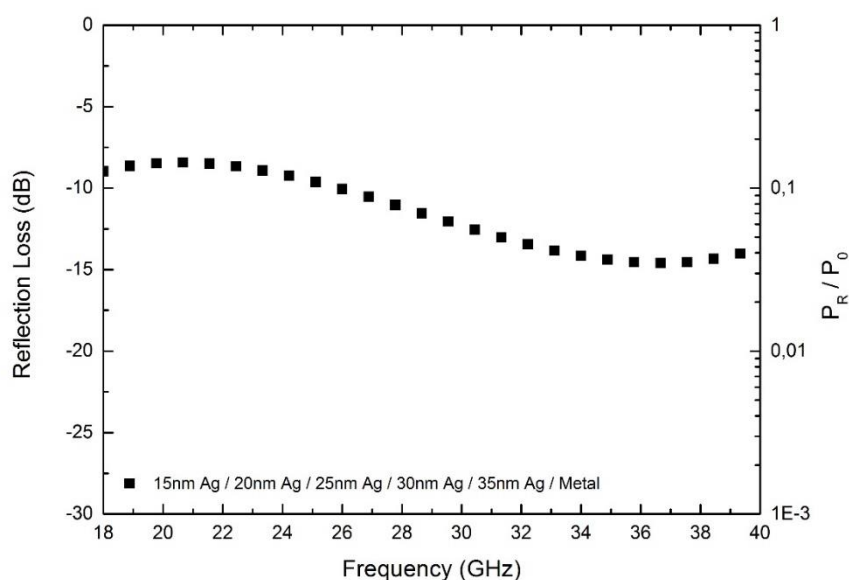


Figure 4.21 EM wave reflection loss varying with frequency in silver surface modified multilayered (5-layered) glass fiber woven fabric with metallic backing plate.

Literally, studies on silver surface modification and glass fiber woven fabrics have resulted in remarkable results in terms of the targets of the current study. However, there is a drawback for this system. It was observed that silver thin films on woven fabrics oxidized in very short time under open air condition. Possible expected variations in electrical conductivities, and hence, electromagnetic properties caused by oxidation added another view to the ongoing study. After this observation, surface modified samples have been left to oxidize for two weeks under room conditions (298 K and 1 atm). Then, same EM measurements were repeated for these samples. Obtained results can be seen in Figure 4.22-Figure 4.27 in the same order discussed

above. According to these results, following the oxidation of silver thin films reflection decreased and transmission increased for both single and multilayered samples. This has led to an increase in the EM wave reflection and decrease in the EM wave absorption for the configuration which includes a backing metallic plate. 90% EM wave absorption value for 5- layered structure has dropped down to 70% absorption with the effect of oxidization.

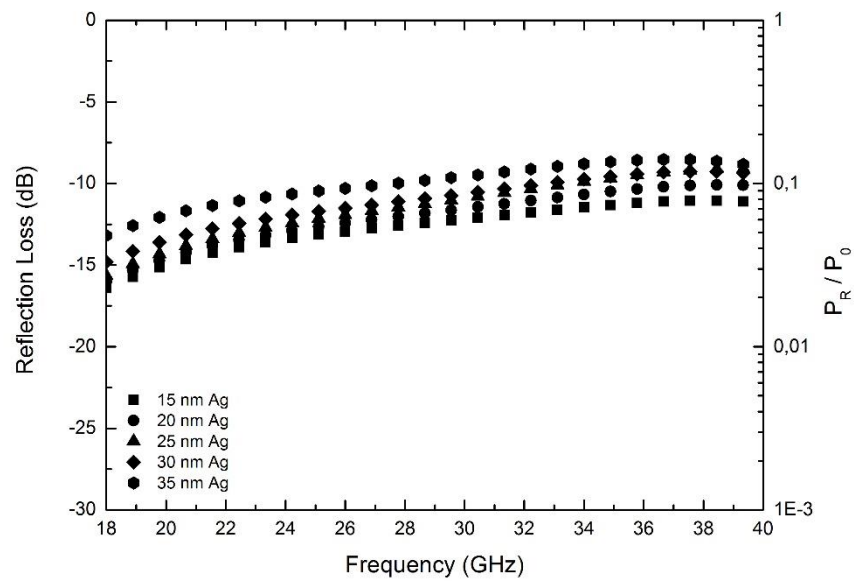


Figure 4.22 EM wave reflection loss varying with frequency in oxidized silver surface modified single layered glass fiber woven fabrics.

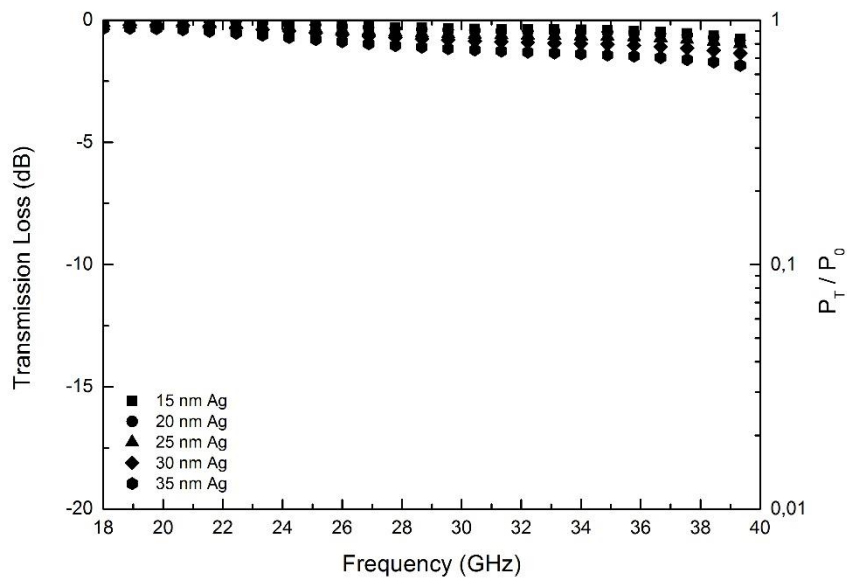


Figure 4.23 EM wave transmission loss varying with frequency in oxidized silver surface modified single layered glass fiber woven fabrics.

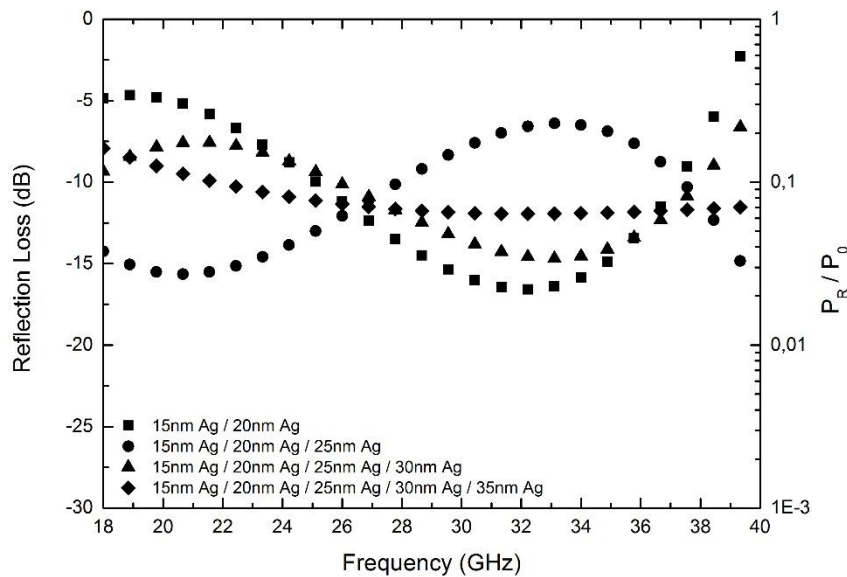


Figure 4.24 EM wave reflection loss varying with frequency in oxidized silver surface modified multilayered glass fiber woven fabrics.

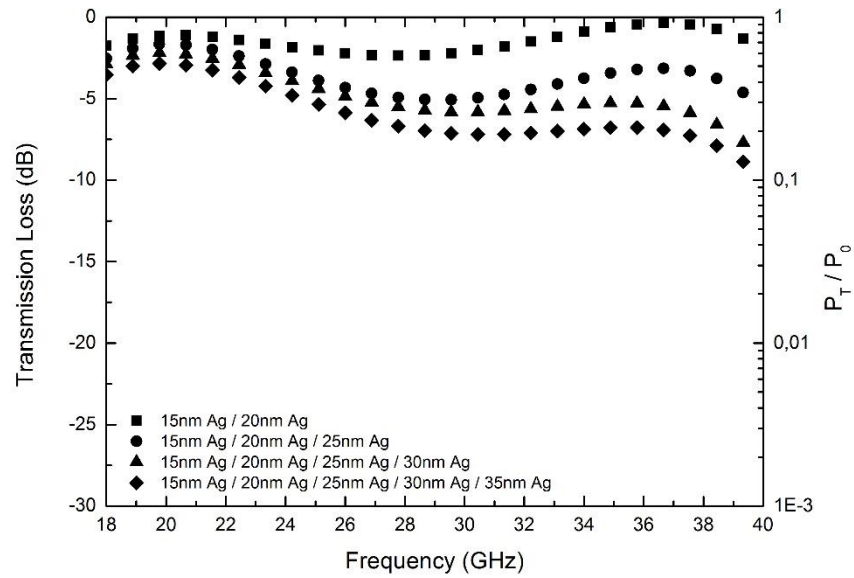


Figure 4.25 EM wave transmission loss varying with frequency in oxidized silver surface modified multilayered glass fiber woven fabrics.

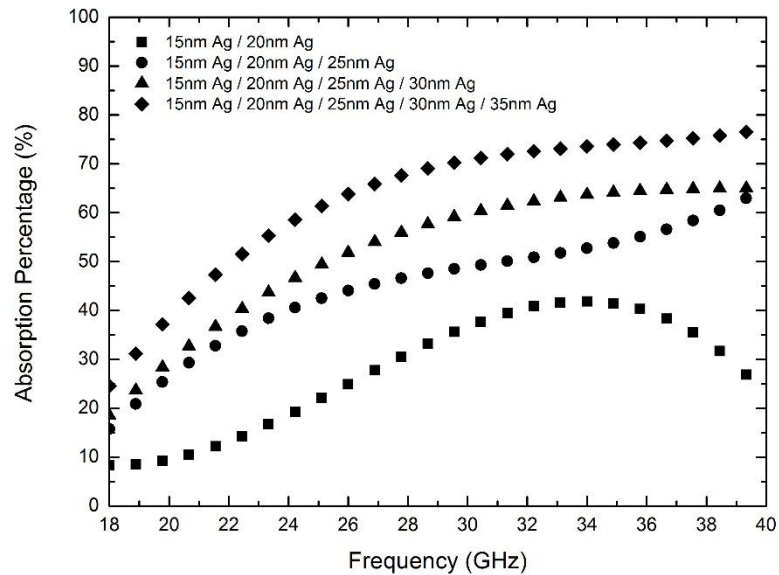


Figure 4.26 EM wave absorption percentage varying with frequency in oxidized silver surface modified multilayered glass fiber woven fabrics.

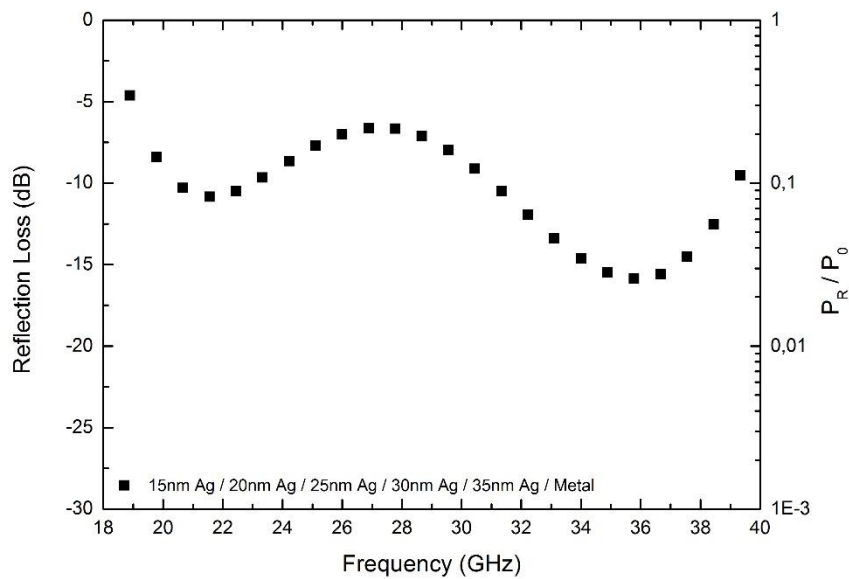


Figure 4.27 EM wave reflection loss varying with frequency in oxidized silver surface modified 5-layered glass fiber woven fabric with metallic backing plate.

To sum up, obtained results showed that effect of oxidation can be a criteria for choosing the coating metals in radar absorbing materials (RAM). Moreover, it showed that there is another point of view for surface modified radar absorbing materials. Finally, although, it showed high EM wave absorption in multilayered form, it is decided that silver is not a suitable metal in order to participate in radar absorbing materials as a surface modification due to possibility of oxidation.

4.3.1.2 EM Measurement Results of Glass Fiber Woven Fabrics Surface Modified with Gold

Gold is a diamagnetic metal with high electrical conductivity and corrosion resistance. These properties of gold make it desirable to be used in EM wave absorbers. Surface modifications by gold on glass fiber woven fabrics were studied in [5]. In the light of

this study, it was decided that thinner gold layers on glass fiber woven fabrics can be more efficient for EM wave absorption. Therefore, in this study surface modification of glass fiber woven fabrics was done by 15 nm, 20 nm, 25 nm, 30 nm and 35 nm thick gold thin films. At first, EM wave reflection and transmission results of single layers were analyzed. Secondly, EM wave reflection, transmission and absorption behavior of multilayered structures as well as their reflection behavior with backing metal were characterized. Finally, since satisfactory results were obtained on the samples mentioned, gold surface modified multilayered structures were used in prototype composite fabrication including silanization efforts explained in Section 3.3.1. Therefore, silane treated gold surface modified single and multilayered glass fiber woven fabrics were also examined in order to determine the effect of silanization treatment on the EM characteristics.

Results of EM wave reflection and transmission measurements of gold surface modified single layer glass fiber woven fabrics can be seen in Figure 4.28 and Figure 4.29, respectively. As it can be seen from these figures, there is a regular trend in the change of the EM wave reflection and transmission behavior with varying surface modification film thickness. It can be seen clearly that as the thickness of gold film increases, EM wave reflection is also increasing while transmission is vice versa. EM wave reflection loss of these samples are changing between -3 dB and -10 dB and transmission loss are varying between -2 dB and -8 dB, both of which correspond to more than %10 of the incident EM wave energy (see the right-side vertical axes showing the percentage of reflection or transmission with respect to the incident energy).

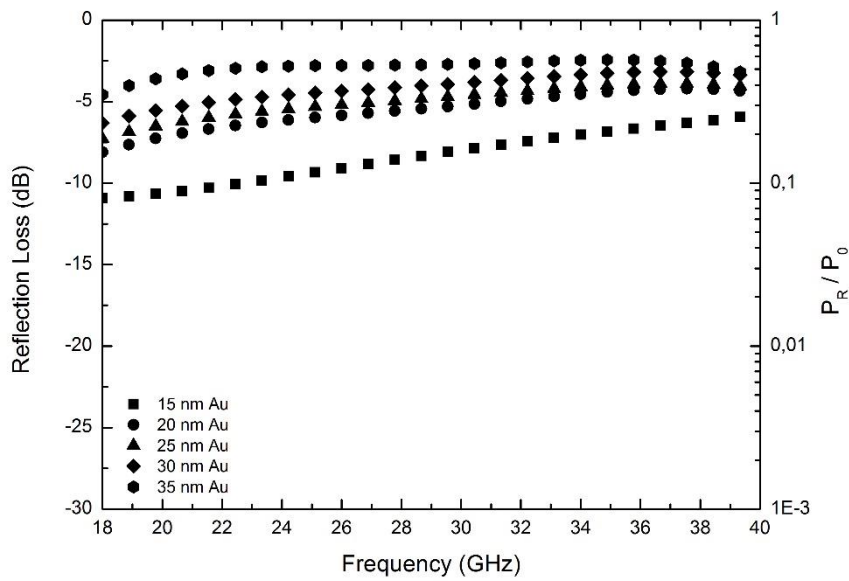


Figure 4.28 EM wave reflection loss varying with frequency in gold surface modified single layer glass fiber woven fabrics.

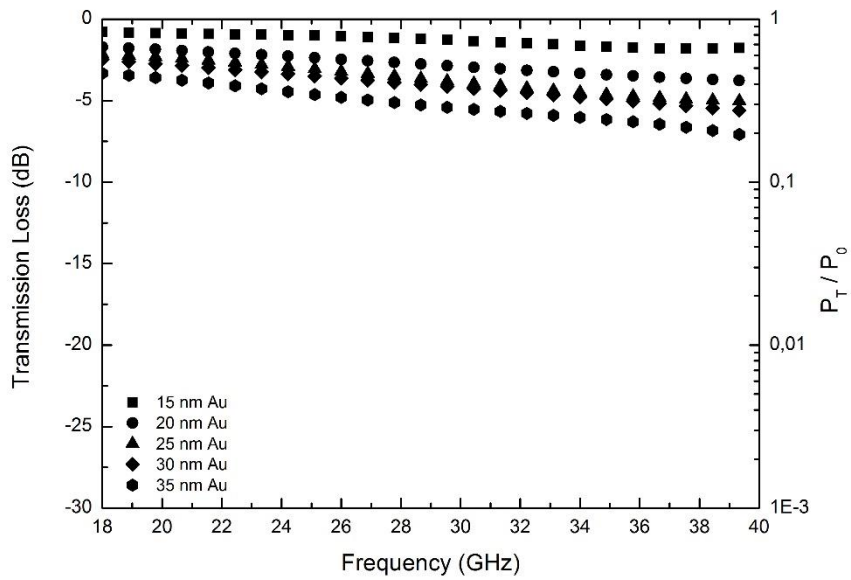


Figure 4.29 EM wave transmission loss varying with frequency in gold surface modified single layer glass fiber woven fabrics.

Four different multilayered structures were also examined in terms of their EM characteristics. Considering the results obtained on the gold surface modified single layered glass fiber woven fabrics, it was expected to achieve remarkable results for EM wave reflection and transmission with multilayered samples. Results can be seen in Figure 4.30-Figure 4.31. EM wave reflection loss of gold surface modified multilayered glass fiber woven fabrics show similar results to those of the silver surface modified glass fiber woven fabrics. As the number of layers increases in the structure, reflection loss of the two metals fluctuate similarly with changing frequency. This means that EM wave interactions in multilayered structures show similar constructive and destructive interferences. Similar magnetic properties and close electrical conductivities were thought to be the reasons for this result.

EM wave reflection loss results of gold surface modified samples are fluctuating between -5 dB and -20 dB. However, the most important multilayered structure, 5-layered one, shows consistent behavior with \sim -13 dB reflection loss. This corresponds to \sim 4% reflection of the incident EM wave. Secondly, EM wave transmission loss results of gold surface modified samples show that increasing number of layers leads to less EM wave transmission. Analysis also shows that EM wave transmission decrease with increasing frequency. As it can be seen from Figure 4.31, EM wave transmission loss results are changing between -2 dB and -13 dB. Moreover, using EM wave reflection and transmission loss results, EM wave absorption values were calculated and results are given in Figure 4.32. In this figure it can be seen that 5-layered structure shows 90% EM wave absorption in 33-40 GHz frequency range. EM wave absorption results of gold surface modified samples are similar to those of non-oxidized silver modified samples; however, gold modified ones show higher absorption in a broader frequency range.

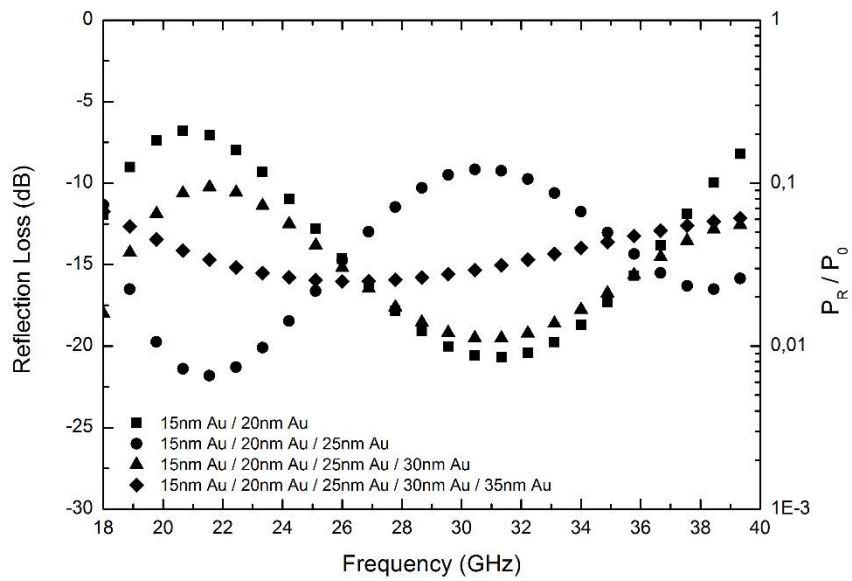


Figure 4.30 EM wave reflection loss varying with frequency in gold surface modified multilayered glass fiber woven fabrics.

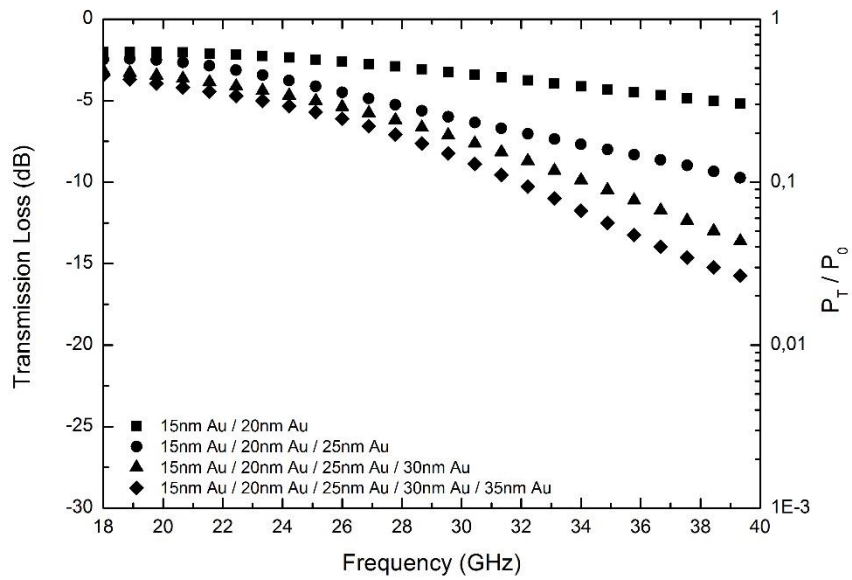


Figure 4.31 EM wave transmission loss varying with frequency in gold surface modified multilayered glass fiber woven fabrics.

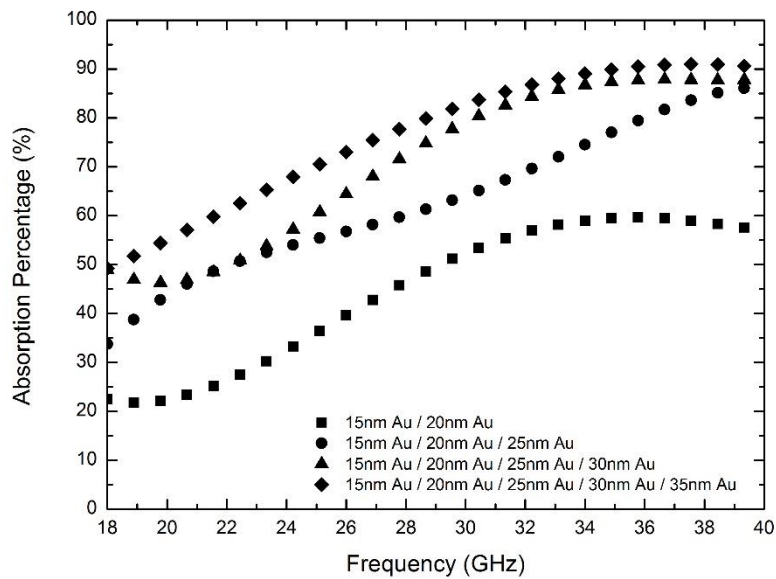


Figure 4.32 EM wave absorption percentage varying with frequency in gold surface modified multilayered glass fiber woven fabrics.

EM wave reflection behavior of gold surface modified 5-layered glass fiber woven fabric structure has also been examined under the presence of a metallic backing plate. Results of this study can be seen in Figure 4.33. As it can be seen, fully reflective metallic plate shows %10 and less EM wave reflection through nearly the whole frequency range, when the 5-layered structure is placed in front of it. As high as 98% EM wave absorption was obtained at high frequencies (34-38 GHz). This shows that gold surface modified glass fiber woven fabrics are suitable materials for using them as reinforcement materials in EM wave absorber composites.

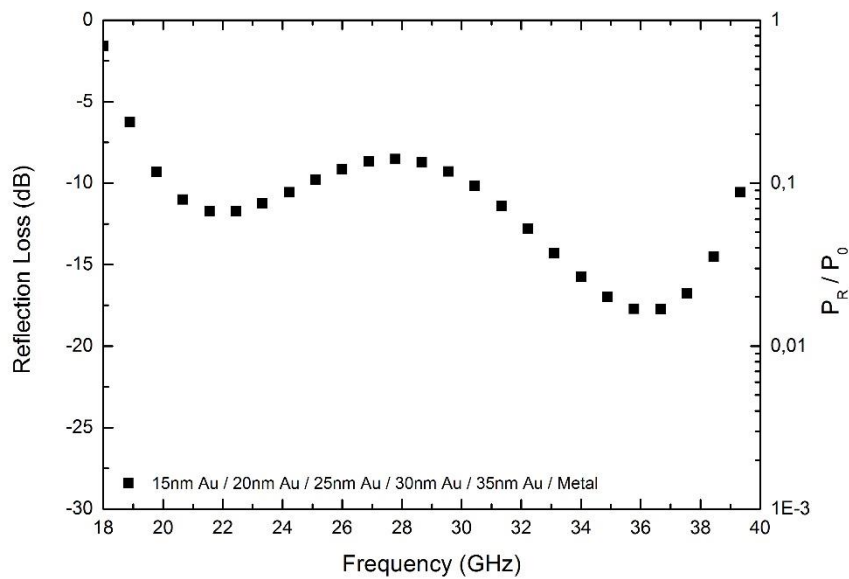


Figure 4.33 EM wave reflection loss varying with frequency in gold surface modified 5-layered glass fiber woven fabrics with metallic backing plate.

Promising results of gold surface modified glass fiber woven fabrics make these materials potential reinforcements to be used in composite structures. In order to increase the mechanical strength of the resulting composite structures by controlling the interfacial properties between the fibers and the matrix, silanization treatment was applied to the surface modified reinforcement materials. Effects of silanization treatment on the EM wave characteristics were analyzed for both single layer and multilayered glass fiber woven fabrics. Results of gold surface modified single layer and multilayered glass fiber woven fabrics can be seen in the Appendix in Figure A.1 to Figure A.6. In these figures, it can be seen that there is no significant effect of silanization treatment on the EM characteristics of the samples. Overall, achieved results demonstrated that gold surface modification and silanization are suitable treatments in terms of improving EM characteristics.

4.3.1.3 EM Measurement Results of Glass Fiber Woven Fabrics Surface Modified with Nickel

Nickel is a ferromagnetic metal with relatively low (compared to silver and gold) electrical conductivity. Surface modifications by nickel on glass fiber woven fabrics were also studied in reference [5]. Considering the results of the preceding study, it was decided that nickel thin films with lower thickness on glass fiber woven fabrics can be more efficient for EM wave absorption. For this reason, surface modification of glass fiber woven fabrics was done with 15 nm, 20 nm, 25 nm, 30 nm and 35 nm thick nickel thin films. Similar to previously mentioned studies, EM wave reflection and transmission results of single layers were analyzed at first, and then, multilayered structures were characterized by adding analyses of EM wave absorption and EM wave reflection loss with metallic backing plate. Similar to studies conducted with gold, silanization treatment was applied to nickel surface modified samples, and their EM characteristics were examined.

EM wave reflection and transmission measurement results of gold surface modified single layer glass fiber woven fabrics can be seen in Figure 4.34 and Figure 4.35, respectively. As it can be seen, similar to silver and gold surface modification cases, there is a regular trend in EM wave reflection and transmission behaviors with varying film thickness. As thickness increases, EM wave reflection becomes more dominant and EM wave transmission becomes more passive. EM wave reflection loss of nickel surface modified single layer glass fiber woven fabrics is changing between -3 dB and -10 dB, and their transmission loss is varying between -3 dB and -8 dB corresponding to more than %10 reflection or transmission of the incident EM wave energy, respectively. Presented results are similar to those of the gold surface modification case; however, there is a remarkable gap between the reflection and transmission loss values of the 15 nm thick nickel applied glass fiber woven fabric and those of the rest. This shows that nickel films thinner than 20 nm starts to behave more transparent to EM waves between 18-40 GHz.

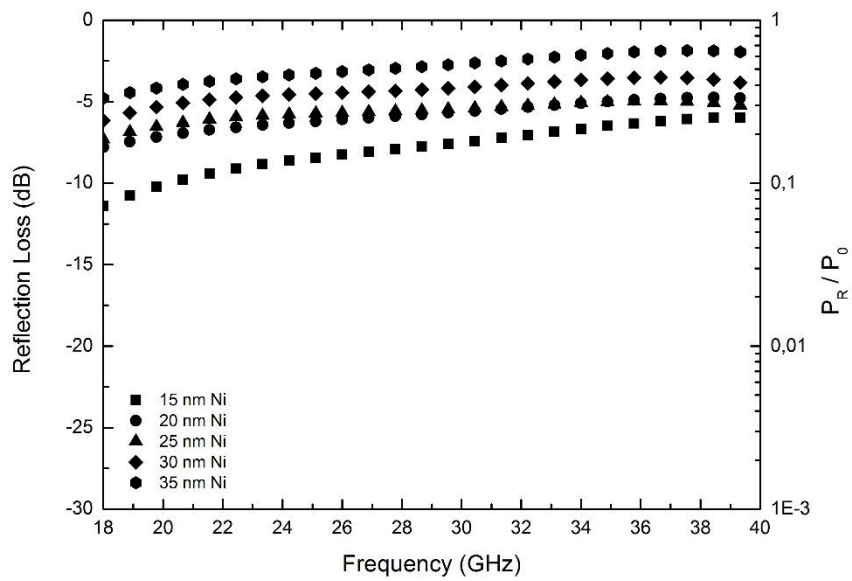


Figure 4.34 EM wave reflection loss varying with frequency in nickel surface modified single layer glass fiber woven fabrics.

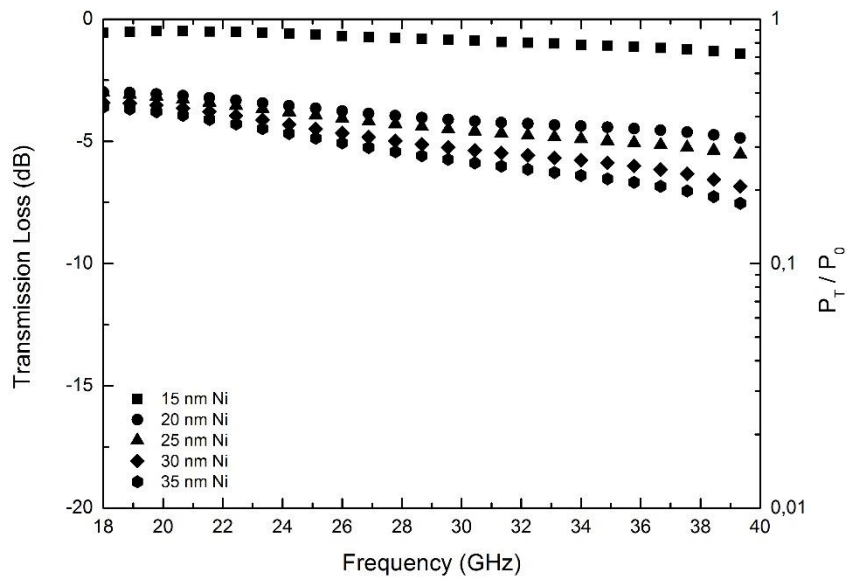


Figure 4.35 EM wave transmission loss varying with frequency in nickel surface modified single layer glass fiber woven fabrics.

Multilayered structures with four different cascading arrangements were characterized in terms of their EM behavior. Results are presented in Figure 4.36-Figure 4.38. EM wave reflection loss of nickel surface modified glass fiber woven fabrics show different results than those of silver and gold surface modified ones. EM wave reflection loss value of nickel surface modified samples shows a unique fluctuation; however, there is again no regular trend with varying number of layers. Possible reason for this might be related to the electrical and magnetic properties of nickel. Nickel is a ferromagnetic metal which has lower electrical conductivity, while silver and gold are diamagnetic with far higher electrical conductivities. EM wave reflection loss results of gold surface modified samples are changing between -5 dB and -15 dB.

Analyzing further, three layer structure shows the highest EM wave reflection loss at 22-34 GHz (Figure 4.36). This shows that rather than the number of layers, forming arrangements to obtain destructive interference is more important for improved EM wave reflection loss. On the other hand, EM wave transmission loss results of nickel surface modified samples show that increasing number of layers renders the multilayered structure to be less transparent against EM waves. Trends similar to silver and gold surface modified samples can be seen in nickel surface modified ones in terms of the EM wave transmission loss dependence on frequency. Increase in frequency results in decay on EM wave transmission. In Figure 4.37, it can be seen that EM wave transmission loss results are varying between -3 dB and -21 dB. Furthermore, EM wave absorption values were calculated from reflection and transmission data, and results of this are presented in Figure 4.38. It can be seen that 5 layered structure shows the maximum EM wave absorption at 40 GHz with a value of 85%. Comparing with gold surface modified samples, nickel surface modified ones show a lower maximum value; however, in these samples 80% EM wave absorption is obtained in broader frequency range.

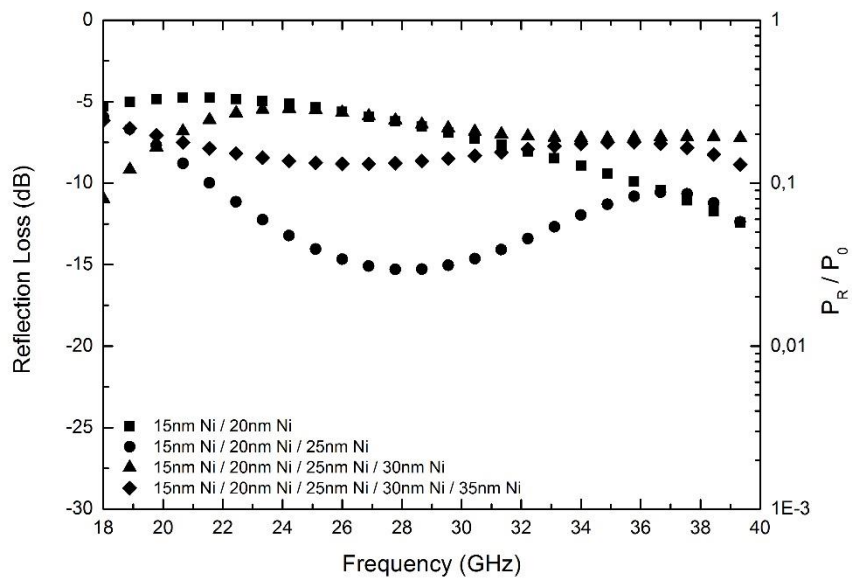


Figure 4.36 EM wave reflection loss varying with frequency in nickel surface modified multilayered glass fiber woven fabrics.

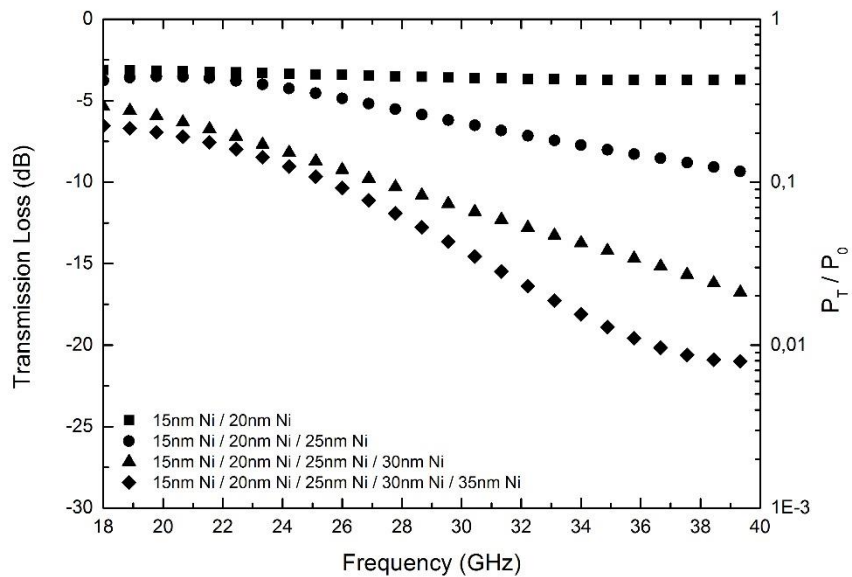


Figure 4.37 EM wave transmission loss varying with frequency in nickel surface modified multilayered glass fiber woven fabrics.

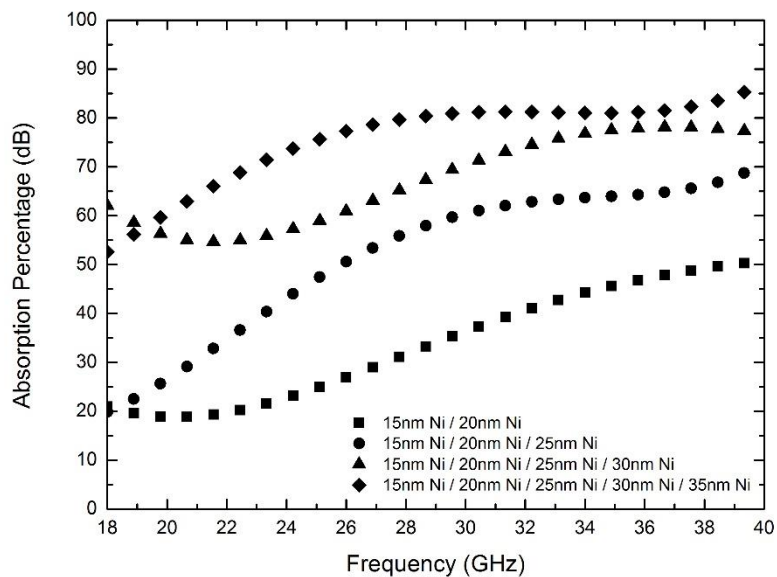


Figure 4.38 EM wave absorption percentages varying with frequency in nickel surface modified multilayered glass fiber woven fabrics.

Metallic backing plate was also used with nickel surface modified samples, and achieved EM wave reflection loss results are presented in Figure 4.39. From this figure, it can be understood that there is consistency in EM wave reflection with varying frequency. EM wave reflection loss values are almost constant at ~ 7.5 dB for all frequencies. This corresponds to $\sim 20\%$ EM wave reflection which is lower than the value obtained with gold surface modified samples. Nevertheless, nickel surface modification still provides promising EM wave absorption characteristics to be used in reinforcement materials.

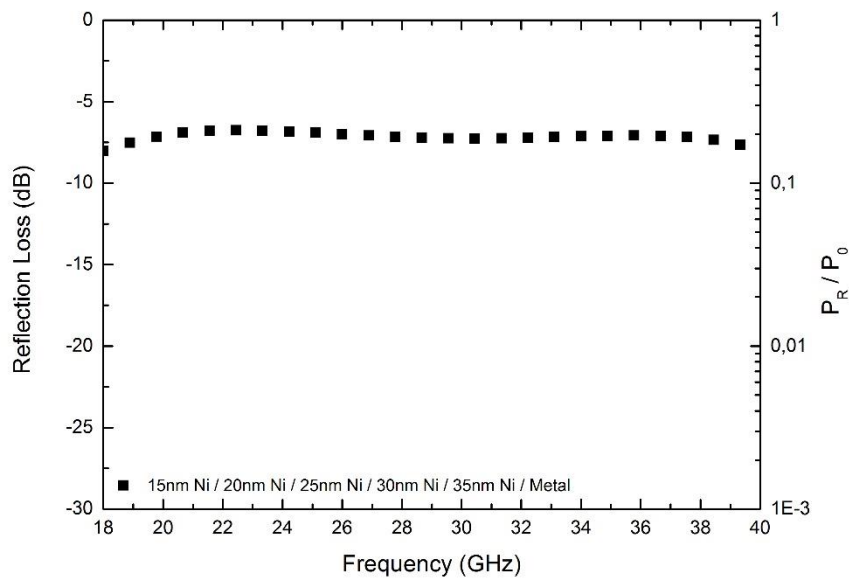


Figure 4.39 EM wave reflection loss varying with frequency in nickel surface modified 5-layered glass fiber woven fabrics with metallic backing plate.

Silanization treatment was also applied on nickel surface modified samples in order to tailor the mechanical properties of their composite structures. EM wave reflection, transmission and absorption characteristics of nickel surface modified glass fiber woven fabrics after silanization can be seen in Figure A.7-Figure A.12. Results show that being different than gold surface modified samples, there is observable effect of silanization over nickel surface modified ones. First of all, sample with 15 nm thick nickel film behaved far more transparent than the others; however, after silanization this distinct behavior of that sample has disappeared. There is also difference between the EM wave reflection behaviors of multilayered structures. Magnitude of fluctuations were suppressed with silanization. Due to small differences between the transmission behavior of the silanized and non-silanized samples, resulting EM wave absorptions were controlled directly by the effects in EM wave reflection. Suppression in the magnitude of the fluctuations of the reflection loss resulted in more consistent

EM wave absorption values through the whole frequency range for nickel surface modified samples. On the other hand, consistency in the EM wave reflection behavior of non-silanized samples with metallic backing plate has disappeared after silanization especially at lower frequencies. Consequently, obtained results demonstrated that nickel is a promising surface modification metal to be used on glass fiber woven fabrics.

4.3.2 Electromagnetic Measurement Results of Surface Modified Aramid Fiber Woven Fabrics

In this study, electromagnetic wave reflection, transmission, and hence absorption of surface modified aramid fiber woven fabrics were also investigated. Surface modifications were done using gold and nickel on aramid fiber woven fabrics. Silver has not been applied as a modifier on the aramid fiber woven fabrics due to the oxidation related complications of silver explained previously. Electromagnetic characteristics of gold and nickel surface modified aramid fiber woven fabric combinations were examined in single-layered and multi-layered form along with in silanized and non-silanized condition. As it was stated in reference [5], aramid (Kevlar) fiber woven fabrics are more promising to be used as reinforcement materials in EM wave absorbing polymer composites due to their more convenient dielectric properties compared to glass fiber woven fabrics.

4.3.2.1 EM Measurement Results of Aramid Fiber Woven Fabrics Surface Modified with Gold

As it has been stated previously, gold is a promising metal as surface modifier of woven fabrics. Similar to previously discussed studies on gold surface modifications on glass fiber woven fabrics, aramid fiber woven fabrics were also coated with gold. Aramid fiber woven fabrics modified with gold thin films with five different thickness, 15 nm, 20 nm, 25 nm, 30 nm, 35 nm, were characterized identically in terms of their EM characteristics. EM wave reflection and transmission loss of single layered samples can be seen in Figure 4.40 and Figure 4.41 as a function of frequency. Results

show that gold surface modified aramid fiber woven fabrics are less reflective than glass fiber woven fabrics. However, there is no significant change in EM wave transmission loss compared to the results of the gold surface modified glass fiber woven fabrics. As it is demonstrated in Figure 4.40 and Figure 4.41, EM wave reflection loss varies between -5 dB and -13 dB, while EM wave transmission loss changes between 0 dB and -5dB. Similar to the previous observations, it is obvious that as thickness of the gold film increases, reflection part of EM waves rises while transmission part of EM waves decays. Major difference between gold surface modified aramid and glass samples is the consistency of either loss values with frequency. In the case of aramid fiber woven fabrics, there is almost no variation in the loss values with frequency. This behavior seems to be quite critical towards achieving broadband EM wave absorption.

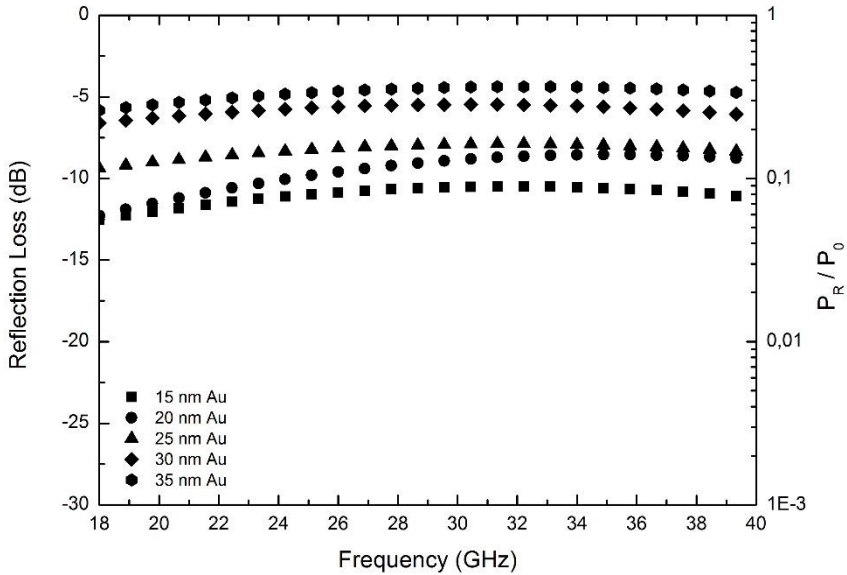


Figure 4.40 EM wave reflection loss varying with frequency in gold surface modified single layer aramid fiber woven fabrics.

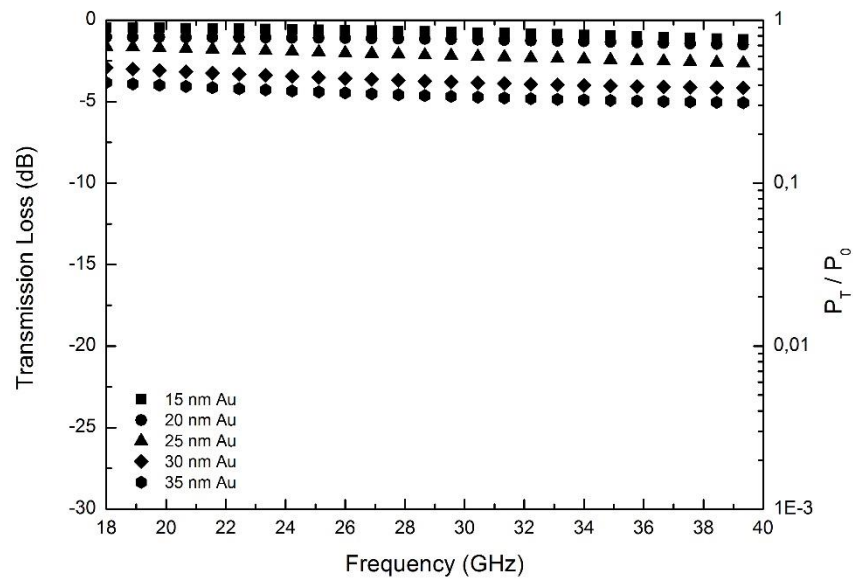


Figure 4.41 EM wave transmission loss varying with frequency in gold surface modified single layer aramid fiber woven fabrics.

Gold surface modified single layer woven fabrics were cascaded to form multilayered structures according to increasing film thickness. Four different multilayered structures were created and characterized similar to the previous discussions. EM wave reflection, transmission and absorption characteristics of multilayered samples are presented in Figure 4.42-Figure 4.44. As in the case of the previous studies, EM wave reflection loss does not follow regular trend with increasing number of layers. However, one significant difference is that magnitude of fluctuations in reflection with changing frequency is larger. As a result of this, EM wave reflection loss values fluctuate between 0 dB and -25 dB. On the other hand, EM wave transmission reduces with increasing number of layers, as observed in the previous cases. While transmission loss of two, three and four layered structures are changing between 0 dB and -5 dB, that of the five layered structure decreases from -5 dB to -15 dB with increasing frequency. This change may possibly lead to high EM wave absorption. EM

wave absorption calculated using obtained reflection and transmission results, confirms this statement. Five layered structure presents more than 90% absorption above 30 GHz, where it exceeds 95% at high frequencies. This is the highest absorption level obtained throughout this study.

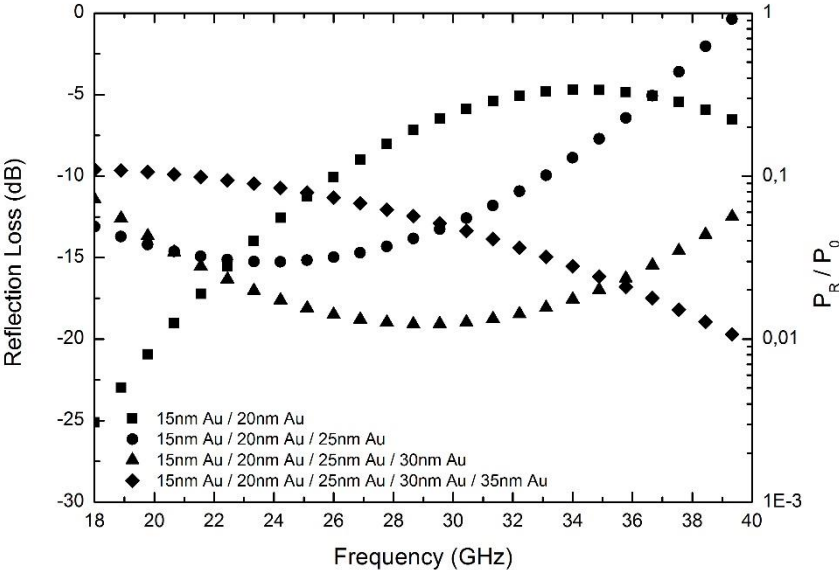


Figure 4.42 EM wave reflection loss varying with frequency in gold surface modified multilayered aramid fiber woven fabrics.

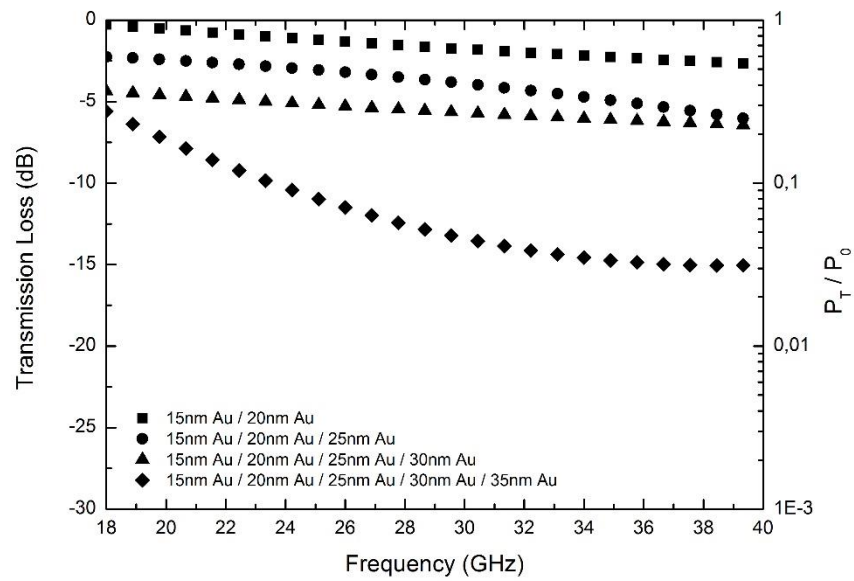


Figure 4.43 EM wave transmission loss varying with frequency in gold surface modified multilayered aramid fiber woven fabrics.

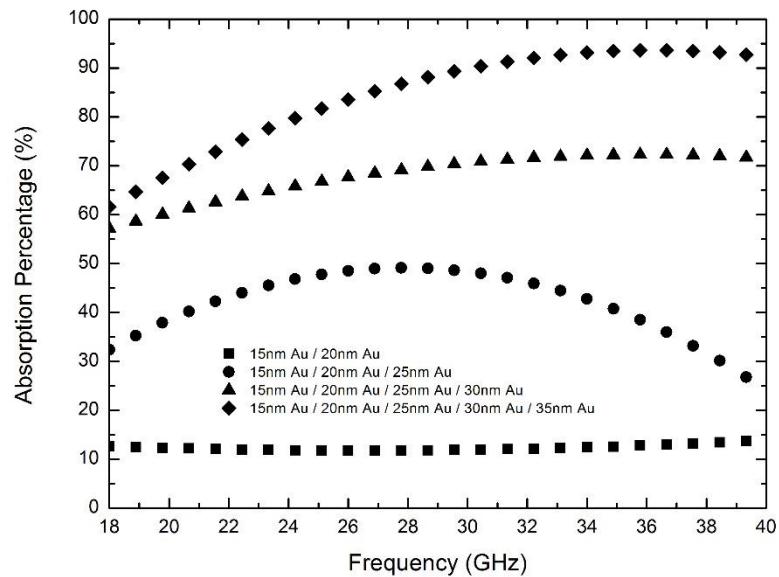


Figure 4.44 EM wave absorption percentage varying with frequency in gold surface modified multilayered aramid fiber woven fabrics.

Metallic backing plate was also used for surface modified aramid fiber woven fabrics in order to determine their behavior when structures are used in shielding conditions. Obtained results are represented in Figure 4.45. Reflection loss values are fluctuating with frequency. In the mid frequency range, there is an absorption close to 98% achieved by less than -15 dB reflection, while at low and high frequency ranges absorption decays to 20%. This represents that EM wave absorption can be tuned for varying frequency. In this study, metallic plate backed five layered arrangement showed the highest absorption at 25-33 GHz. It is possible to obtain similarly high absorption values at other frequency ranges by changing arrangements in the multilayered structures.

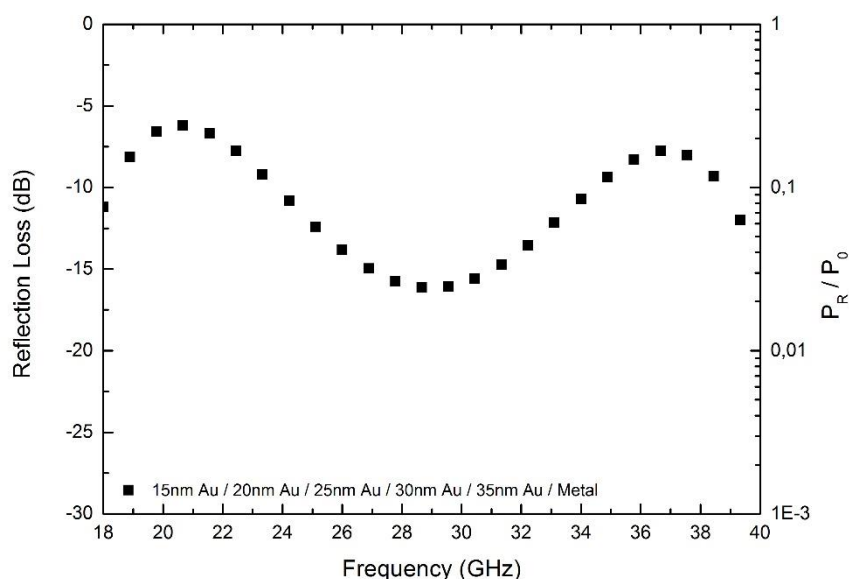


Figure 4.45 EM wave reflection loss varying with frequency in gold surface modified 5-layered aramid fiber woven fabrics with metallic backing plate.

Gold surface modified aramid fiber woven fabrics structures revealing the highest EM wave absorption were subjected to silanization. Silanization treatments applied on gold

surface modified glass fiber woven fabrics had no remarkable effect in their EM characteristics. However, in this case silanization treatment resulted in changes in the geometry of the aramid fiber woven fabrics, and hence in their EM characteristics. The change in the geometry of the gold surface modified aramid fiber woven fabrics after silanization is presented in Figure 4.46. In this figure, it can be seen that silanization causes variations in the diameter of the fiber yarns. Most probably aramid fiber woven fabrics soaked the sprayed silane solution which has resulted in their swelling.

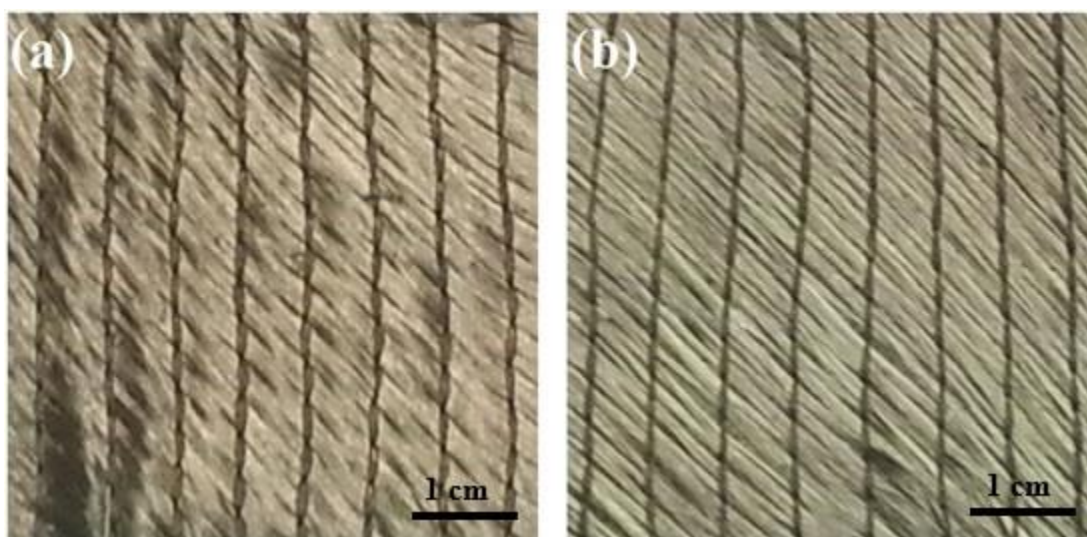


Figure 4.46. Aramid fiber woven fabrics with gold surface modification as (a) non-silanized and (b) silanized.

Results of EM wave reflection, transmission; hence absorption measurements of silanized gold surface modified aramid fiber woven fabrics are represented in Figure A.13-Figure A.18. Despite the geometry changes observed, there is no remarkable change in the EM characteristics after silanization. Again, silanization affected the reflection behavior of the multilayered structures and changed the fluctuations. However, these changes in reflection did not affect the absorption characteristics significantly. The only difference in the EM wave absorption characteristics is the

broadening of the frequency range for high absorption. Furthermore, silanization has changed the EM wave reflection characteristic of the structure with metallic backing plate in a beneficial way. Fluctuation in the reflection loss was suppressed, and this resulted in approximately 92% absorption consistent throughout the whole frequency range.

4.3.2.2 EM Measurement Results of Aramid Fiber Woven Fabrics Surface Modified with Nickel

Identical studies were conducted on nickel surface modified aramid fiber woven fabric structures. EM wave reflection and transmission loss characteristics of single layered nickel surface modified aramid fiber woven fabrics are represented in Figure 4.47- Figure 4.48. Reflection and transmission loss values are changing between -7 and -14 dB and 0 dB and -3 dB, respectively. Notable difference of this combination is the shift in the reflection characteristic. Obtained maximum reflection is around -7 dB.

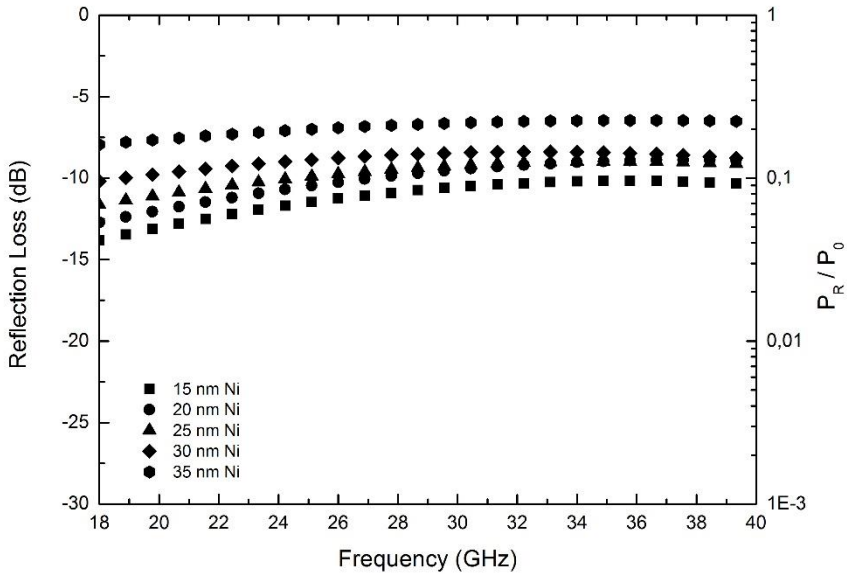


Figure 4.47 EM wave reflection loss varying with frequency in nickel surface modified single layer aramid fiber woven fabrics.

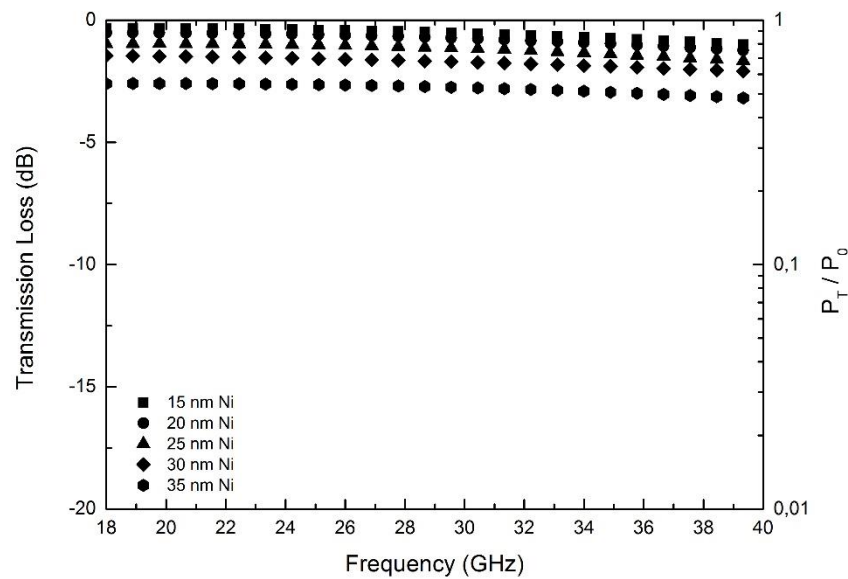


Figure 4.48 EM wave transmission loss varying with frequency in nickel surface modified single layer aramid fiber woven fabrics.

EM wave reflection, transmission and absorption measurement results of nickel surface modified aramid fiber woven fabric multilayered structures are demonstrated in Figure 4.49-Figure 4.51. Similar to single layered structures, multilayered structures show relatively low EM wave reflection compared to gold surface modified samples where their loss values are fluctuating between -7dB and -25 dB. On the contrary, structures behave more transparent for all number of layers. EM wave transmission loss results are changing between 0 dB and -5 dB. These results point out that EM wave absorption capability of these multilayered structures is probably deficient. In Figure 4.51, it can be seen clearly that maximum EM wave absorption achieved is ~55% for the five layered structure. This illustrates that nickel surface modification and aramid fiber woven fabric combinations are not suitable reinforcement materials for EM wave absorbing composites.

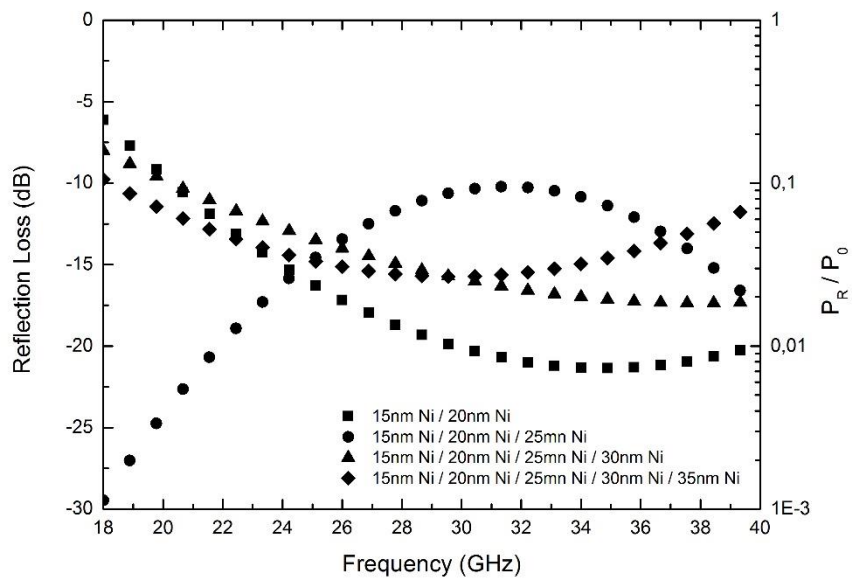


Figure 4.49 EM wave reflection loss varying with frequency in nickel surface modified multilayered aramid fiber woven fabrics.

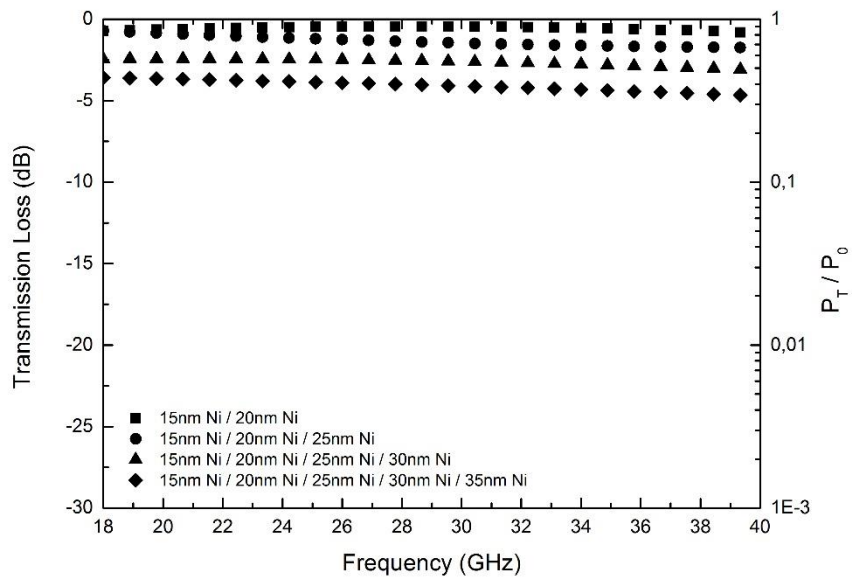


Figure 4.50 EM wave transmission loss varying with frequency in nickel surface modified multilayered aramid fiber woven fabrics.

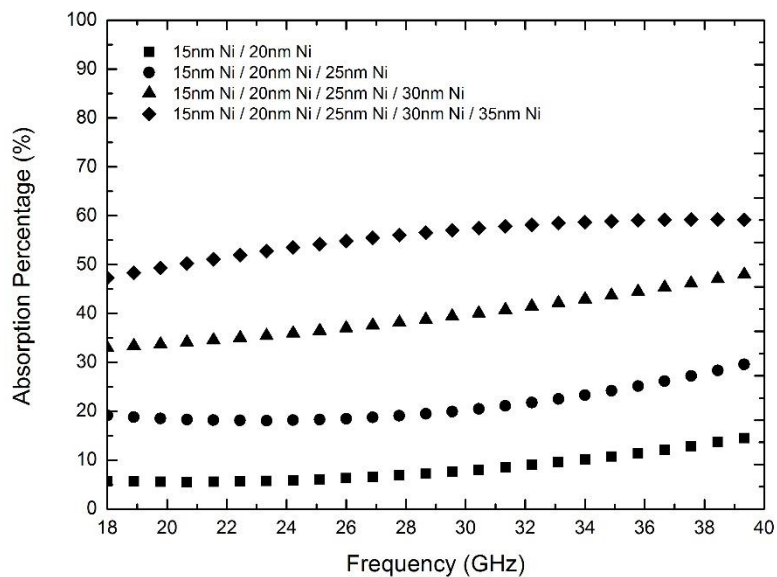


Figure 4.51 EM wave absorption percentage varying with frequency in nickel surface modified multilayered aramid fiber woven fabrics.

EM wave reflection measurements were also done for nickel surface modified aramid fiber woven fabrics backed with a metallic plate, even though their absorption values were relatively low. Obtained results are indicated in Figure 4.52. As it is expected due to the low absorption capability of the multilayered structures, reflection loss of the metallic plate backed 5-layered structure changes between -5 dB and -10 dB corresponding to 60-90% absorption of the incident EM energy.

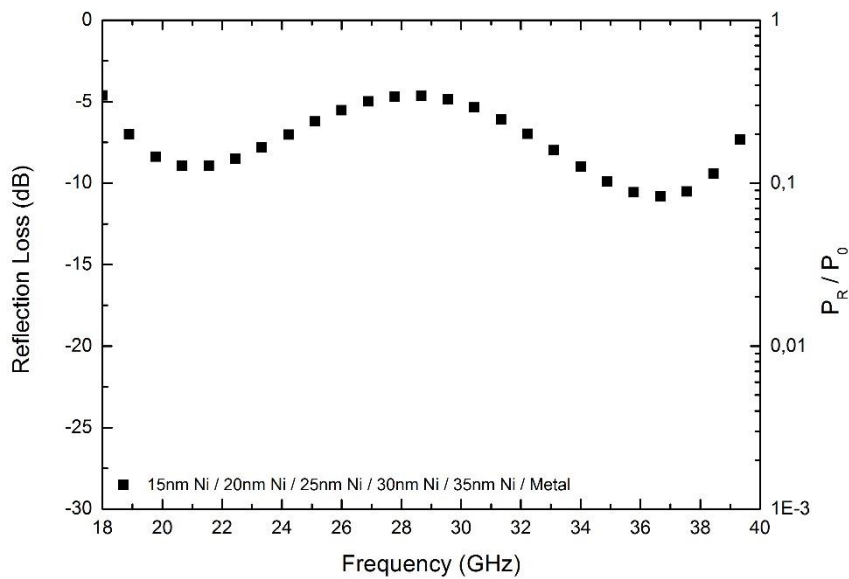


Figure 4.52 EM wave reflection loss varying with frequency in nickel surface modified 5-layered aramid fiber woven fabrics with metallic backing plate.

Silanization treatments were also applied on the nickel surface modified aramid fiber woven fabric combinations. EM wave reflection, transmission and absorption measurements were also conducted on these combinations after silanization. No significant change in the EM characteristics of these combinations has been observed after silanization as demonstrated in Figure A.19-Figure A.24.

4.3.3 Electromagnetic Measurements Results of Surface Modified PET Sheets

In this part of the study, effect of substrate material and its surface topography on the resulting EM characteristics were examined. Different than the previous studies, gold thin films with 4 different thickness have been applied on smooth PET sheets. As the representative surface modification metal gold was chosen due to the superior EM characteristics it presented in this studies.

15 nm, 20 nm, 25 nm and 30 nm thick gold thin films were coated on PET sheets using thermal evaporation method applying identical parameters used in previous cases. Firstly, single layers of gold surface modified PET sheets were analyzed and results are demonstrated in Figure 4.53 and Figure 4.54. As it can be seen, 20 nm, 25 nm and 30 nm thick thin film containing samples show almost fully reflective behavior. Only 15 nm thick Au film containing PET sample show EM wave reflection loss different than 0 dB, which is ~ -4 dB. On the other hand, 20 nm, 25 nm and 30 nm thick thin film containing samples do not allow the transmission of the EM waves evident from the reflection loss values changing between ~ -25 and -35 dB (Figure 4.54). However, 15 nm thick Au thin film containing PET sheet shows ~ -10 dB transmission loss, which corresponds to $\sim 10\%$ transmission of the incident EM wave through the material.

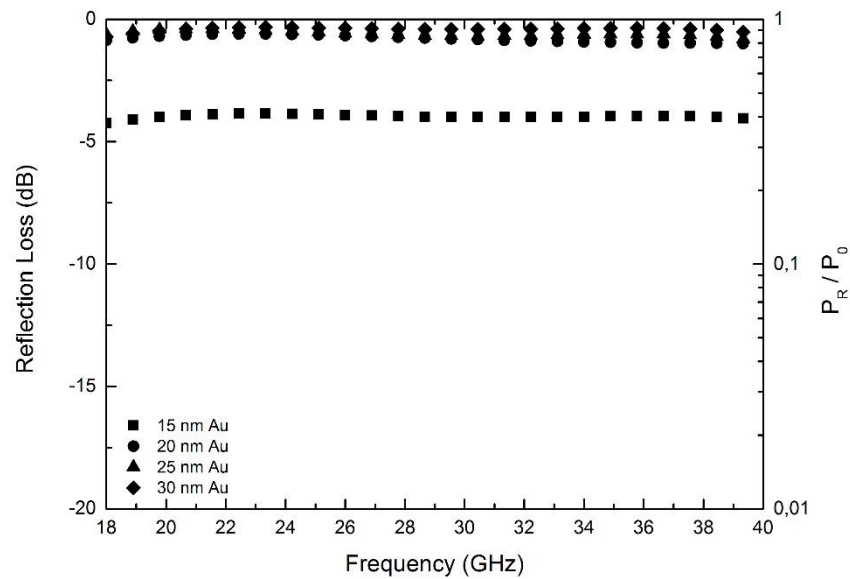


Figure 4.53 EM wave reflection loss varying with frequency in gold surface modified single layer PET sheets.

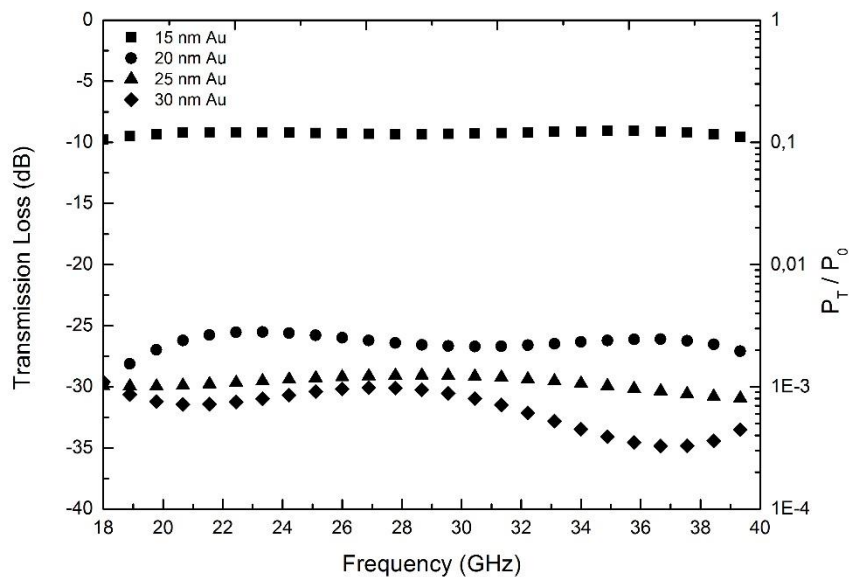


Figure 4.54 EM wave transmission loss varying with frequency in gold surface modified single layer PET sheets.

In the light of the results obtained from single layered gold surface modified PET sheets, it is expected that multilayered structures cannot show high EM wave absorption. EM wave reflection, transmission and absorption measurement results of multilayered structures are shown in Figure 4.55-Figure 4.57. Comparing the EM wave reflection and transmission loss values of single layers and multilayered structures, it is understood that multilayered structures provided destructive interference which has resulted in a weaker reflective behavior. Moreover, multilayered structures show less transmission as expected. Despite the weakening in both reflection and transmission by forming multilayered structures, calculated absorption values do not exceed 30%.

Studies have shown that surface topography and geometry of the reinforcement materials are major factors controlling the EM wave absorption. Same surface modification material, gold, with the same applied thickness resulted in far different

EM characteristics on different substrate materials. This important finding incorporated a different viewpoint to the current study. Consequently, it was decided that effects of surface topography and geometry of the surface modified substrate materials on their EM characteristics should be investigated within the scope of a different project that should be based on modelling and simulation.

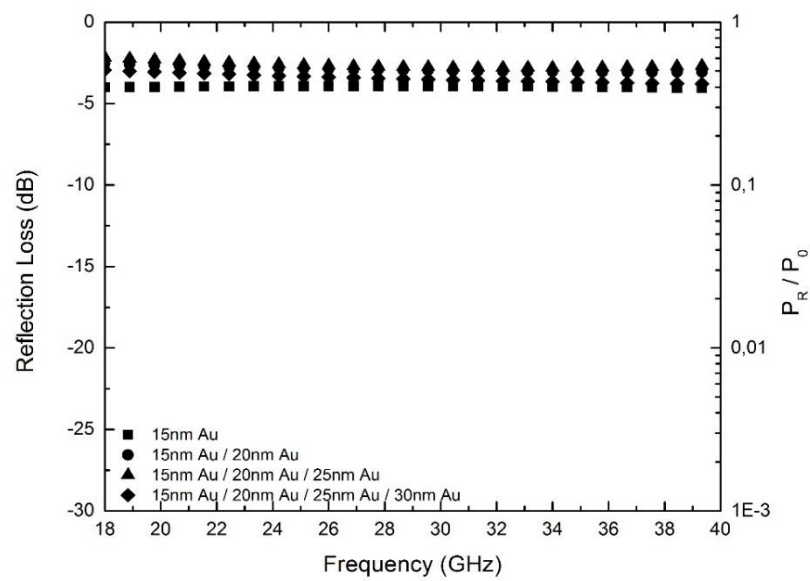


Figure 4.55 EM wave reflection loss varying with frequency in gold surface modified multilayered PET sheets.

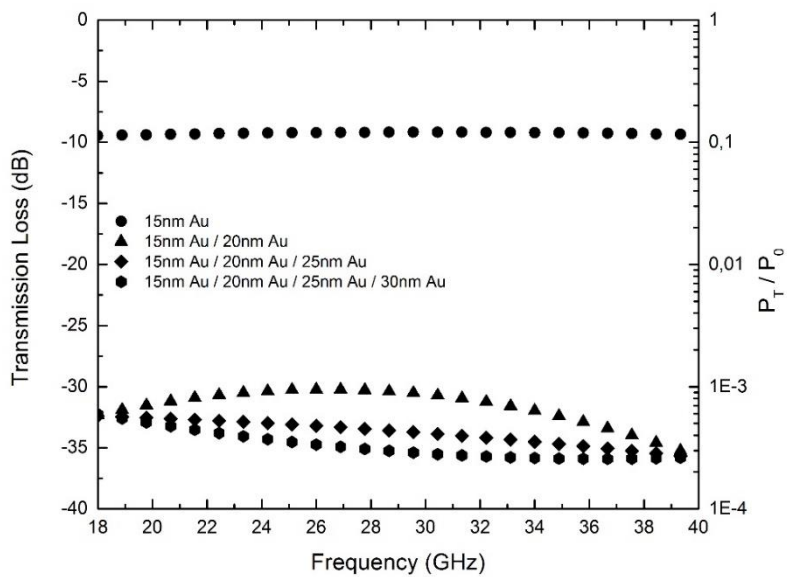


Figure 4.56 EM wave transmission loss varying with frequency in gold surface modified multilayered PET sheets.

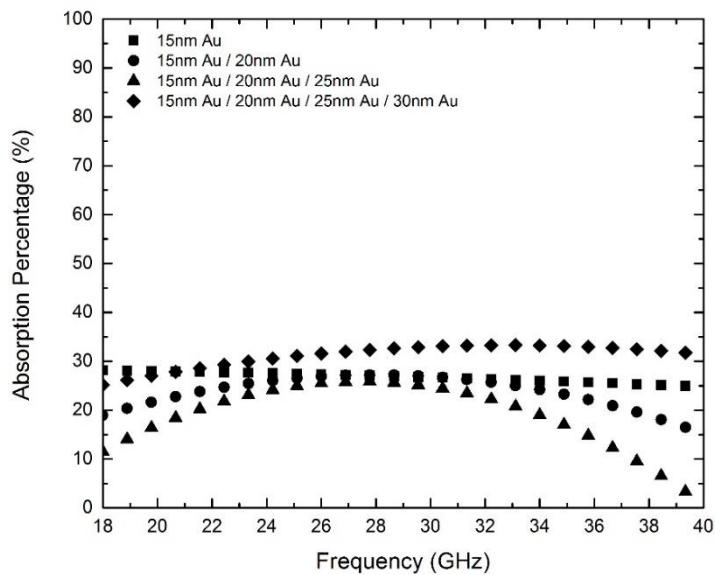


Figure 4.57 EM wave absorption percentage varying with frequency in gold surface modified multilayered PET sheets.

4.3.4 Electromagnetic Measurements and Results of Prototype Composite Structures

In this study, EM wave reflection, transmission and absorption characterization were done on prototype composites fabricated using the surface modified multilayered reinforcement materials which are the most promising in terms of EM wave absorption as discussed above. The most promising combinations, namely gold-glass fiber, gold-aramid fiber, nickel-glass fiber and nickel-aramid fiber, of multilayered reinforcement materials were incorporated in the epoxy matrix. EM characterizations were done on the composites containing silanized and non-silanized versions of these 4 combinations. Moreover, in order to determine the EM wave absorption/shielding capability of the fabricated composites in a fully reflective condition, EM characteristics of the composite were also investigated with the presence of a metallic backing plate.

In this study, effect of silanization on the EM characteristics of the composites could be seen clearly. Especially in terms of EM wave reflection, composites showed different behaviors with and without silanization. Remarkable point of this study is the harmony obtained between the surface modifiers and reinforcement materials in forming the combinations. Although, multilayered structures of the surface modified woven fabrics showed high absorption values, their composite structures resulted in lower absorptions. This demonstrated the fact that there should be a compatibility between the reinforcement materials, surface modifiers and matrix materials. Furthermore, silanization and surface geometry of the reinforcement structures are also effective on the EM characteristics of the resulting composites.

4.3.4.1 Electromagnetic Measurement Results of Gold Surface Modified Multilayered Glass Fiber Woven Fabric Containing Prototype Composites

EM characterization measurement results; namely reflection, transmission, absorption and reflection with the presence of a metallic backing plate, of the composites containing gold surface modified multilayered glass fiber woven fabrics can be seen in Figure 4.58-Figure 4.61. According to these results, it can be seen that there is

significant effect of silanization of reinforcement materials on the EM properties of the composites. Silanized samples showed more reflection and less transmission against EM waves. Due to the differences between the amount of shifts for both reflection and transmission loss values, silanized samples are expected to reveal lower EM wave absorption. Possibly, improved interfacial bonding with silanization created geometry variations in the composite structure affecting the EM characteristics of the composite.

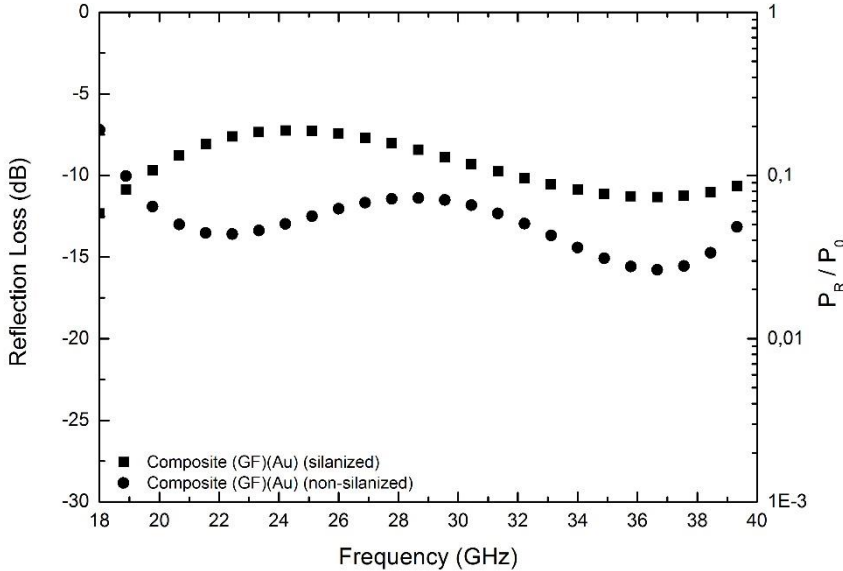


Figure 4.58 EM wave reflection loss varying with frequency in silanized and non-silanized composites containing gold surface modified multilayered glass fiber woven fabrics.

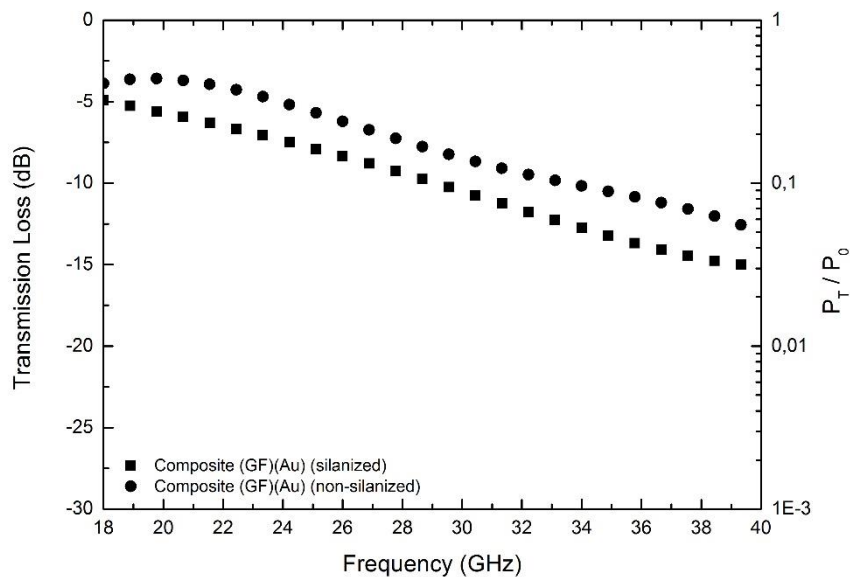


Figure 4.59 EM wave transmission loss varying with frequency in silanized and non-silanized composites containing gold surface modified multilayered glass fiber woven fabrics.

Analysis of EM wave absorption results proved the accuracy of the prediction made previously. In the large portion of frequency range, non-silanized composite revealed higher EM wave absorption. The maximum EM wave absorption achieved by the composites is ~80%. According to the previous results, gold surface modified 5-layered glass fiber woven fabric revealed 90% EM wave absorption. Comparing these two cases, it can be said that both silanization and incorporation of the epoxy matrix into the composite structure decreased the EM wave absorption capability of the surface modified fiber woven reinforcements.

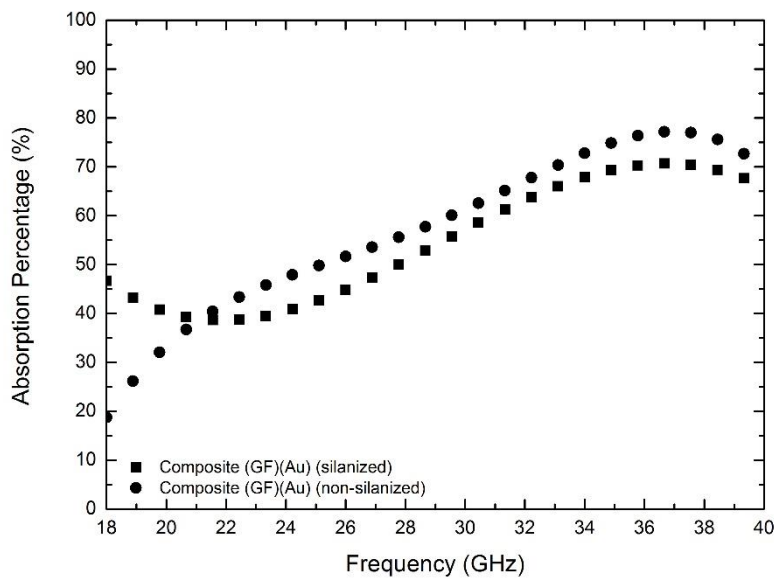


Figure 4.60 EM wave absorption percentage varying with frequency in silanized and non-silanized composites containing gold surface modified multilayered glass fiber woven fabrics.

Study with the presence of a metallic backing plate demonstrated that even though, composites show low EM wave absorptions, their usage in shielding condition can be quite promising. Non-silanized composite revealed a maximum of 98% EM wave absorption at 29 GHz and through a large portion of the investigated frequency range it revealed more than 90% absorption. Results showed that surface modified reinforcement materials introduced in polymeric matrices have high potential to used in EM wave absorbing/shielding composites.

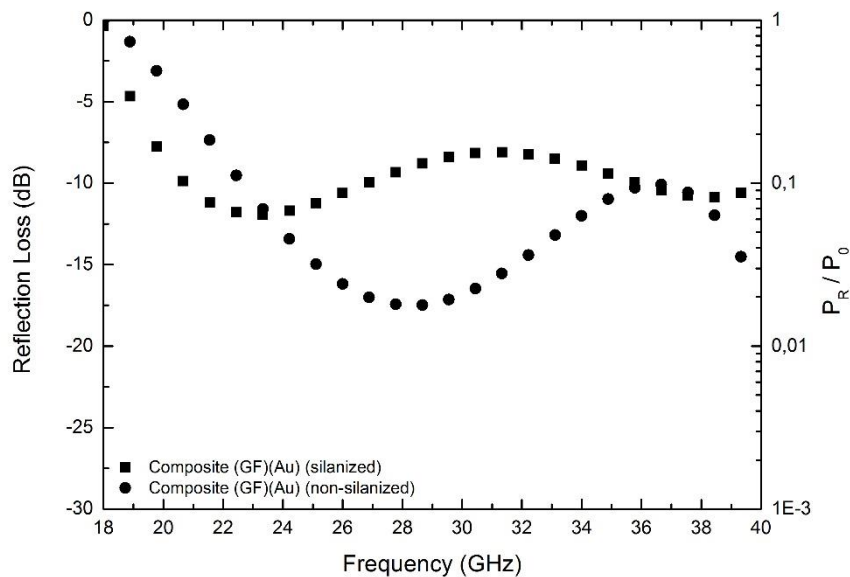


Figure 4.61 EM wave reflection loss varying with frequency in silanized and non-silanized composites containing gold surface modified multilayered glass fiber woven fabrics under the presence of a metallic backing plate.

4.3.4.2 Electromagnetic Measurement Results of Nickel Surface Modified Multilayered Glass Fiber Woven Fabric Containing Prototype Composites

EM characterization measurement results; namely reflection, transmission, absorption and reflection with the presence of a metallic backing plate, of the composites containing nickel surface modified multilayered glass fiber woven fabrics can be seen in Figure 4.62-Figure 4.65. Analyzing these results, significant effect of silanization on the EM characteristics of the surface modified reinforcement materials can be seen. Silanized samples revealed more EM wave reflection; however, also more EM wave transmission as opposed to the previous case. Reflection loss is shifted by ~6 dB, where shift in transmission loss is about 5 dB on average for the silanized composite compared to those of the non-silanized one. This pointed out that difference in the absorption percentages of the two cases should be remarkable.

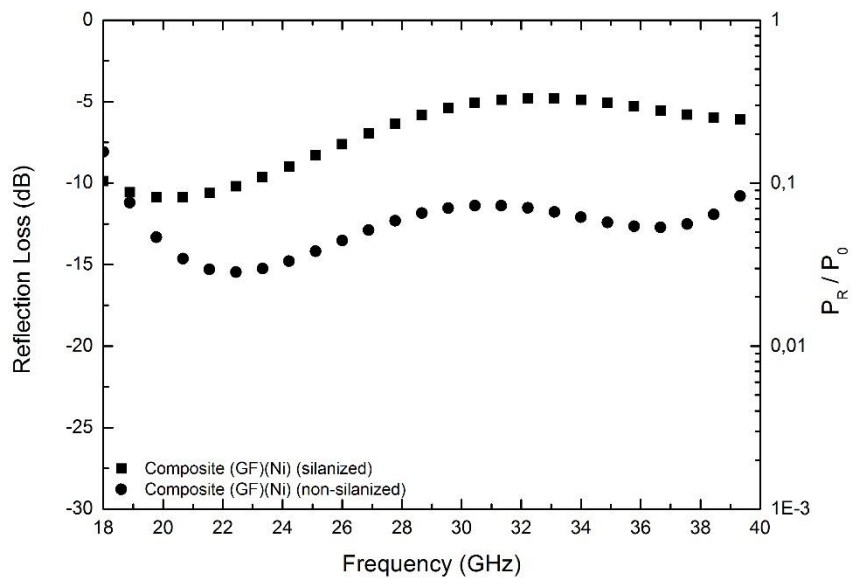


Figure 4.62 EM wave reflection loss varying with frequency in silanized and non-silanized composites containing nickel surface modified multilayered glass fiber woven fabrics.

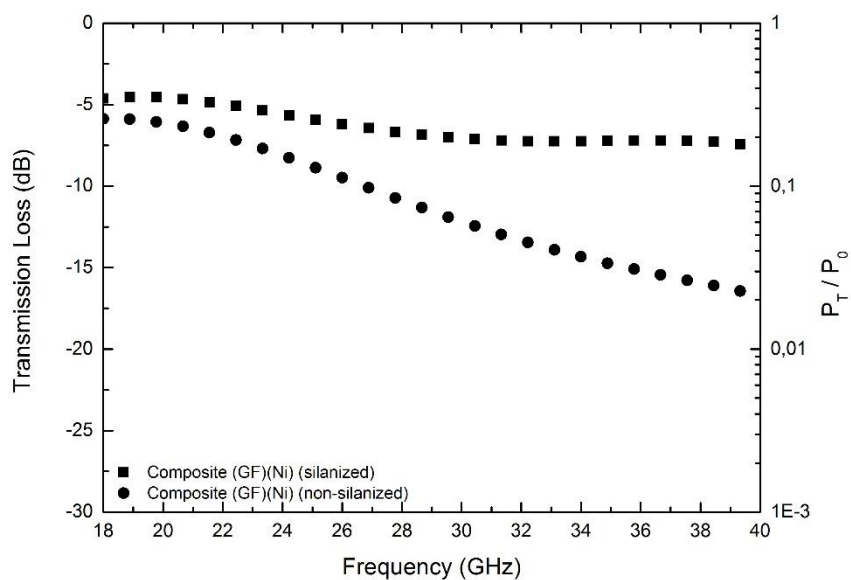


Figure 4.63 EM wave transmission loss varying with frequency in silanized and non-silanized composites containing nickel surface modified multilayered glass fiber woven fabrics.

As it is expected, there is a considerable difference between the absorption percentages of the silanized and non-silanized composites. While silanized composite showed a maximum of 60% absorption, 92% EM wave absorption has been reached by the non-silanized one. In addition, as discussed earlier nickel surface modified multilayered glass fiber woven fabrics revealed 80% absorption. This indicated that there are variations between the EM absorption percentages of surface modified reinforcement materials and their composites. Gold containing composites revealed lower absorption than their multilayered structures, while nickel containing ones behaved inversely.

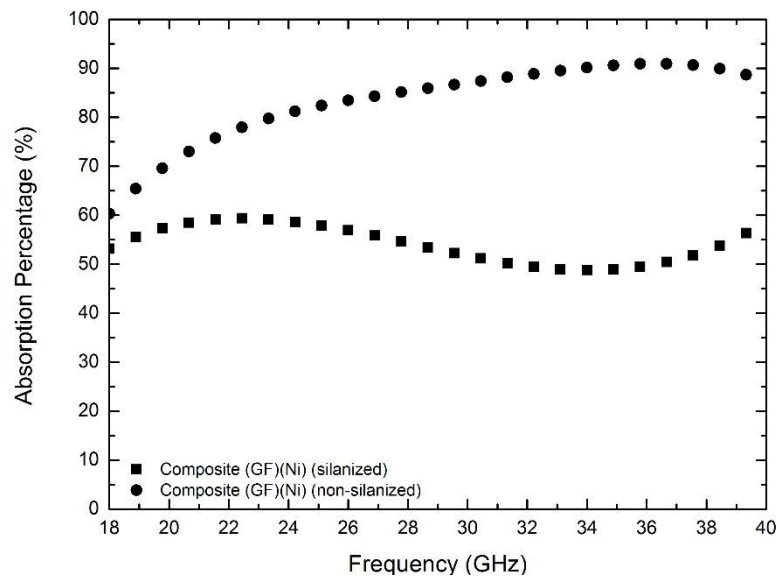


Figure 4.64 EM wave absorption percentage varying with frequency in silanized and non-silanized composites containing nickel surface modified multilayered glass fiber woven fabrics.

According to reflection measurements on these composites under the presence of a metallic backing plate, it is clear that silanization is not suitable for glass fiber woven

fabric reinforcement materials. While a maximum of 93% absorption is obtained by non-silanzed composite, under 80% absorption can be obtained by silanzed composite for broadband frequency range (Figure 4.65).

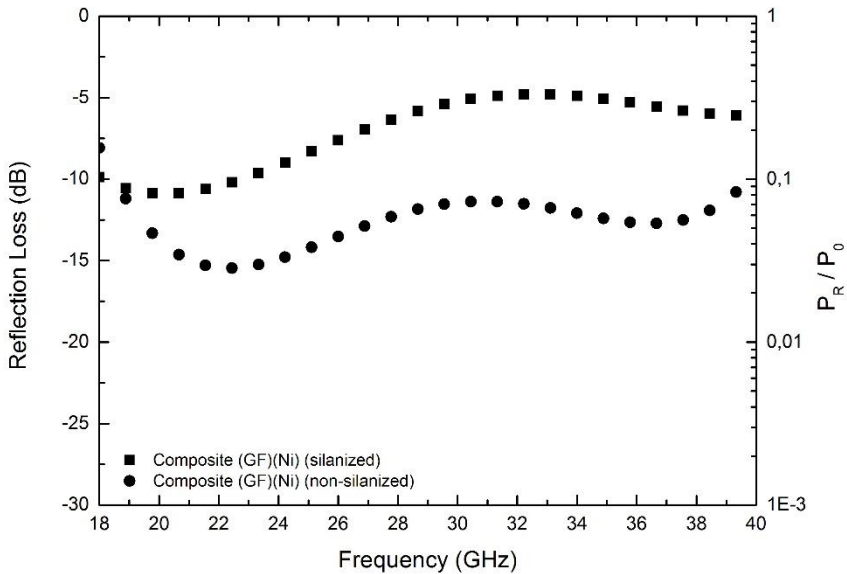


Figure 4.65 EM wave reflection loss varying with frequency in silanzed and non-silanzed composites containing nickel surface modified multilayered glass fiber woven fabrics under the presence of a metallic backing plate.

4.3.4.3 Electromagnetic Measurement Results of Gold Surface Modified Multilayered Aramid Fiber Woven Fabric Containing Prototype Composites

EM wave characterization measurement results; reflection, transmission, absorption and reflection with metallic backing plate, of composites containing gold surface modified multilayered aramid fiber woven fabrics can be seen in Figure 4.66-Figure

4.69. According to these results, effect of silanization of reinforcement materials on the resulting EM characteristics can be seen. Silanized samples showed more reflection against EM waves in the lower frequency range, while at higher frequencies the situation is just the opposite. EM wave reflection loss values are changing between -7 dB and -20 dB. Moreover, non-silanized composite shows more transparent behavior against EM waves through the whole frequency range.

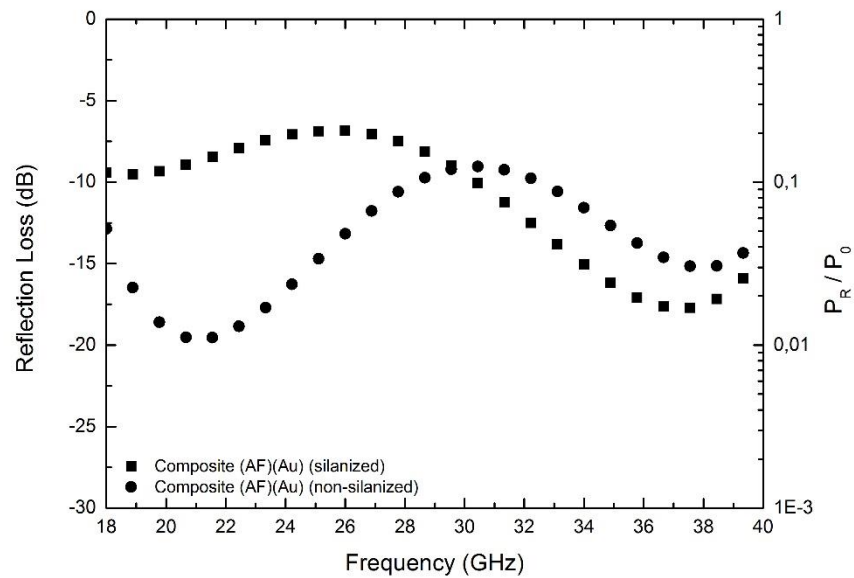


Figure 4.66 EM wave reflection loss varying with frequency in silanized and non-silanized composites containing gold surface modified multilayered aramid fiber woven fabrics.

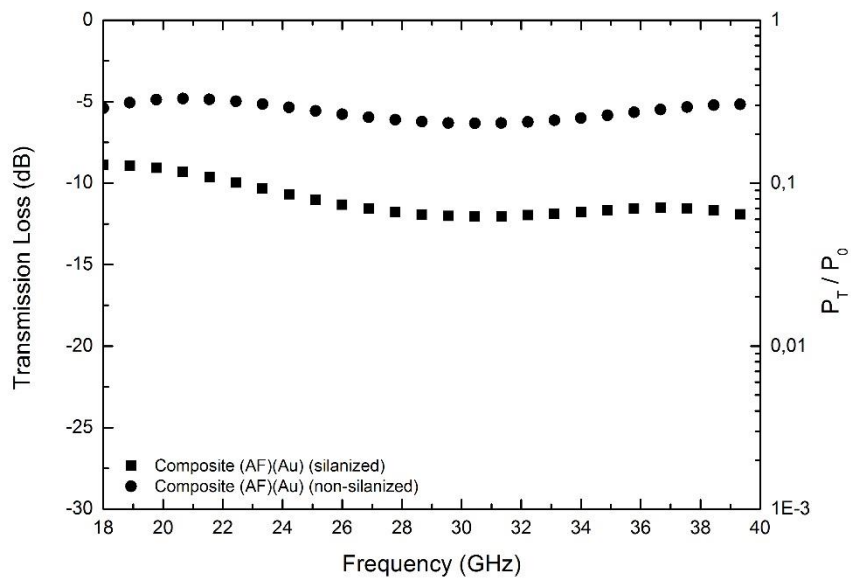


Figure 4.67 EM wave transmission loss varying with frequency in silanized and non-silanized composites containing gold surface modified multilayered aramid fiber woven fabrics.

Comparing the EM wave absorption of multilayered structures of gold surface modified aramid fiber woven fabrics (Figure 4.44) and that of their composites (Figure 4.68), it is seen that absorption values are changing between ~70 and 90% in the latter case, which is comparable with that of the former. This shows that formation of the composite structure does not deteriorate the EM wave absorption capability of the surface modified multilayered aramid fiber woven fabrics.

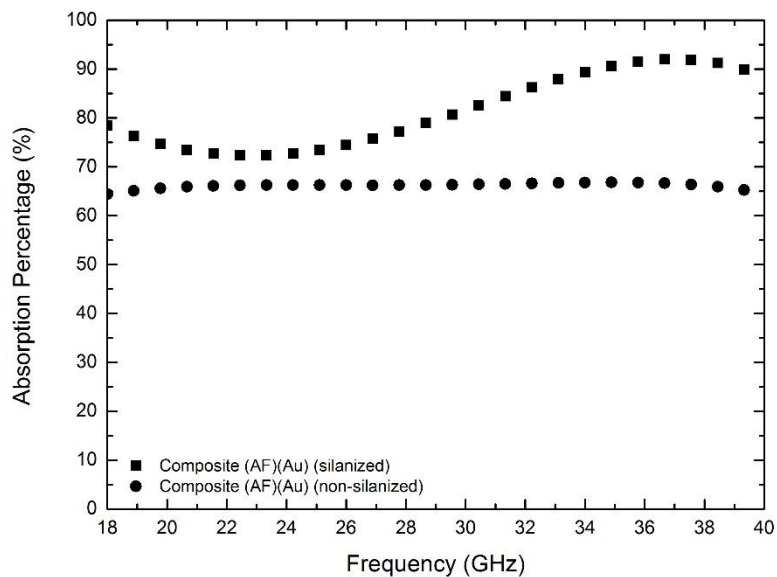


Figure 4.68 EM wave absorption percentage varying with frequency in silanized and non-silanized composites containing gold surface modified multilayered aramid fiber woven fabrics.

Furthermore, with metallic backing plate, composite structures again revealed high EM wave absorption values. Silanized composite revealed ~90% absorption through a large portion of the investigated frequency range while EM wave absorption as high as 99% has been obtained within 36-40 GHz range. In this particular composite, silanization seems to have a positive effect on the resulting absorption behavior by changing the reinforcement geometry.

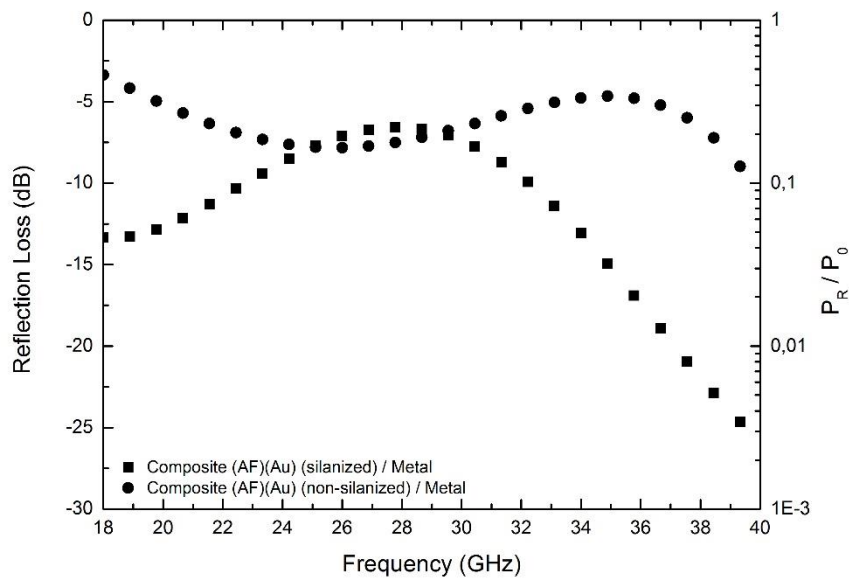


Figure 4.69 EM wave reflection loss varying with frequency in silanized and non-silanized composites containing gold surface modified multilayered aramid fiber woven fabrics under the presence of a metallic backing plate.

4.3.4.4 Electromagnetic Measurement Results of Nickel Surface Modified Multilayered Aramid Fiber Woven Fabric Containing Prototype Composites

EM wave characterization measurement results; reflection, transmission, absorption and reflection with metallic backing plate, of composites containing nickel surface modified multilayered aramid fiber woven fabrics can be seen in Figure 4.70-Figure 4.73. In this particular case, silanized composites showed both more reflective and more transparent behavior against the EM waves. This should result in lower absorption capability of silanized composites compared to non-silanized ones.

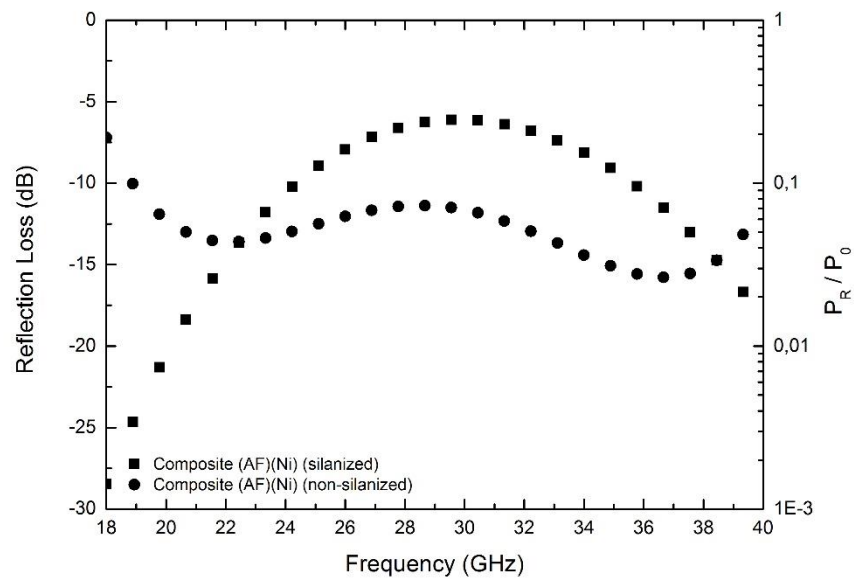


Figure 4.70 EM wave reflection loss varying with frequency in silanized and non-silanized composites containing nickel surface modified multilayered aramid fiber woven fabrics.

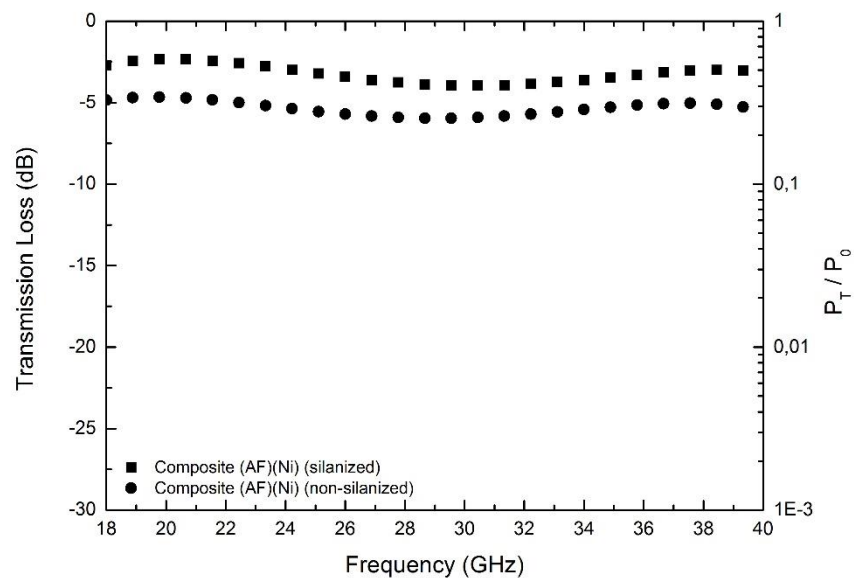


Figure 4.71 EM wave transmission loss varying with frequency in silanized and non-silanized composites containing nickel surface modified multilayered aramid fiber woven fabrics.

Low absorption capability was expected for the silanized composite, and Figure 4.72 shows that there is in fact a significant difference in the determined absorption values. While non-silanized composite revealed over 68% absorption in the higher frequency range, obtained maximum EM wave absorption is ~48% for the silanized composite. Furthermore, the highest EM wave absorption obtained with the nickel surface modified multilayered aramid fiber woven fabrics was 55% (Figure 4.51) while it is above 68% in its composite (Figure 4.72). This shows that as in the case of the gold surface modification formation of the composite structure does not deteriorate the EM wave absorption capability of the nickel surface modified multilayered aramid fiber woven fabrics.

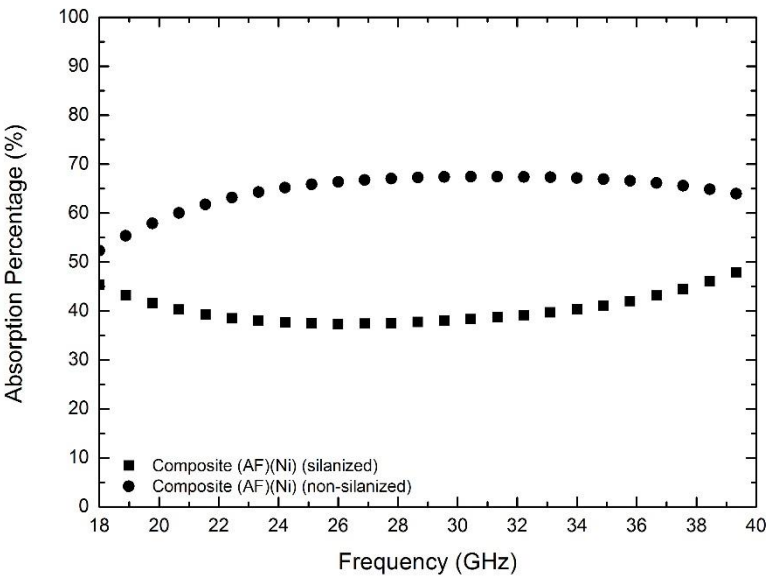


Figure 4.72 EM wave absorption percentage varying with frequency in silanized and non-silanized composites containing nickel surface modified multilayered aramid fiber woven fabrics.

Overall, although low absorption values were obtained under the presence of a metallic backing plate, non-silanzed composite revealed lower reflection, and hence higher absorption under fully reflective condition. It showed higher than 90% absorption in 24-40 GHz frequency range (Figure 4.73).

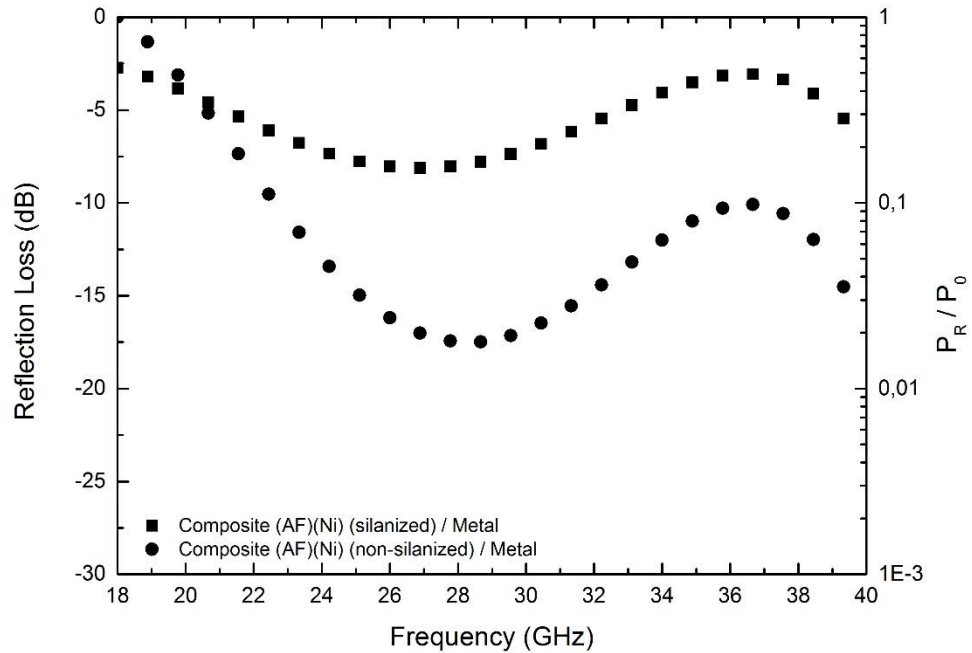


Figure 4.73 EM wave reflection loss varying with frequency in silanzed and non-silanzed composites containing nickel surface modified multilayered aramid fiber woven fabrics under the presence of a metallic backing plate.

4.3.5 Electromagnetic Measurement Simulation Studies

In the last part of the EM measurement studies, EM characteristics of the multilayered structures were simulated and achieved results were compared with the previously presented experimental data. Gold-glass fiber, nickel-glass fiber, gold-aramid fiber and nickel-aramid fiber multilayered structures were subjected to this mathematical

simulation. According to simulation studies, EM wave reflection results do not show similarities with the experimental values, whereas transmission results are promising. For all of the four different combinations, studies demonstrated that reflection predictions are not matching with the experimental values, while they are very well matching in terms of transmission. This conclusion suggests that prediction of the EM wave absorption characteristics may be achieved poorly (Figure 4.76).

Applied simulation method causes this discrepancy probably due to the virtually formed circuit within this method. Mathematical calculations for simulations are based on electrical and magnetic behaviors of materials. For the used software mathematically calculating the model, virtually formed circuits are shaped in the form of exact arrangements of surface modified single layers. Due to this reason, software cannot put human and geometry related factors into calculations. Human and geometry related factors result in different arrangements of layers in millimetric sizes, and this leads to unpredictable destructive or constructive interferences of EM waves. Because of this, EM wave reflections could not be predicted correctly, while calculation of EM wave transmission is possible. These calculation results were presented in study.

Due to similarity in the results achieved from the simulations of different types of structural combinations, in this chapter only calculations on gold-glass fiber multilayered structures were given. Simulation results of gold-glass fiber structures can be seen in Figure 4.74-Figure 4.76. Simulation results of the other three structural combinations can be seen in Appendix (Figure A.25-A.33).

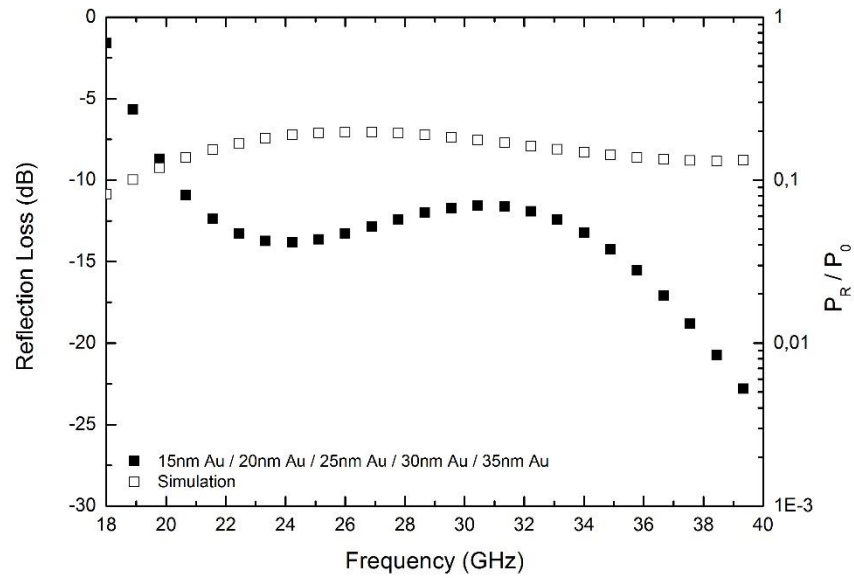


Figure 4.74 Comparison of measured and simulated EM wave reflection loss of gold surface modified 5-layered glass fiber woven fabric structure.

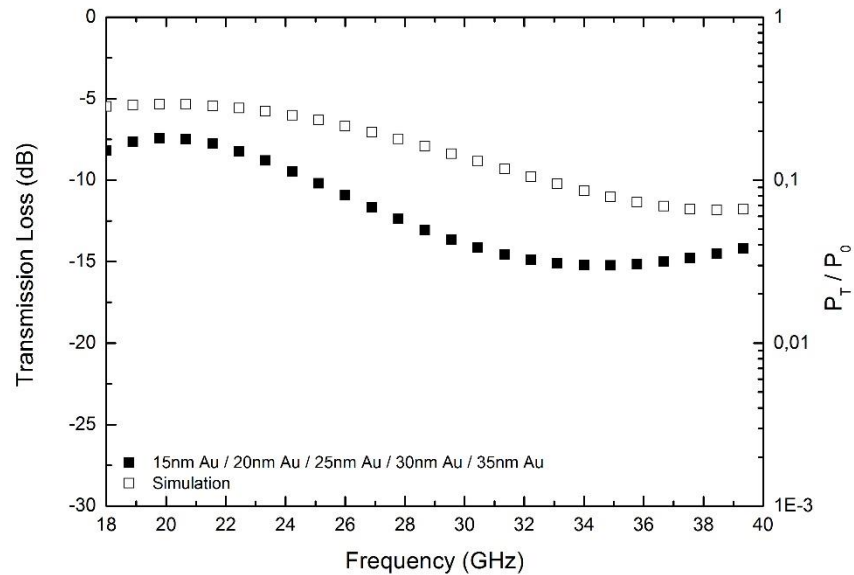


Figure 4.75 Comparison of measured and simulated EM wave transmission loss of gold surface modified 5-layered glass fiber woven fabric structure.

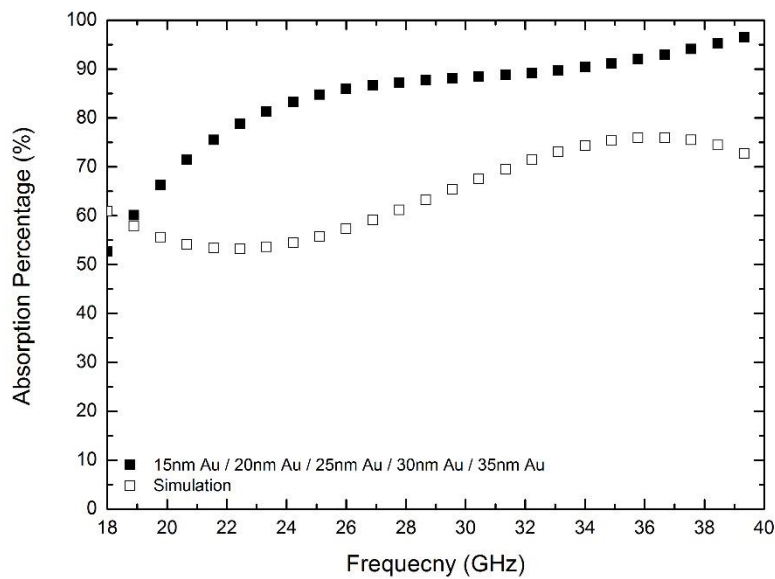


Figure 4.76 Comparison of measured and simulated EM wave absorption percentage of gold surface modified 5-layered glass fiber woven fabric structure.

4.4 Mechanical Test Results

In the scope of this study, glass and aramid fiber woven fabrics were modified with metallic coatings, and four multilayered reinforcement configurations providing the highest EM wave absorption characteristics were used for the fabrication of prototype composites. Surface modified glass and aramid fiber woven fabrics were incorporated into these prototype composites in silanized or non-silanized condition. EM wave reflection, transmission and absorption properties of the resulting prototype composites were investigated.

In last part of this study, mechanical behavior of the fabricated prototype EM wave absorbing composites has been investigated. In order to analyze the mechanical behavior of these prototype composites three-point bending tests were conducted.

Three-point bending test results were analyzed under six different comparative conditions. These comparisons were done based on the obtained flexural stress (MPa) - strain (%) graphs given in Figure 4.77 - Figure 4.82. As the control samples, three-point bending test results were conducted on the prototype composites containing silanized and non-silanized as-received glass fiber (Figure 4.77) and aramid fiber (Figure 4.80). Using the data from the control samples, effect of gold and nickel surface modification along with silanization applied on the glass and aramid fiber woven fabrics on the mechanical properties of the resulting composites has been investigated. According to the preliminary tests on the control samples, it has been observed that silanized composite structures show significantly higher mechanical strength both in the case of glass and aramid fiber woven fabric reinforcements. This shows that applied silane treatment affects the mechanical strength of as-received glass and aramid fiber woven fabric reinforced composites positively.

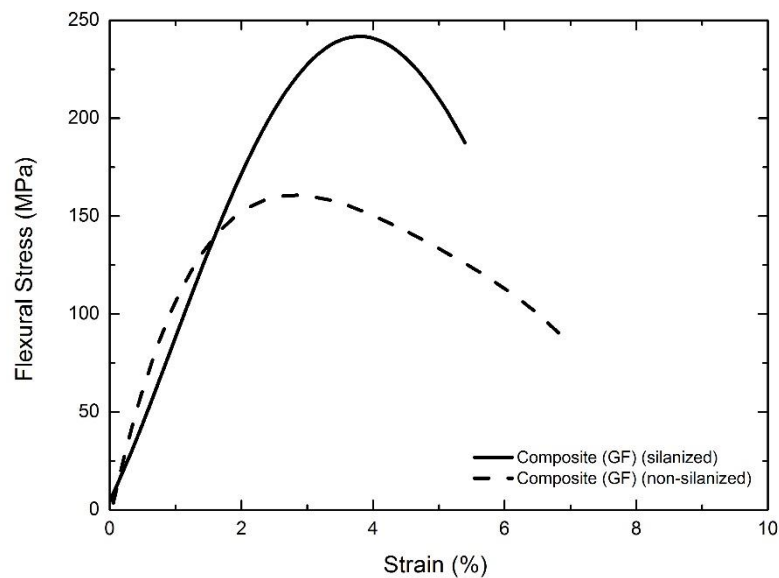


Figure 4.77 Three-point bending test results of prototype composites containing silanized and non-silanized as-received glass fiber woven fabrics.

Graph showing the mechanical behavior of the prototype EM wave absorbing composites containing silanized and non-silanized gold surface modified glass fiber woven fabrics can be seen in Figure 4.78. According to the results, silanization showed a positive effect on these composites in terms of strength. When Figure 4.77 and 4.78 are compared, there is no remarkable effect of the gold surface modification on the mechanical strength of the composites. In both cases the strength of the composite is around 150 MPa. On the other hand, it was observed that silanization increases mechanical strength after gold surface modification, even though this increase is not as high as the control sample which does not contain gold surface modification.

In Figure 4.79, flexural stresses (MPa) - strain (%) plot of composites with nickel surface modified glass fiber woven fabrics before silanization and after silanization are given. On the contrary to gold surface modification, mechanical strength of the composite increases remarkably by the application of the nickel surface modification on the glass fiber woven fabric. However, application of silane on the nickel surface modified glass fiber woven fabric leads to lower mechanical strength in the resulting composite. In addition, during the three-point bending test, non-silanized composite was broken immediately following the maximum load, where the silanized composite continued to carry load while bending to almost 2 times more strain compared to non-silanized one. This shows that although silanization does not improve strength for nickel surface modified glass fiber woven fabrics, it leads to higher toughness in these composites.

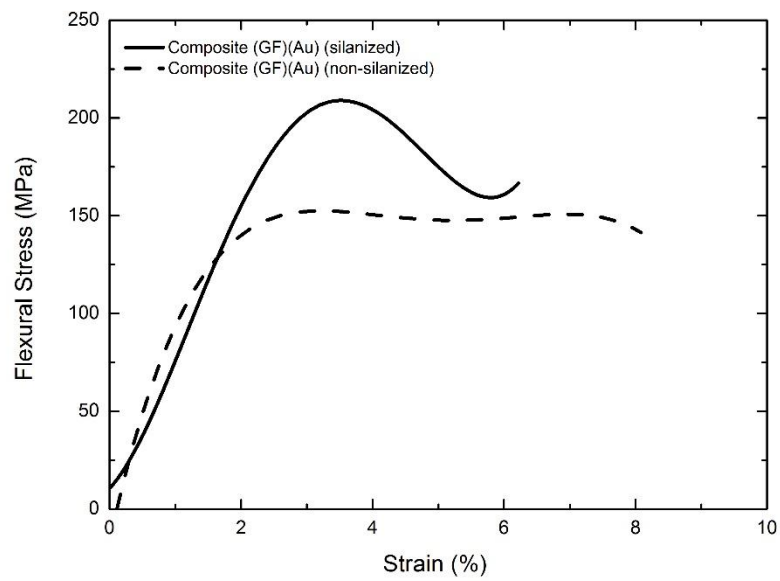


Figure 4.78 Three-point bending test results of prototype composites containing silanized and non-silanized gold surface modified glass fiber woven fabrics.

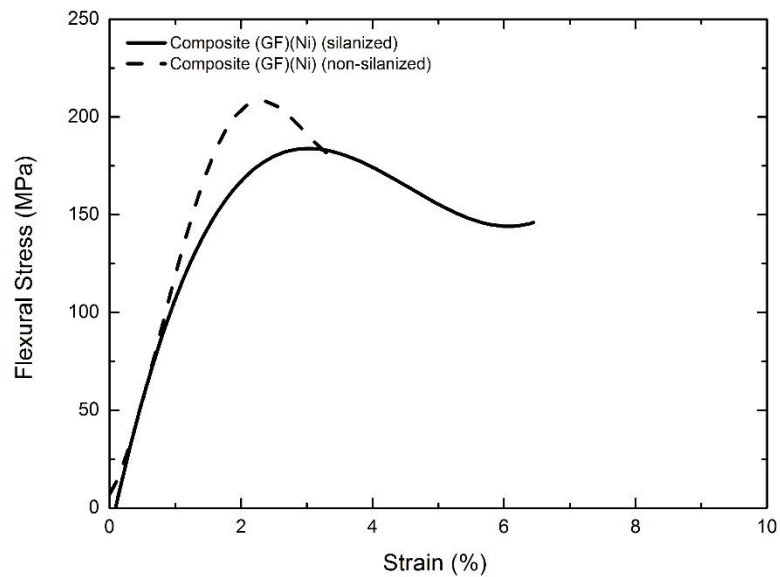


Figure 4.79 Three-point bending test results of prototype composites containing silanized and non-silanized nickel surface modified glass fiber woven fabrics.

In this part, mechanical test results of composites containing aramid fiber woven fabrics are illustrated. Flexural stress (MPa) - strain (%) results of the composites containing silanized and non-silanized as-received aramid fiber woven fabrics are shown in Figure 4.80. According to this plot, silanization provides both increase in strength and elongation. However, both silanized and non-silanized composites demonstrated lower mechanical strength than their glass fiber containing counterpart (Figure 4.77).

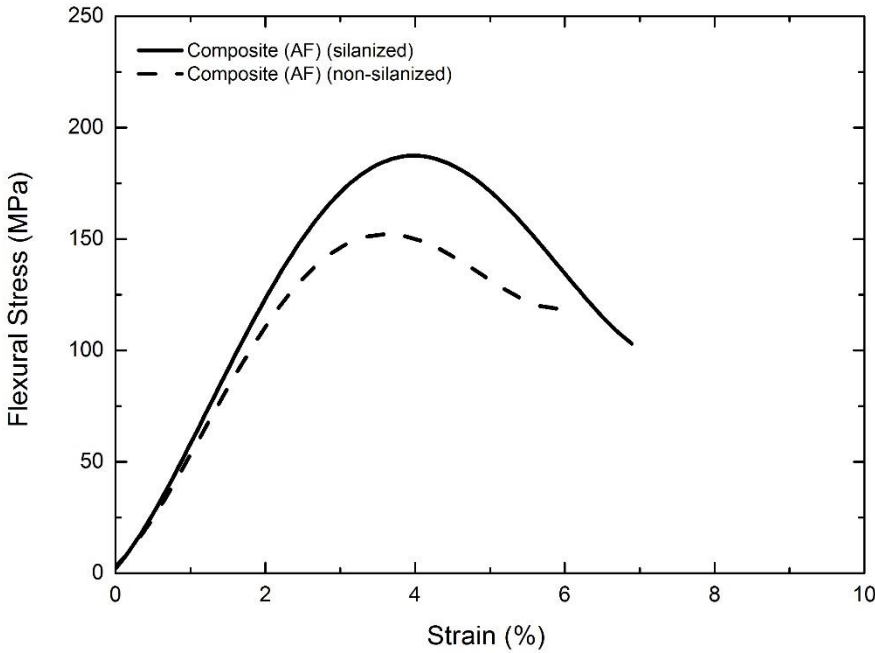


Figure 4.80 Three-point bending test results of prototype composites containing silanized and non-silanized as-received aramid fiber woven fabrics.

In Figure 4.81, mechanical test data of EM wave absorbing prototype composites containing silanized and non-silanized gold surface modified aramid fiber woven fabrics are shown. Comparing the plots in Figure 4.80 and 4.81, it is clear that gold surface modification decreases mechanical strength for aramid fiber woven fabric reinforcements. Especially, silanization seems to result in a further deterioration in mechanical properties both in terms of lower strength and strain. However, there was significant decay in mechanical properties. This study showed that aramid fiber woven fabrics, applied silane treatment and gold surface modification are not compatible with the used epoxy matrix.

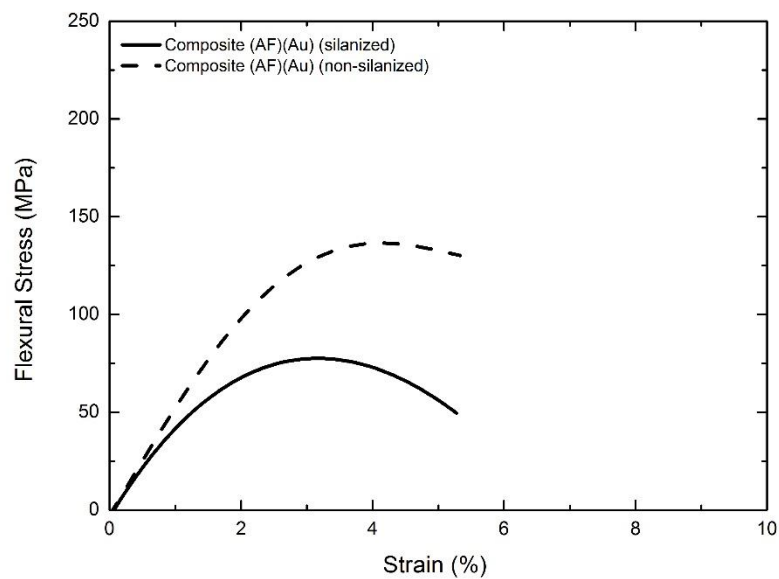


Figure 4.81 Three-point bending test results of prototype composites containing silanized and non-silanized gold surface modified aramid fiber woven fabrics.

Similar mechanical tests were conducted on the EM wave absorbing prototype composites containing silanized and non-silanized nickel surface modified aramid fiber woven fabrics. These silanized and non-silanized composites are compared in Figure 4.82. Nickel thin film addition into the reinforcement results in decrease in mechanical properties and this effect seems to be comparable to that observed in the gold containing counterpart. Applied silanization seems to have a further negative effect on the mechanical properties of the resulting composites. Due to this reason, it can be said that applied silanization is also not suitable for the nickel surface modified aramid fiber woven fabrics and the used epoxy matrix.

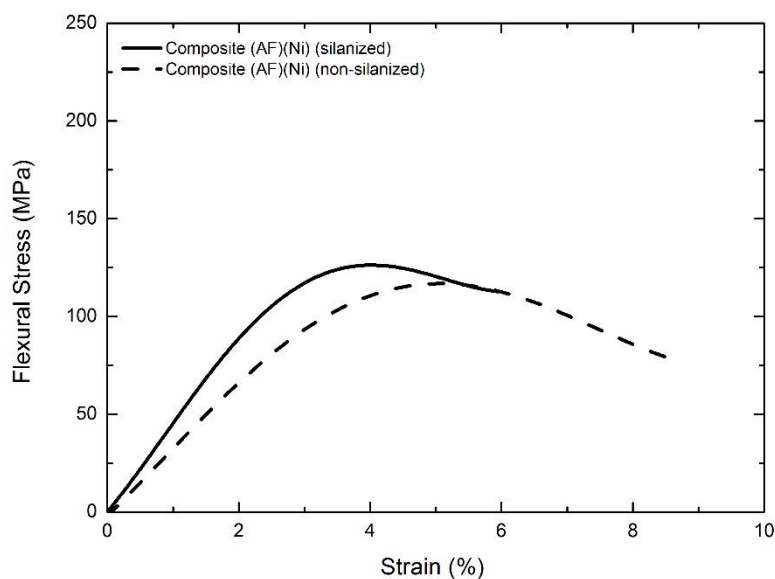


Figure 4.82 Three-point bending test results of prototype composites containing silanized and non-silanized aramid surface modified aramid fiber woven fabrics.

4.5 Summary of Achievements

As discussed in Chapter 2, "Salisbury screens" and "Jaumann absorbers" are being used for EM shielding in specific frequencies. Moreover, graded absorbers are being used as EMI shielding materials for broader frequency ranges. Using same principles, multilayered composite structures which were developed in this study can be used as EM wave absorber or EMI shielding materials for K-K_a frequency range (18-40 GHz).

Correlation between the EM properties of the composite structures developed in this study and the parameters varied throughout the study was tried to be established. Nevertheless, EM wave absorption and EMI shielding potential of these novel composite structures depend on the matrix and reinforcement material, the type and surface topography of the reinforcement material, the type and thickness of the metallic thin film applied as well as the composite fabrication method used etc. Because of this high number of variables, there is a huge number of material related parameter combinations controlling the EM absorption and EMI shielding potential of the developed composites. Therefore, in this study achieved results were presented and discussed on an empirical basis. This empirical approach can be extended to simulation studies, also demonstrated preliminarily in this study, in order to predict the EM wave behavior of the potential multilayered composites involving complex input parameter combinations.

To sum up, EM wave absorption and EMI shielding potential of most promising composite structures developed in this study were compared. Highest EM absorption (Figure 4.83) or EMI shielding (Figure 4.84) results achieved by silanized or non-silanized composites have been summarized. Surface modifications applied on the reinforcements seems to have affected the EM wave absorption and EMI shielding of the fabricated composites positively when compared to the their counterparts containing as received reinforcements (Composite (GF) or (AF) in Figure 4.83 and Figure 4.84.

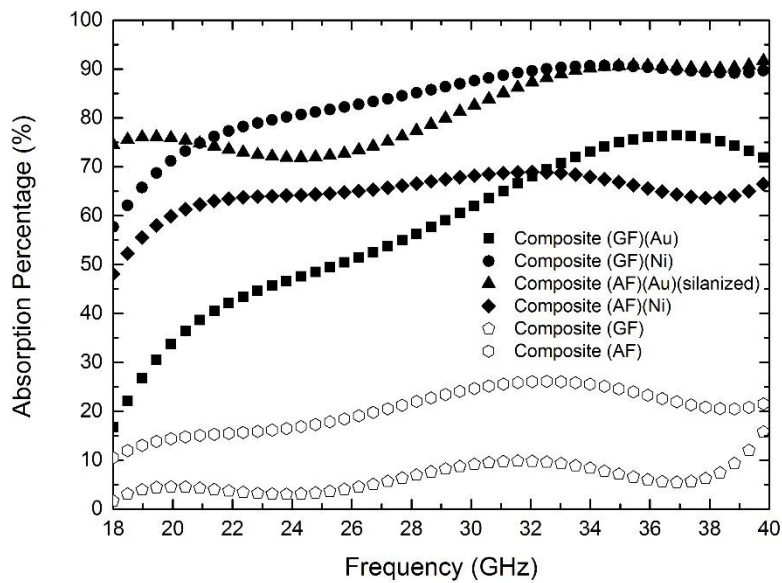


Figure 4.83 EM wave absorption percentage of the selected composites varying with frequency.

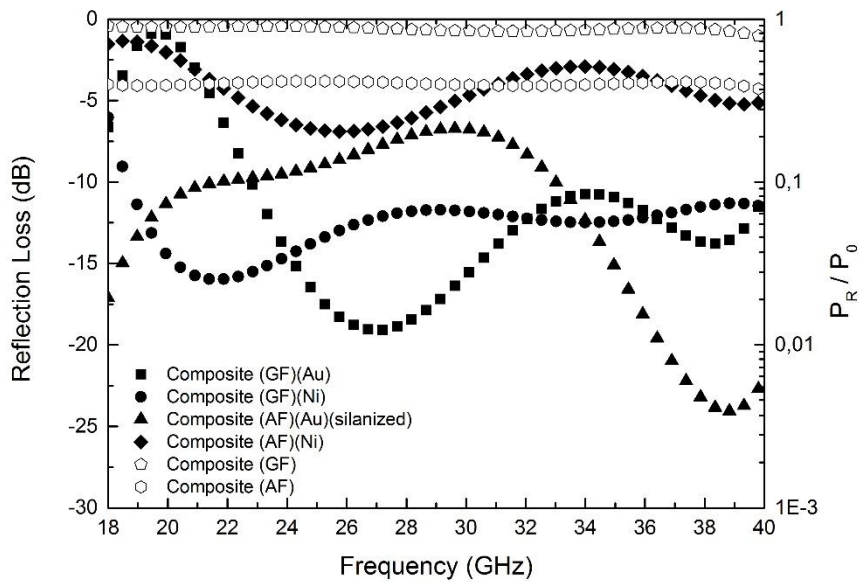


Figure 4.84 EM wave reflection loss of selected composites varying with frequency.

In addition to the EM studies, effect of the applied surface modifications on the reinforcement materials on the mechanical properties of the fabricated composites was compared based on the maximum flexural stress measured during the three-point bending tests. In Figure 4.85, maximum flexural stress values achieved in Au or Ni surface modified glass fiber and aramid fiber woven fabric composites with silanization (S) or without silanization (NS) treatment are summarized. As it can be seen, although the applied metallic surface modification deteriorates the mechanical strength of the composites, silanization process improves the mechanical strength of the fabricated composites with some exceptions. Moreover, obtained results illustrates that mechanical strength of composites containing glass fiber woven fabrics are generally higher than those of the composites containing aramid fiber woven fabrics.

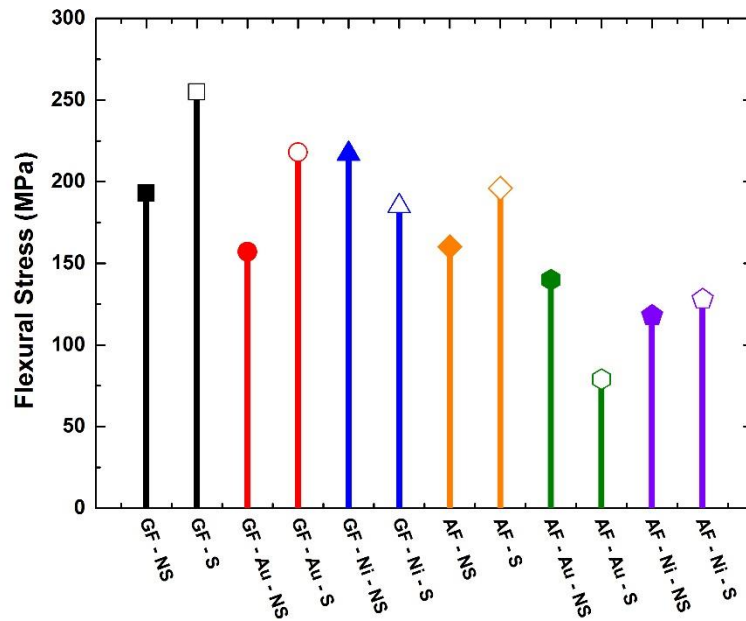


Figure 4.85 Maximum flexural stress values achieved in 12 different composite types.

CHAPTER 5

CONCLUSION

In the current study, effect of surface modifications by silver, gold and nickel on glass fiber and aramid fiber woven fabrics on their EM wave absorption characteristics were investigated within 18-40 GHz frequency range by free-space method. Gold thin films on silicon wafers were examined under FESEM and AFM in order to gain information about the structural morphology of the applied thin film surface modifications. Surface modifications by silver, gold and nickel were done on glass fiber woven fabrics and their electromagnetic wave reflection, transmission and absorption characteristics were measured for both single and multilayered structures. Effect of oxidization in silver thin film surface modifications on glass fiber woven fabrics were examined. Similar EM characterization was also done for single and multilayered aramid fiber woven fabrics surface modified by gold and nickel. Effect of silanization on EM wave behaviors was also investigated. Moreover, in order to indicate the effect of surface topography and geometry of the used substrates on the resulting EM characteristics, PET sheets were coated with gold thin films, and EM measurements were conducted on these structures.

Reinforcement materials were selected according to their EM wave absorption potentials in order to be used in prototype composites. Composite structures were fabricated by vacuum bagging method by introducing gold and nickel surface modified glass and aramid fiber woven fabrics as reinforcement materials into the epoxy matrix. EM measurements were also conducted on the prototype composites for both silanized and non-silanized cases. In addition to these studies, EM characteristics of the surface modified multilayered structures were also simulated using a commercial software. EM wave reflection, transmission, and hence absorption behavior of the multilayered

structures were tried to be predicted. Furthermore, mechanical properties of the fabricated prototype EM wave absorbing composites were examined by three-point bending tests. Effect of silanization treatment on the mechanical behavior was studied.

- In the light of these studies, materials to be used as reinforcement material in EM wave absorbing composites were tried to be chosen according to their EM wave absorption potential. Results showed that gold and nickel are strong surface modifiers for both glass and aramid fiber woven fabrics especially in terms of shielding on fully reflective surfaces. All of the fabricated prototype composites revealed high potential to be used as EM wave absorbers; however, composites with aramid fibers showed poor mechanical strength. Nevertheless, composites containing surface modified aramid fiber woven fabrics can be used as EM wave absorbers in devices where absorption consistency is crucial in 18-40 GHz.
- Numbers of combinations of multilayered structures can be increased with using simulation studies and their potentials for EM wave absorbing and EMI shielding can be obtained close to real situations. This can be a method for determining the best EM wave absorber or EMI shielding composites in future studies.
- This study showed that by changing arrangements, thickness of surface modifications, surface geometries of the reinforcement materials etc. it is possible to increase the EM wave absorption potential of structural polymeric composite. This renders fiber reinforced polymer matrix composites one of the most promising EM wave absorbing structural material.

REFERENCES

- [1] E. F. Knott, J. F. Schaeffer and M. T. Tuley, Radar Cross Section, SciTech Publisher, 1993.
- [2] P. S. Neelakanta, Handbook of Electromagnetic Materials, Washington D.C.: CRC Press, 1995.
- [3] K. K. Chawla, Composite Materials: Science and Engineering, London: Springer, 2008.
- [4] IEEE, "IEEE Standard Letter Designations for Radar-Frequency Bands," in *Revision of Std 521-1984*, IEEE Std 521, 2003.
- [5] G. Gürer, Design and Characterization of Electromagnetic Wave Absorbing Structural Composites, M.Sc Thesis, Ankara: METU, Graduate School of Natural and Applied Sciences, 2010.
- [6] M. Gupta and E. W. Leong, Microwaves and Metals, Wiley, 2007.
- [7] IPAC, Infrared Windows, Infrared Processing and Analysis Center, 2010.
- [8] D. M. Pozar, Microwave Engineering, Addison-Wesley Publishing Company, 1993.
- [9] W. J. D. Callister and D. G. Rethwisch, Materials science and Engineering: An Introduction (8th Edition), Wiley, 2010.

- [10] J. Huo, L. Wang and H. Yu, "Polymeric Nanocomposites for Electromagnetic Wave Absorption," *Journal of Materials Science*, vol. 44, no. 15, pp. 3917-3927, 2009.
- [11] D. G. Fink and D. Christiansen, *Electronics Engineers' Handbook*, McGraw-Hill, 1989.
- [12] D. S. Dai, F. Q. Shi, Y. Q. Chen and S. L. Chu, *Ferromagnetics*, Beijing: Science Press, 1976.
- [13] K. Foster and M. F. Littmann, *Journal of Applied Physics*, vol. 8, p. 351, 1985.
- [14] S. W. Phang and R. Daika, "Poly(4,4'-diphenylene diphenylvinylene) as a non-magnetic microwave absorbing conjugated polymer," *Thin Solid Films*, vol. 477, no. 1-2, pp. 125-130, 2005.
- [15] S. V. Marshall and G. G. Skitek, *Electromagnetic Concepts and Applications 3rd Ed.*, New Jersey: Prentice-Hall, 1990.
- [16] W. S. Chin and D. G. Lee, "Composite Structures," *Article in Press*, 2005.
- [17] W. S. Chin and D. G. Lee, "Laminating Rule for Predicting the Dielectric Properties of E-glass/epoxy laminate composites," *Composite Structures*, vol. 77, no. 3, pp. 373-382, 2007.
- [18] K. Y. Park, S. E. Lee, C. G. Kim and J. H. Han, "Fabrication and Electromagnetic Characteristics of Electromagnetic Wave Absorbing Sandwich Structures," *Composites Science and Technology*, vol. 66, no. 3-4, pp. 576-584, 2006.
- [19] K. J. Vinoy and M. R. Jha, *Radar Absorbing Materials from Theory to Design and Characterization*, Kluwer Academic Publishers, 1996.

- [20] M. Cao, B. Wang, Q. Li, J. Yuan, G. Xu, S. Qin and X. Fang, "Towards an Intelligent CAD System for Multilayer Electromagnetic Absorber Design," *Materials and Design*, vol. 19, no. 3, pp. 113-120, 1998.
- [21] X. Luo and D. D. Chung, "Electromagnetic Interference Shielding Using Continuous Carbon-Fiber Carbon-Matrix and Polymer-Matrix Composites," *Composites Part B*, vol. 30, pp. 227-231, 1999.
- [22] C. Y. Lee, H. G. Song, K. S. Jang, E. J. Oh, A. J. Epstein and J. Joo, "Electromagnetic Interference Shielding Efficiency of Polyaniline Mixtures and Multilayer films," *Synthetic Metals*, vol. 102, no. 1-3, pp. 1346-1349, 1999.
- [23] A. Ghasemi, A. Hossienpour, A. Morisako, A. Saatchi and M. Salehi, "Electromagnetic Properties and Microwave Absorbing Characteristics of Doped Barium Hexaferrite," *Journal of Magnetism and Magnetic Materials*, vol. 302, no. 2, pp. 429-435, 2006.
- [24] C. Wang, L. Li, J. Zhou, X. Qi, Z. Yue and X. Wang, "Microstructures and High-frequency Magnetic Properties of Low-temperature Sintered Co-Ti Substituted Barium Ferrites," *Journal of Magnetism and Magnetic Materials*, vol. 257, no. 1, pp. 100-106, 2003.
- [25] M. C. Rezende, I. M. Martin, M. A. Miacci and E. L. Nohara, "Radar Cross Section Measurements (8-12 GHz) of Flat Plates Painted with Microwave Absorbing Materials," in *Microwave and Optoelectronics Conference*, 2001.
- [26] M. B. Amin and J. R. James, "Techniques for Utilization of Hexagonal Ferrites in Radar Absorbers. Part 1: Broadband Planar Coatings," *Radio and Electronic Engineer*, vol. 51, no. 5, pp. 209-218, 1981.
- [27] W. B. Weir, "Automatic Measurement of Complex Dielectric Constant and Permeability at Microwave Frequencies," *Proceedings of the IEEE*, vol. 62, no. 1, pp. 33-36, 1974.

- [28] R. S. Biscaro, E. L. Nohara, G. G. Peixoto and R. Faez, "Performance evaluation of conducting polymer paints as radar absorbing materials (RAM)," in *Microwave and Optoelectronics Conference*, 2003.
- [29] W. S. Chin and D. G. Lee, "Development of the Composite RAS (Radar Absorbing Structure) for the X-band Frequency Range," *Composite Structures*, vol. 77, no. 4, pp. 457-765, 2007.
- [30] M. S. Pinho, M. L. Gregori, R. C. R. Nunes and B. G. Soares, "Performance of Radar Absorbing Materials by Waveguide Measurements for X- and Ku-band Frequencies," *European Polymer Journal*, vol. 38, no. 11, p. 2321–2327, 2002.
- [31] S. Wen and D. D. Chung, "Partial Replacement of Carbon Fiber by Carbon Black in Multifunctional cement-matrix composites," *Carbon*, vol. 45, pp. 505-513, 2007.
- [32] C. Y. Huang, W. W. Mo and M. L. Roan, "Studies on the Influence of Double-layer Electroless Metal Deposition on the Electromagnetic Interference Shielding Effectiveness of Carbon Fiber/ABS Composites," *Surface and Coatings Technology*, vol. 184, no. 2-3, pp. 163-169, 2004.
- [33] X. Shui and D. D. Chung, "Submicron Diameter Nickel Filaments and Their Polymer-matrix Composites," *Journal of Materials Science*, vol. 35, no. 7, pp. 1773-1785, 2000.
- [34] S. S. Tzeng and F. Y. Chang, "EMI Shielding Effectiveness of Metal-coated Carbon Fiber-reinforced ABS Composites," *Materials Science and Engineering: A*, vol. 302, no. 2, pp. 258-267, 2001.
- [35] J. Wu and D. D. Chung, "Increasing the Electromagnetic Interference Shielding Effectiveness of Carbon Fiber Polymer–matrix Composite by Using Activated Carbon Fibers," *Carbon*, vol. 40, pp. 445-447, 2002.

- [36] N. Zhao, T. Zou, C. Shi, J. Li and W. Guo, "Microwave Absorbing Properties of Activated Carbon-fiber Felt Screens (Vertical-arranged Carbon Fibers)/epoxy Resin Composites," *Materials Science and Engineering: B*, vol. 127, no. 2-3, pp. 207-211, 2006.
- [37] J. H. Oh, K. S. Oh, C. G. Kim and C. S. Hong, "Design of Radar Absorbing Structures Using Glass/epoxy Composite Containing Carbon Black in X-band Frequency Ranges," *Composites Part B: Engineering*, vol. 35, no. 1, pp. 49-56, 2004.
- [38] E. Tan, Characterization of Electromagnetic Wave Absorbing Properties of SiC-Based Alumina Woven Fabrics, M. Sc. Thesis, Ankara: METU, Graduate School of Natural and Applied Sciences, 2008.
- [39] METYX, Artist, *Glass Fiber Reinforcement Catalog*. [Art]. 2005.
- [40] D. K. Ghodgaonkar, V. V. Varadan and V. K. Varadan, "Free-space measurement of complex permittivity and complex permeability of magnetic materials at microwave frequencies," *IEEE Transactions on Instrumentation and Measurement*, vol. 39, no. 2, pp. 387-394, 1990.
- [41] L. F. Chen, C. K. Ong, C. P. Neo, V. V. Varadan and V. K. Varadan, *Microwave Electronics: Measurement and Materials Characterization*, Wiley, 2004.
- [42] M. M. Corporation, "LRL Calibration of Vector Network Analyzers," 1999.
- [43] N. Gagnon, Design and Study of a Free-Space Quasi-Optical Measurement System, Ph. D. Thesis in: School of Information Technology and Engineering University of Ottawa, 2002.
- [44] ASTM D790, Standard Test Methods for Flexural Properties of Unreinforced and Reinforced Plastics and Electrical Insulating Materials, 2010.

- [45] A. T. Caballo and L. A. Acebron, Implementation of the Two Probe Method: A Technique in Measuring Electrical Properties, LaSallian Research Forum, 2009.
- [46] M. Mosleh, N. Pryds and P. V. Hendriksen, "Thickness dependence of the conductivity of thin films (La,Sr)FeO₃ deposited on MgO single crystal," *Materials Science and Engineering B*, vol. 144, pp. 38-42, 2007.
- [47] R. A. Serway, in *Principles of Physics (2nd ed)*, Fort-Worth, Texas, London: Saunders College Pub, 1998, p. 602.
- [48] E. S. Gadelmawla, M. M. Koura, T. A. Maksoud, I. M. Elewa and H. H. Soliman, "Roughness parameters," *Journal of Materials Processing Technology*, vol. 123, pp. 133-145, 2002.

APPENDIX A

EM WAVE MEASUREMENTS AND RESULTS

A.1 EM Wave Measurements and Results of Silanized and Surface Modified Woven Fabrics

A.1.1 EM Wave Measurements and Results of Silanized and Gold Surface Modified Glass Fiber Woven Fabrics

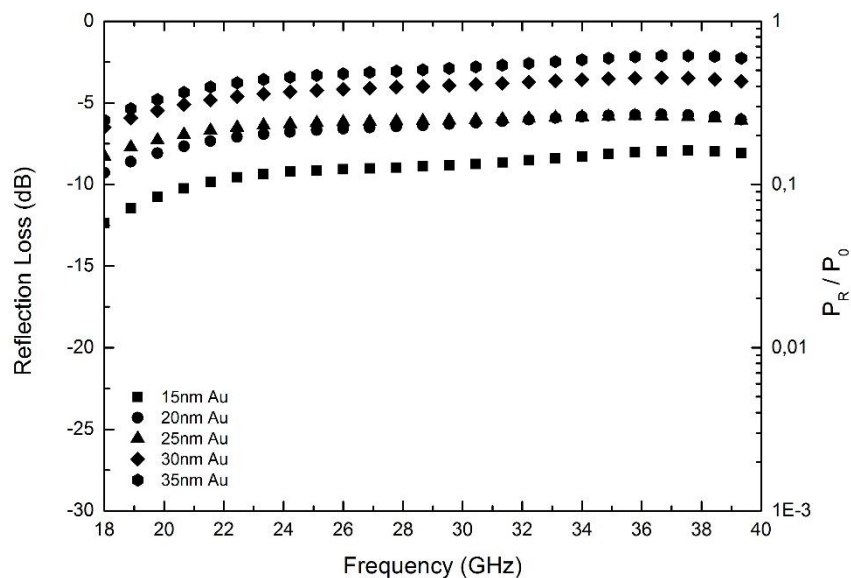


Figure A.1 EM wave reflection loss varying with frequency in silanized gold surface modified single layer glass fiber woven fabrics.

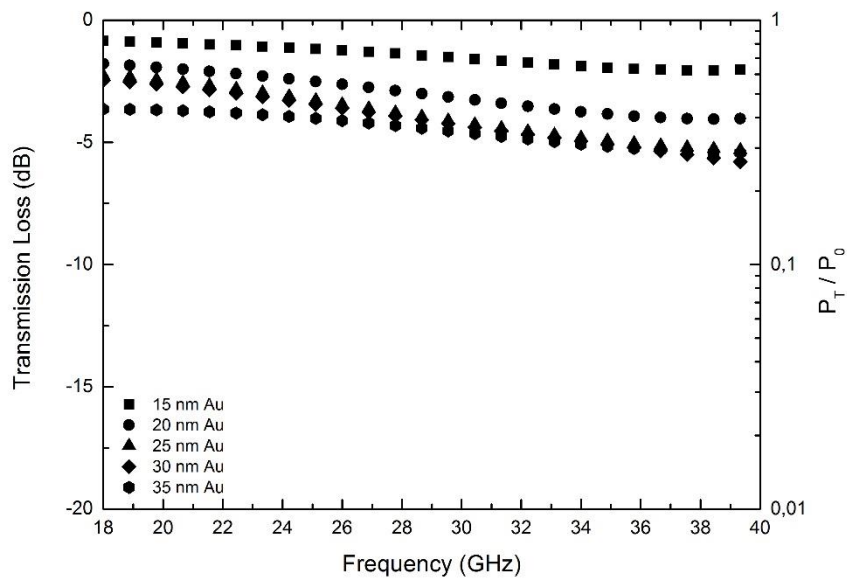


Figure A.2 EM wave transmission loss varying with frequency in silanized gold surface modified single layer glass fiber woven fabrics.

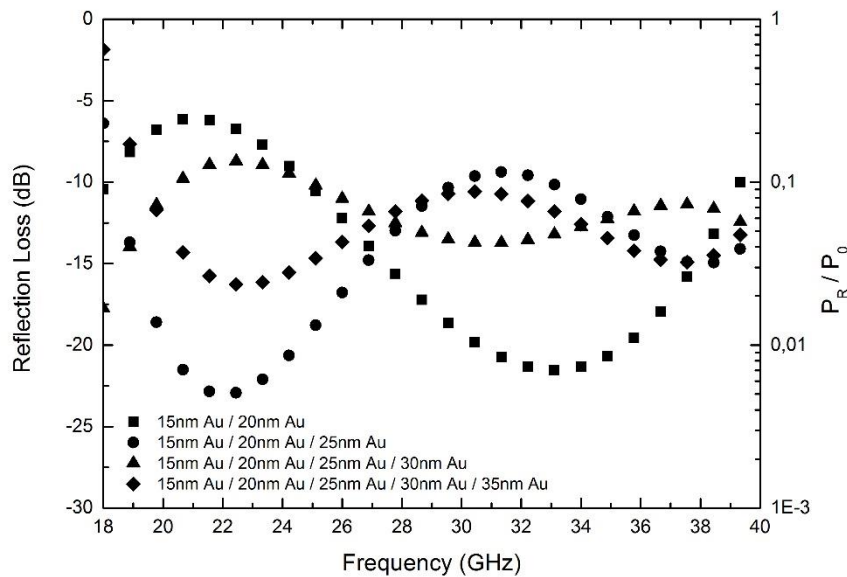


Figure A.3 EM wave reflection loss varying with frequency in silanized gold surface modified multilayered glass fiber woven fabrics.

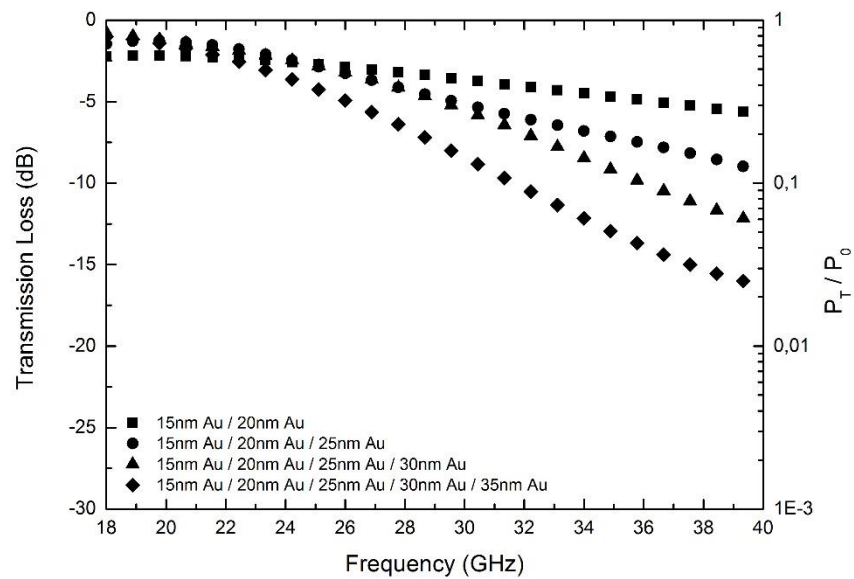


Figure A.4 EM wave transmission loss varying with frequency in silanized gold surface modified multilayered glass fiber woven fabrics.

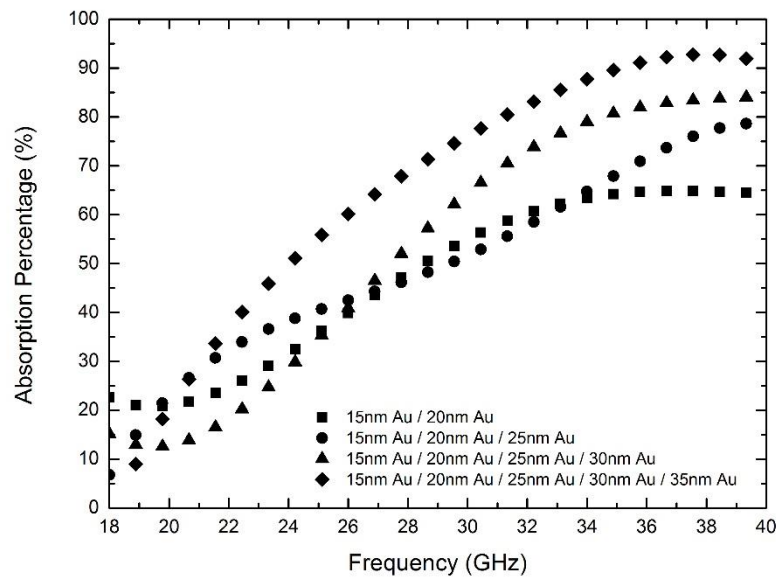


Figure A.5 EM wave absorption percentage varying with frequency in silanized gold surface modified multilayered glass fiber woven fabrics.

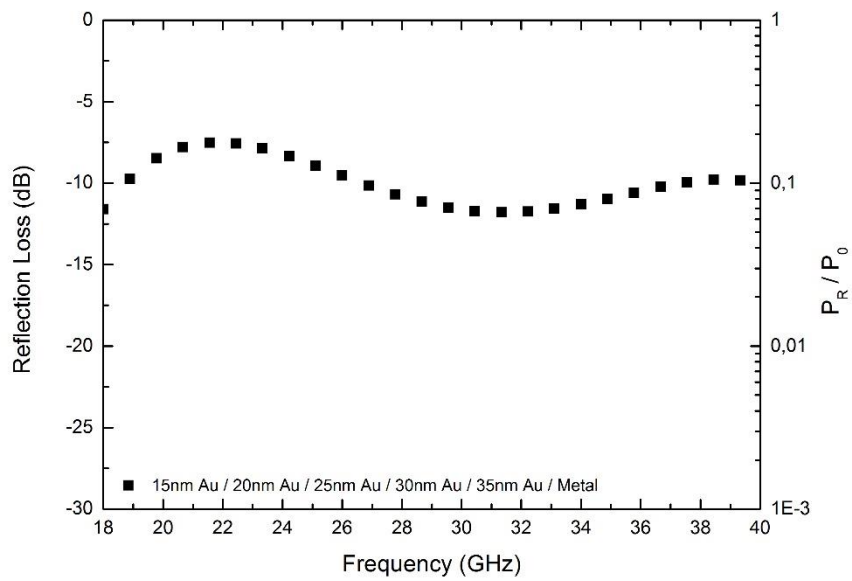


Figure A.6 EM wave reflection loss varying with frequency in silanized gold surface modified multilayered glass fiber woven fabrics with backing metallic plate.

A.1.2 EM Wave Measurements and Results of Silanized and Nickel Surface Modified Glass Fiber Woven Fabrics

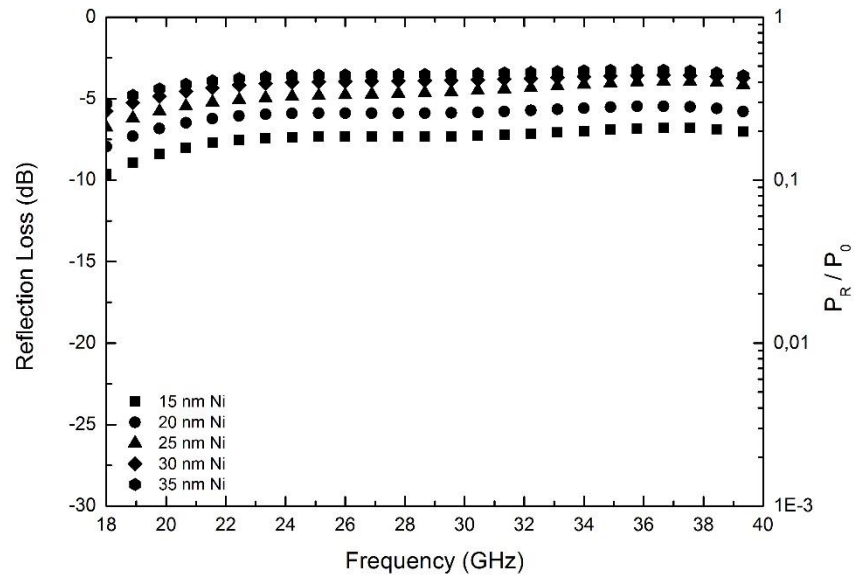


Figure A.7 EM wave reflection loss varying with frequency in silanized nickel surface modified single layer glass fiber woven fabrics.

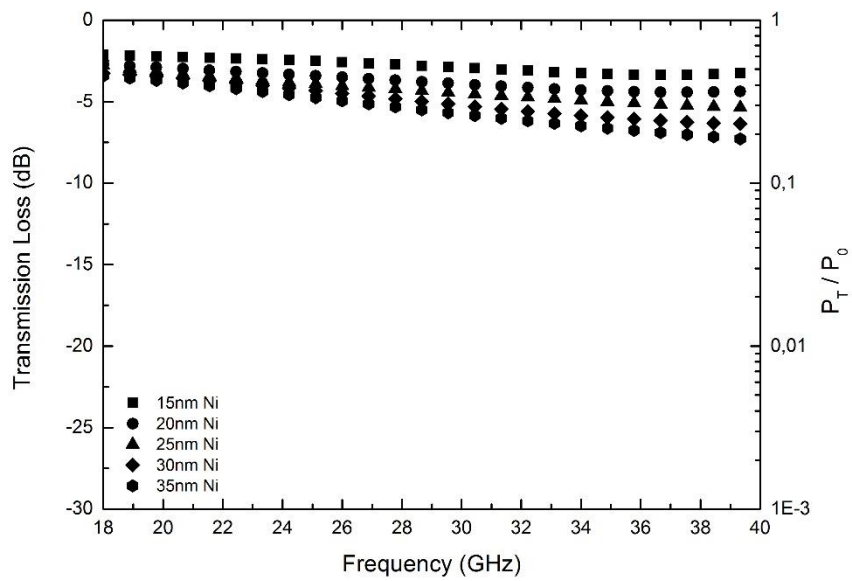


Figure A.8 EM wave transmission loss varying with frequency in silanized nickel surface modified single layer glass fiber woven fabrics.

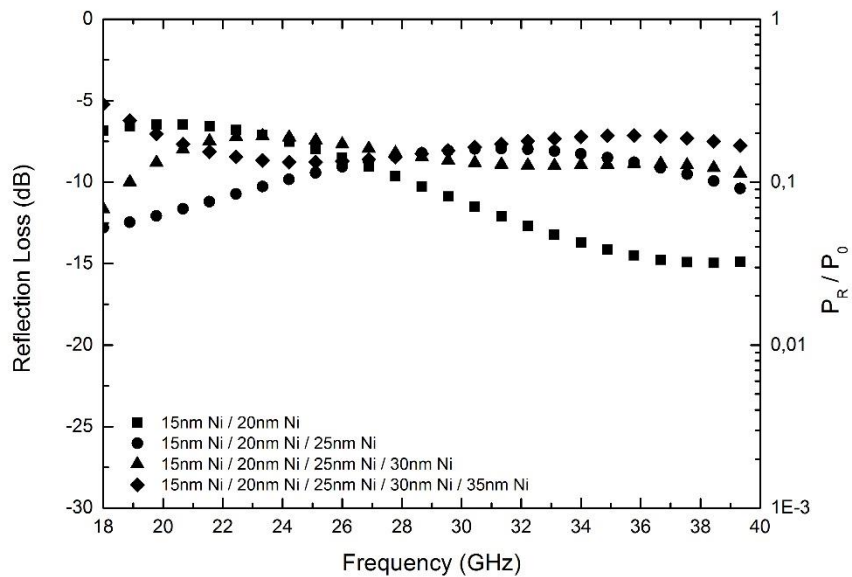


Figure A.9 EM wave reflection loss varying with frequency in silanized nickel surface modified multilayered glass fiber woven fabrics.

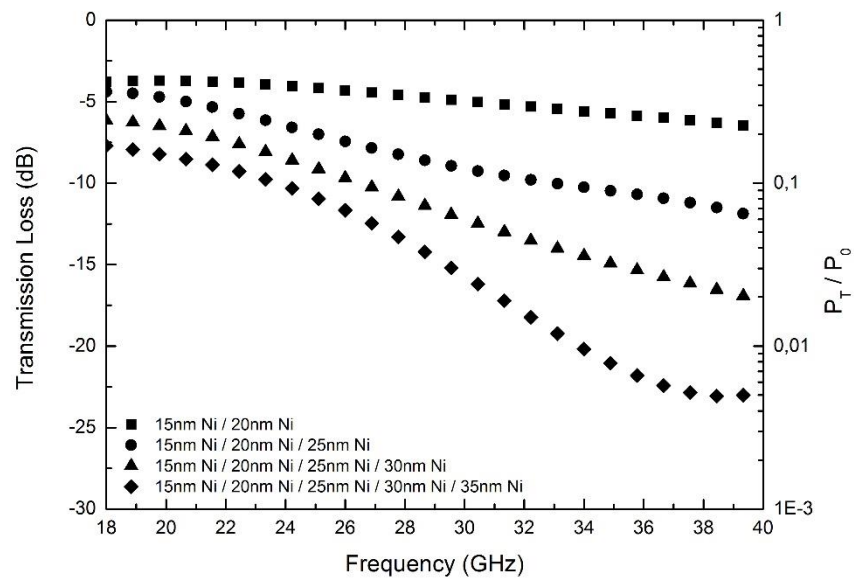


Figure A.10 EM wave transmission loss varying with frequency in silanized nickel surface modified multilayered glass fiber woven fabrics.

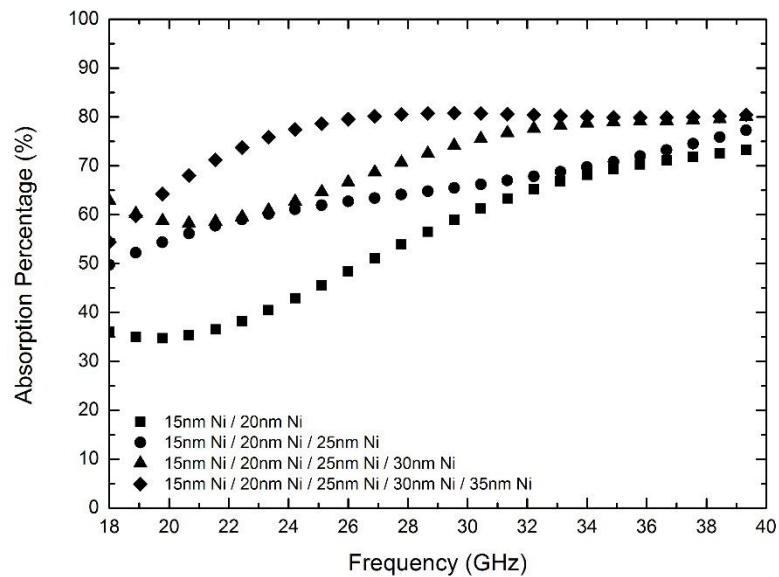


Figure A.11 EM wave absorption percentage varying with frequency in silanized nickel surface modified multilayered glass fiber woven fabrics.

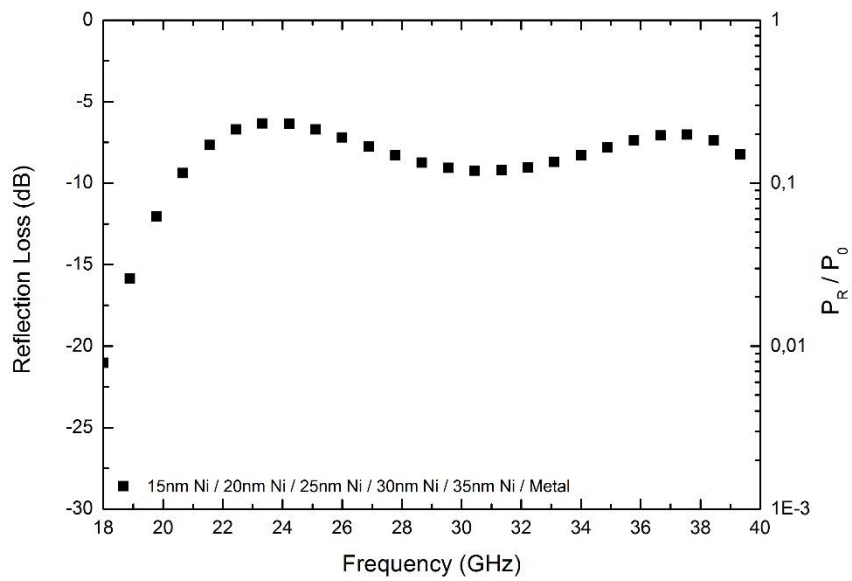


Figure A.12 EM wave reflection loss varying with frequency in silanized nickel surface modified multilayered glass fiber woven fabrics with backing metallic plate.

A.1.3 EM Wave Measurements and Results of Silanized and Gold Surface Modified Aramid Fiber Woven Fabrics

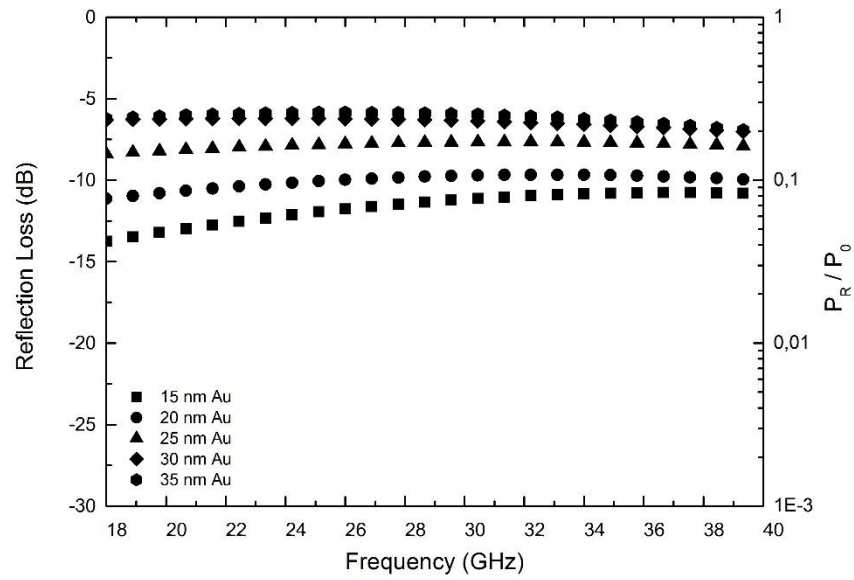


Figure A.13 EM wave reflection loss varying with frequency in silanized gold surface modified single layer aramid fiber woven fabrics.

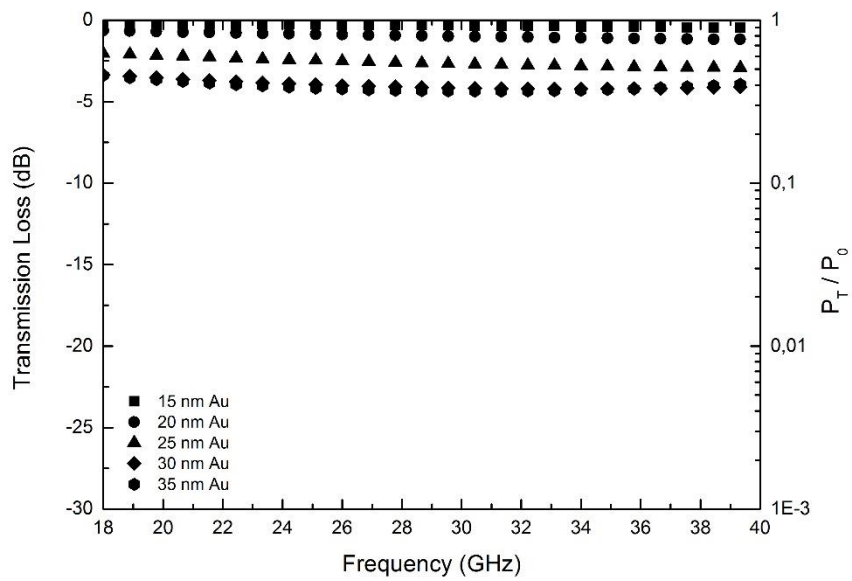


Figure A.14 EM wave transmission loss varying with frequency in silanized gold surface modified single layer aramid fiber woven fabrics.

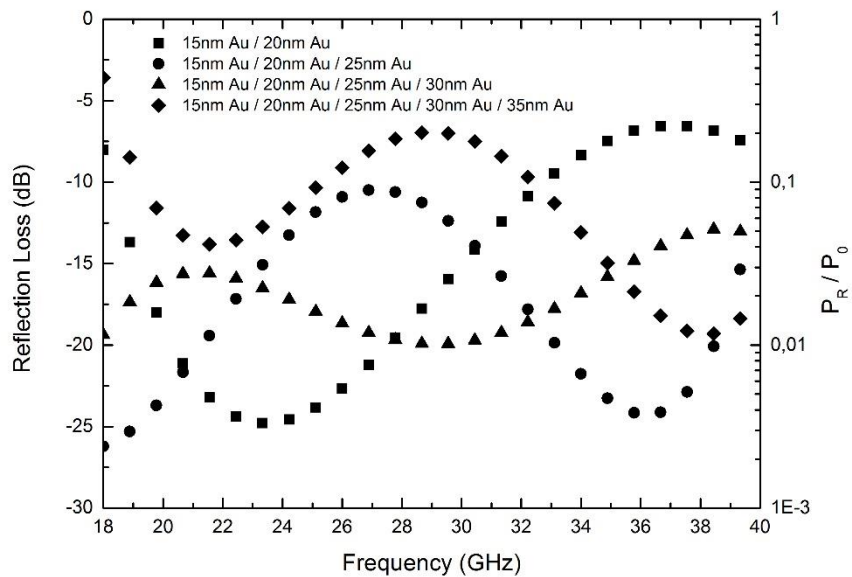


Figure A.15 EM wave reflection loss varying with frequency in silanized gold surface modified multilayered aramid fiber woven fabrics.

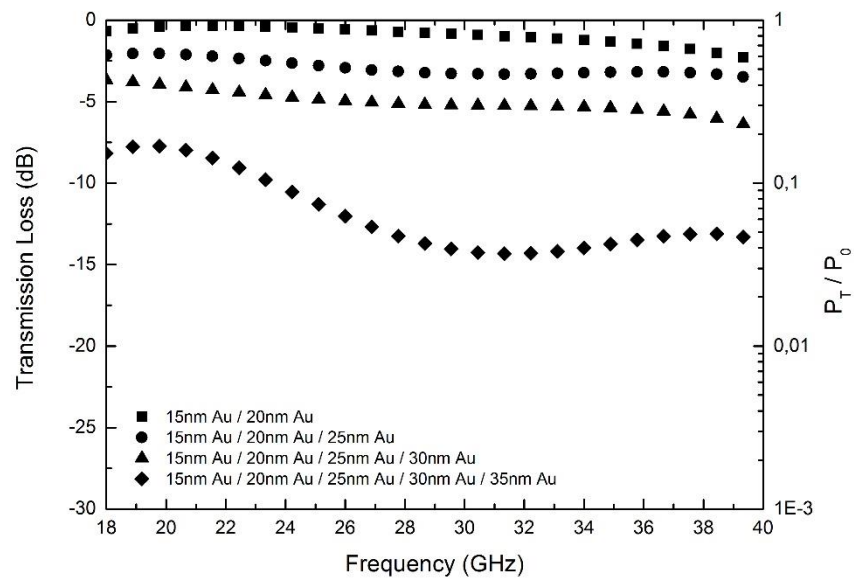


Figure A.16 EM wave transmission loss varying with frequency in silanized gold surface modified multilayered aramid fiber woven fabrics.

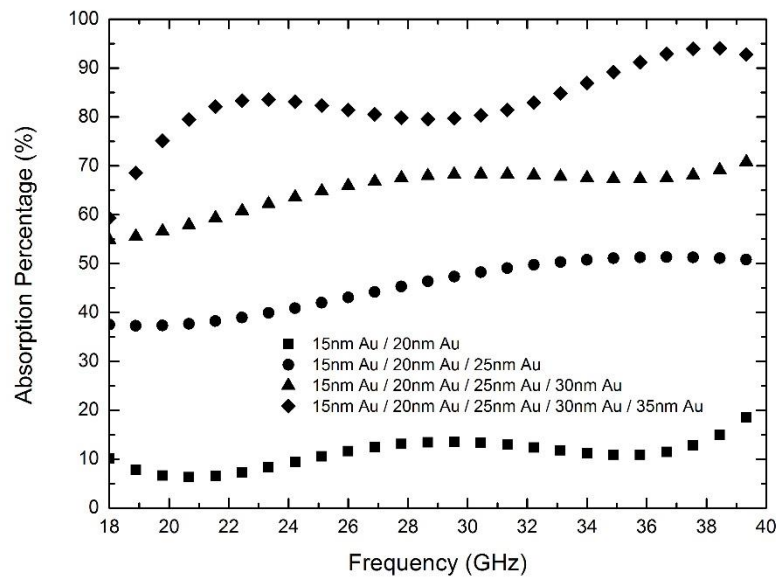


Figure A.17 EM wave absorption percentage varying with frequency in silanized gold surface modified single layer aramid fiber woven fabrics.

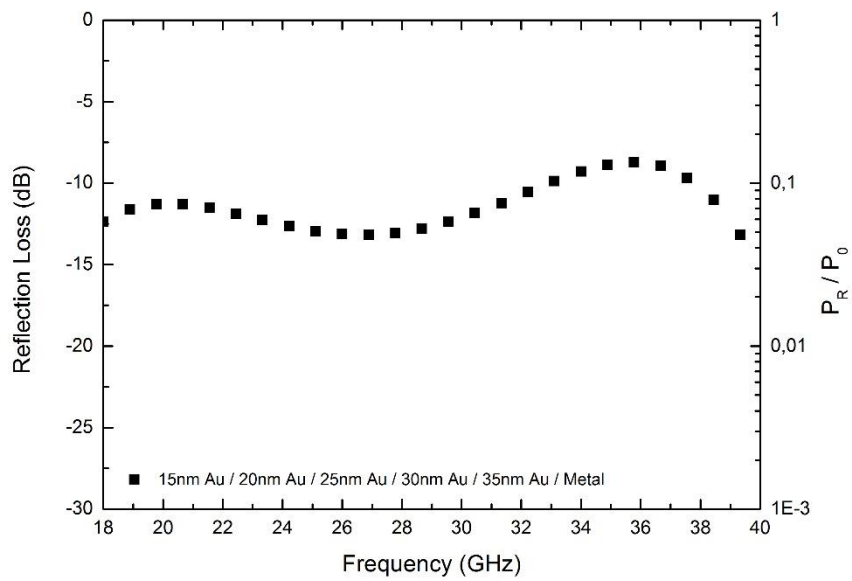


Figure A.18 EM wave reflection loss varying with frequency in silanized gold surface modified multilayered aramid fiber woven fabrics with backing metallic plate.

A.1.4 EM Wave Measurements and Results of Silanized and Nickel Surface Modified Aramid Fiber Woven Fabrics

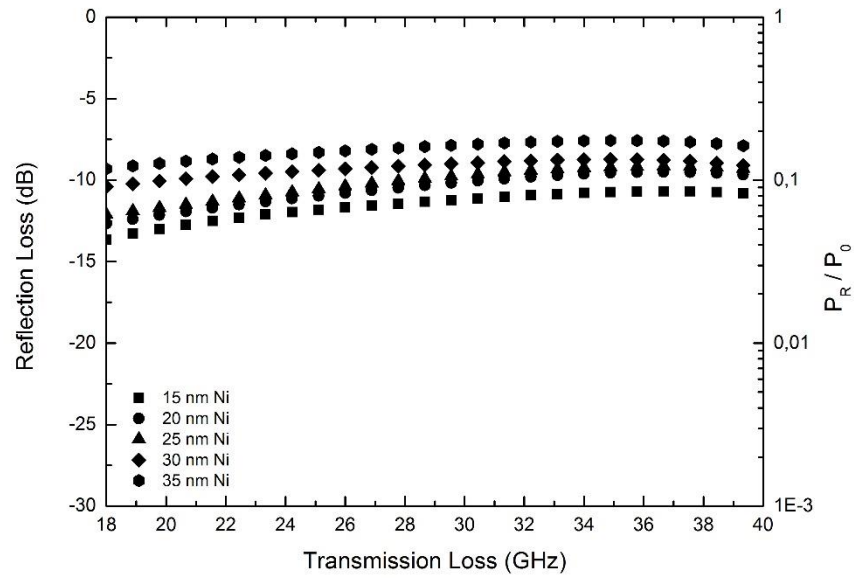


Figure A.19 EM wave reflection loss varying with frequency in silanized nickel surface modified single layer aramid fiber woven fabrics.

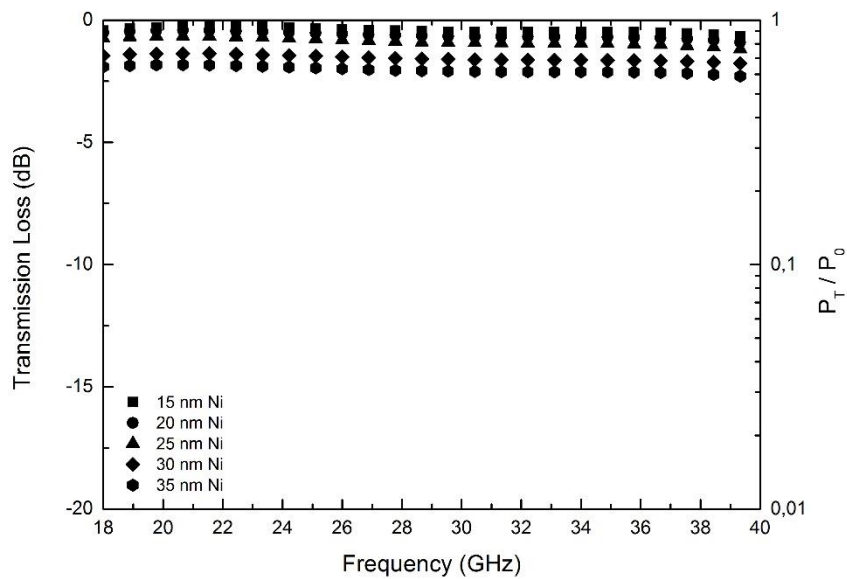


Figure A.20 EM wave transmission loss varying with frequency in silanized nickel surface modified single layer aramid fiber woven fabrics.

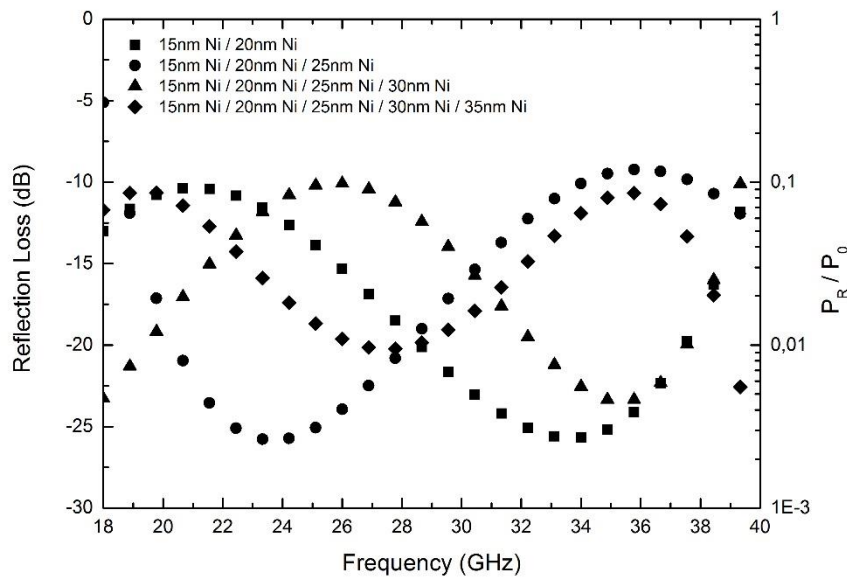


Figure A.21 EM wave reflection loss varying with frequency in silanized nickel surface modified multilayered aramid fiber woven fabrics.

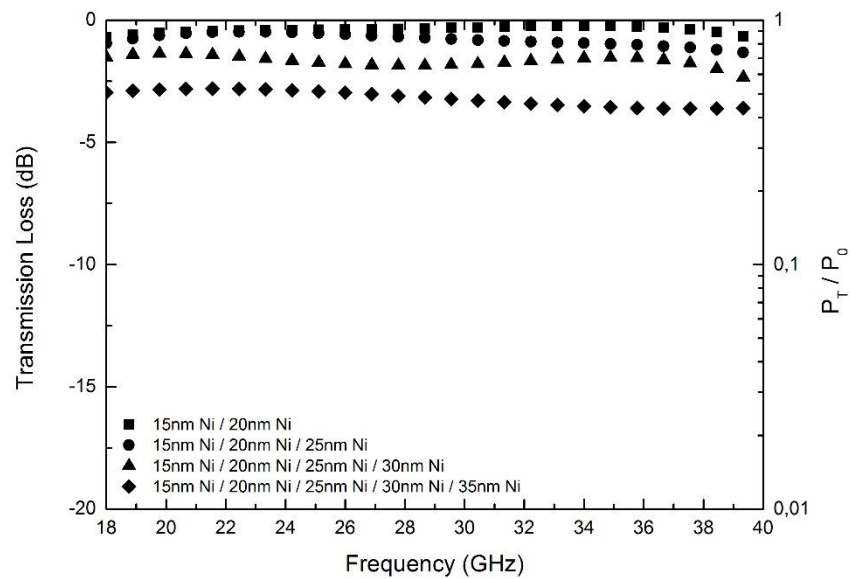


Figure A.22 EM wave transmission loss varying with frequency in silanized nickel surface modified multilayered aramid fiber woven fabrics.

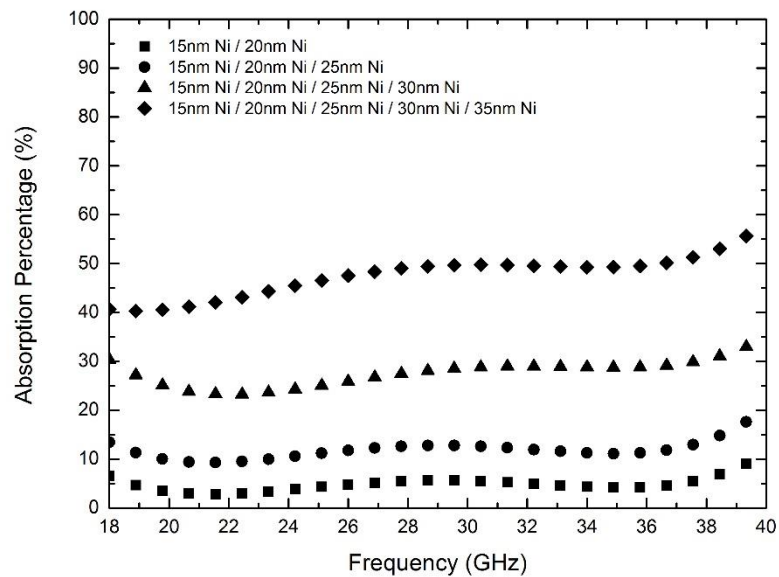


Figure A.23 EM wave absorption percentage varying with frequency in silanized nickel surface modified multilayered aramid fiber woven fabrics.

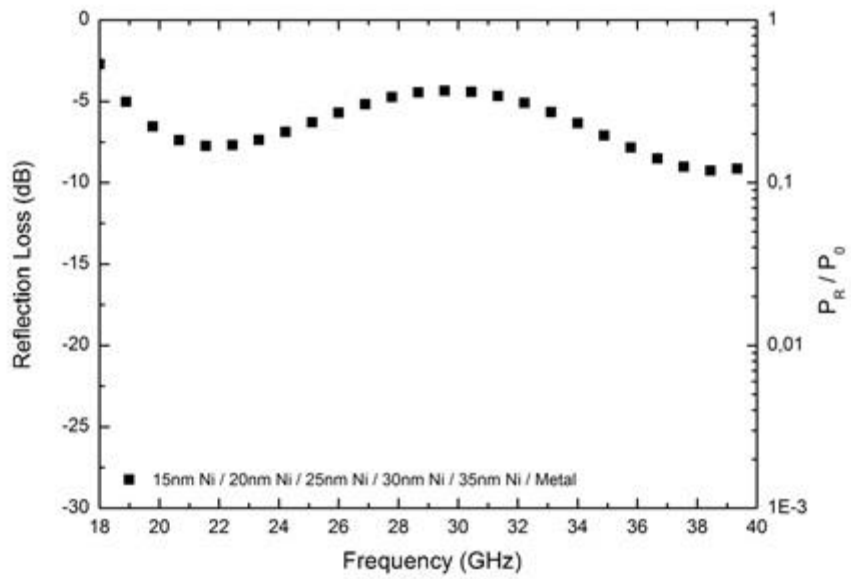


Figure A.24 EM wave reflection loss varying with frequency in silanized nickel surface modified multilayered aramid fiber woven fabrics with backing metallic plate.

A.2 Electromagnetic Measurement Simulation Studies

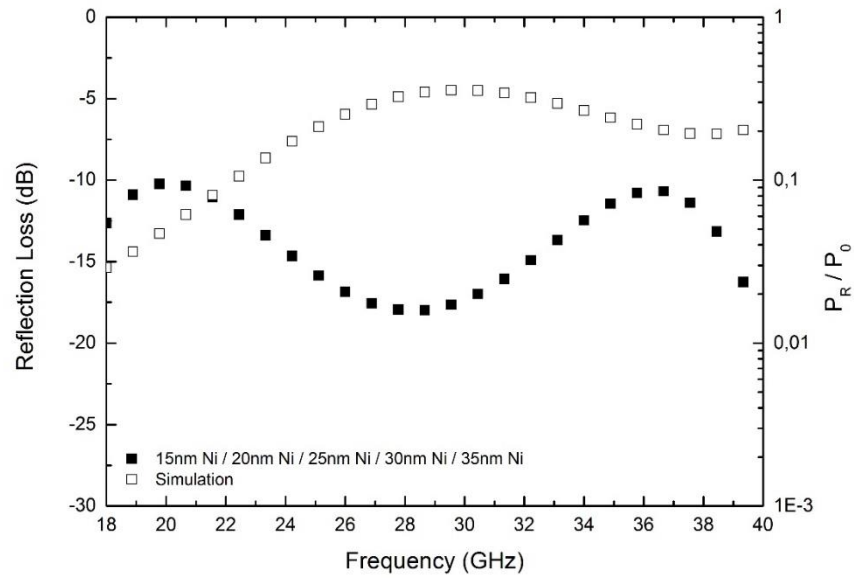


Figure A.25 EM wave reflection loss comparison of five layer nickel surface modified glass fiber structure and its simulation.

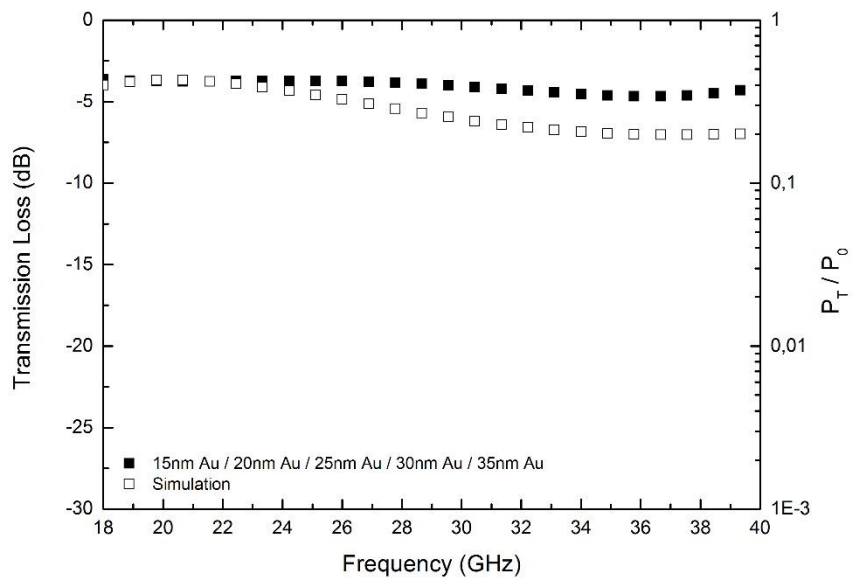


Figure A.26 EM wave transmission loss comparison of five layer nickel surface modified glass fiber structure and its simulation.

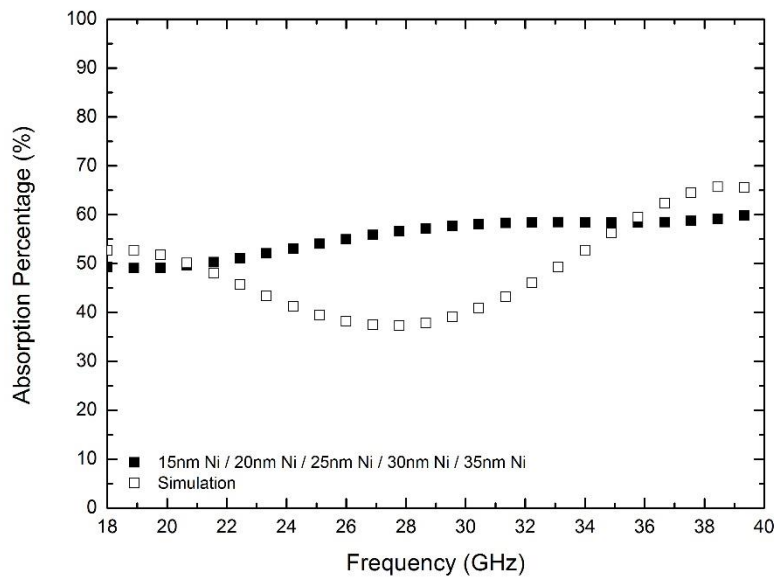


Figure A.27 EM wave absorption percentage comparison of five layer nickel surface modified glass fiber structure and its simulation.

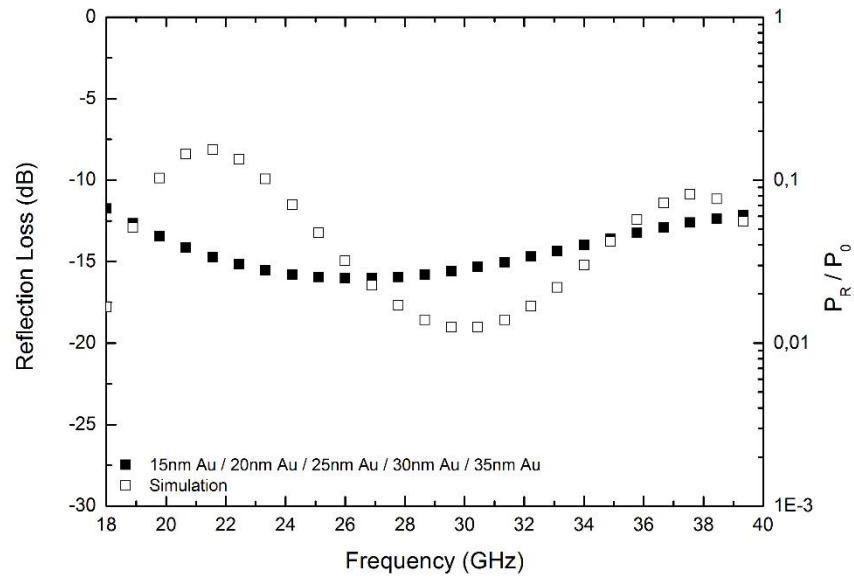


Figure A.28 EM wave reflection loss comparison of five layer gold surface modified aramid fiber structure and its simulation.

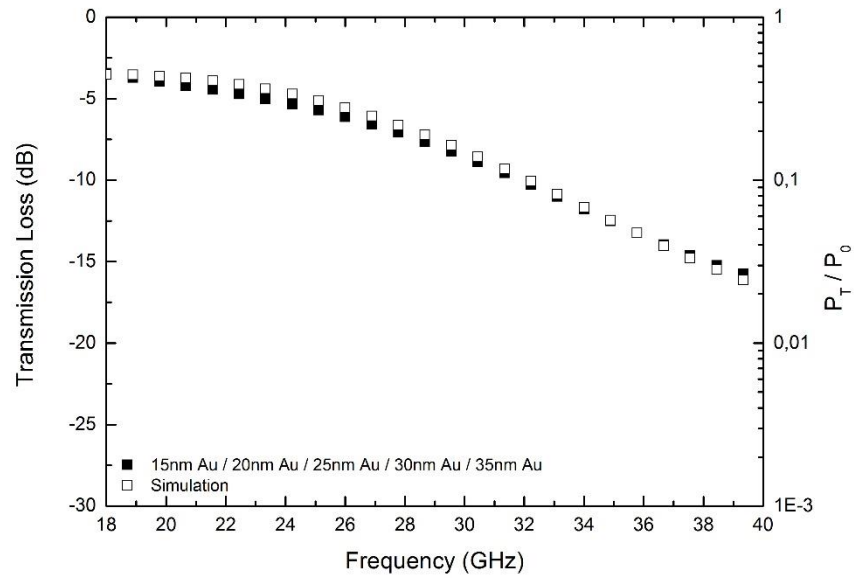


Figure A.29 EM wave transmission loss comparison of five layer gold surface modified aramid fiber structure and its simulation.

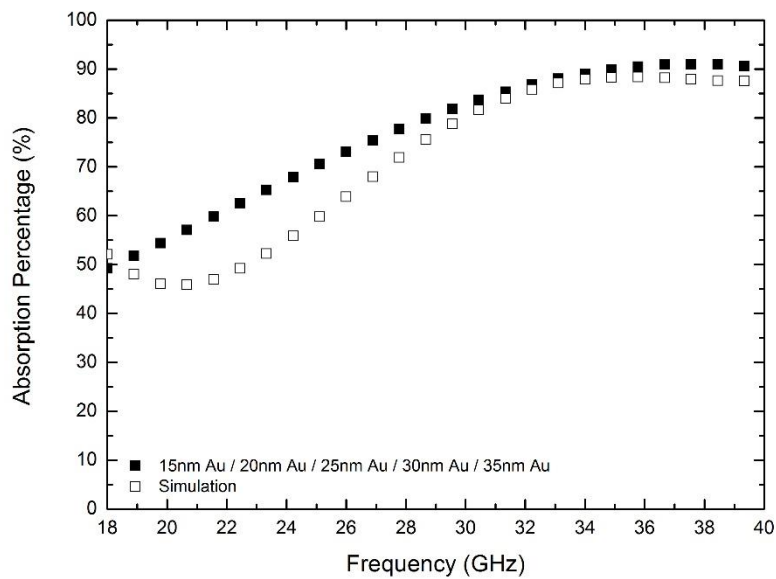


Figure A.30 EM wave absorption percentage comparison of five layer gold surface modified aramid fiber structure and its simulation.

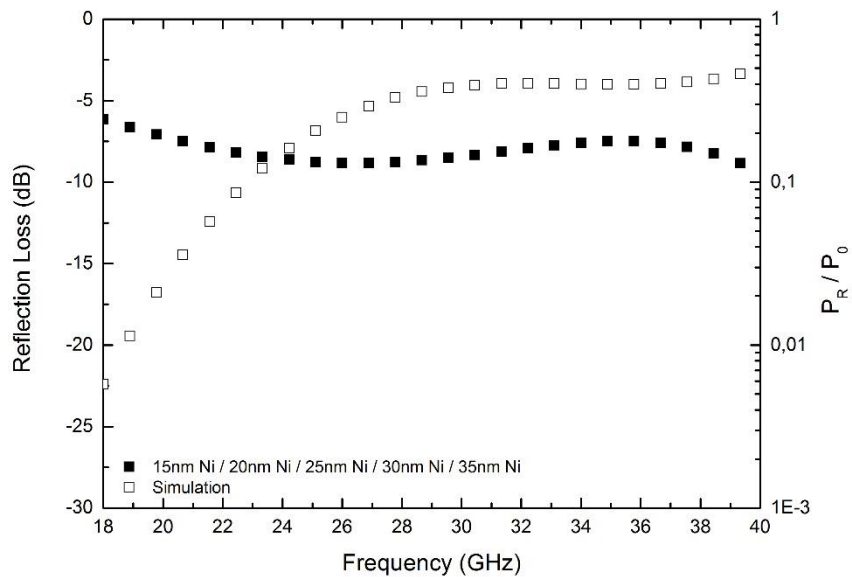


Figure A.31 EM wave reflection loss comparison of five layer nickel surface modified aramid fiber structure and its simulation.

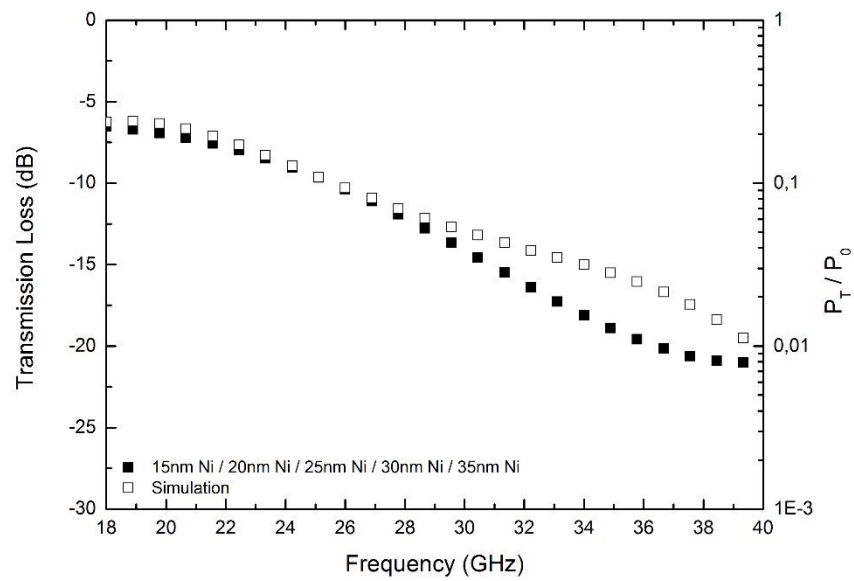


Figure A.32 EM wave transmission loss comparison of five layer nickel surface modified aramid fiber structure and its simulation.

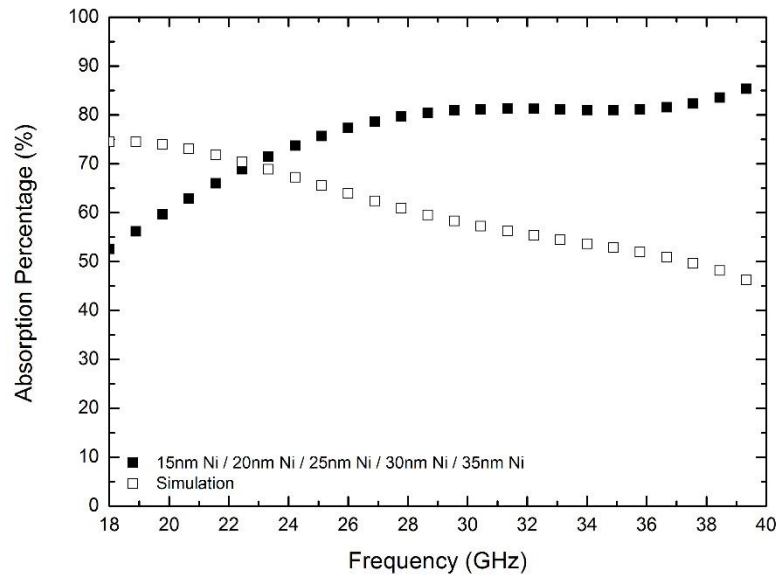


Figure A.33 EM wave absorption percentage comparison of five layer nickel surface modified aramid fiber structure and its simulation.